1-1-2013

Investigation of START Domain Proteins in Human Luteinized Cells and COS-1 Cells

Bo Shi
University of South Carolina

Investigation of START Domain Proteins in Human Luteinized Cells and COS-1 Cells

By

Bo Shi

Bachelor of Science
University of Lanzhou, 2008

Submitted in Partial Fulfillment of the Requirements

For the Degree of Master of Science in

Biomedical Engineering

College of Engineering and Computing

University of South Carolina

2013

Accepted by:

Holly LaVoie, Major Professor

Richard L. Goodwin, Committee Member

Daping Fan, Committee Member

Lacy Ford, Vice Provost and Dean of Graduate Studies

Acknowledgments

First and foremost I would like to thank my mentor, Dr. Holly A. LaVoie for her insight and direction, and also thank her to isolate, culture, transfect, and treat with cells. I would like to thank Dr. Robert L. Price and Anna McNeal belonged to Instrumentation Resource Facility (IRF) for teaching me fluorescent staining and confocal imaging, thank Nicole E. Whitfield belonged to our lab for teaching and helping me do some protein works and do most of RNA isolation, and thank Dr. Steven King of Doug Stocco's laboratory from Texas Tech University, Lubbock, TX, for the work on western blots of STARD1 and phosphorylated-STARD1 of Patient #1376. I would like to thank Richard Kordusfrom and Dr. Gail Whitman-Elisa from Advanced Fertility and Reproductive Endocrinology Institute, LLC in West Columbia, SC, for us obtaining human luteinized granulosa cells, thank Dr. Douglas Stocco and Dr. Steven King for the gifts of STARD1 and phosphorylated-STARD1 antibodies, and thank Dr. Himangshu Bose from Mercer University, Savannah, GA, for the gifts of pSTARD1 and the F2 plasmids. I would also like to offer my sincere gratitude to my thesis committee, Dr. Daping Fan and Dr. Richard L. Goodwin, for their time, comments, and instruction.

Abstract

After the luteinizing hormone surge of the menstrual cycle, the ovarian follicular granulosa and theca cells terminally differentiate to form the luteal cells of the corpus luteum. During this process known as luteinization, granulosa cells begin to synthesize large quantities of progesterone, a hormone essential for pregnancy. The rate limiting step for the de novo synthesis of pregnenolone (the precursor to progesterone) is the transport of cholesterol from the outer to the inner mitochondrial membrane, a process mediated by STARD1. STARD1 contains a C-terminal lipid binding domain holding one molecule of cholesterol, and an N-terminal domain targeting STARD1 to the mitochondrial membrane. STARD1 is the founding member of the mammalian START domain family, which includes 15 members. Two other members, STARD4 and STARD6, have recently been found in the ovary, and there is evidence that both can transfer cholesterol in certain settings, but unlike STARD1, STARD4 and STARD6 lack mitochondrial targeting. In this study, we aimed to determine the regulation of STARD1, STARD4, and STARD6 by protein kinase A (PKA) and Protein Kinase C (PKC) signals and sterol levels in cultured human luteinized granulosa cells. We found that both STARD1 and STARD4 mRNA, but not STARD6, were increased by PKA and PKC signaling agonists. STARD4 mRNA was sensitive to cellular sterol level, and STARD1 mRNA was responsive to cholesterol under low dose phorbol ester (PMA) stimulation. Moreover, STARD1 protein level and phosphorylation was increased by both cAMP analog and PMA. In transfected COS-1 cells, fluorescent confocal images showed that the localization of STARD6 was mostly in

the cytoplasm with some nuclear presence but STARD4 was throughout the cytoplasm and nucleus. In addition, to confirm a prior result in our laboratory to test if STARD6 can facilitate de novo steroidogenesis, COS-1 cells transfected with the components of the P450 cholesterol side chain cleavage complex were co-transfected with vector alone or vectors containing either human STARD1 or STARD6. STARD6 was able to modestly increase pregnenolone production above vector, but not nearly to the extent of STARD1. These studies provide new insight into the regulation of START domain proteins in the human ovary.

Table of Contents

List of Tables

List of Figures

List of Abbreviations

22R-OH-Chol.....22(*R*)-hydroxy-cholesterol

27HC..... 27-Hydroxycholesterol

3β-HSD..... 3β-hydroxysteroid dehydrogenase

8Br-cAMP.....8-Bromoadenosine 3',5'-cyclic monophosphate

ACAT ..... acyl coenzyme A: cholesterolacyltransferase

AG .....Aminoglutethimide

ATF6α ..... activating transcription factor 6α

BSA ..... bovine serum albumin

bHLH-Zip ..... basic helix–loop–helix leucine zipper

C-terminus ..... carboxyl-terminal

cAMP..... 3'-5'-cyclic adenosine monophosphate

CEBP .....CCAAT/enhancer-binding protein

CRAC .....cholesterol recognition / interaction amino acid consensus

CL.....Corpus luteum

CLAH .....congenital lipoid adrenal hyperplasia

CRE .....cAMP-responsive element

CYP11A1..... Cytochrome P450, Family 11, Subfamily A, Polypeptide 1

CYP27A1..... Cytochrome P450, Family 27, Subfamily A, Polypeptide 1

DAPI.....4',6-diamidino-2-phenylindole

DAM-Cy3.....donkey anti-mouse Cyanine 3

DAR-Cy3 ..... donkey anti- rabbit Cyanine 3

DDK ..... aspartic acid aspartic acid lysine

DHE ..... dehydroergosterol

DMSO ..... dimethyl sulfoxide

DOR ..... diminished ovarian reserve

ER ..... endoplasmic reticulum

EGF ..... epidermal growth factor

FBS ..... fetal bovine serum

FGD ..... familial glucocorticoid deficiency

FGF ..... fibroblast growth factor

FRAP ..... fluorescent recovery after photobleaching

FSH ..... follicle-stimulating hormone

HDL ..... high density lipoprotein

hCG ..... human chorionic gonadotropin

HD ..... homeodomain

hLDL ..... human low density lipoprotein

HMG-CoA ..... 3-hydroxy-3-methylglutaryl-coenzyme A

hTBP ..... human TATA-box binding protein

IGF-1 ..... insulin-like growth factor 1

INSIG1 ..... insulin-induced genes 1

INSIG2 ..... insulin-induced genes 2

LH ..... luteinizing hormone

LPDS ..... lipoprotein deficiency serum

LRH-1 ..... liver receptor homologue-1

LXRs ..... liver X receptors

MCD ..... methyl-β-cyclodextrin

N-terminus ..... amino-terminal

NBCS ..... new born calf serum

NCEH ..... neutral cholesterol ester hydrolase

NCLAH ..... non-classic form of lipoid adrenal hyperplasia

NEAA ..... non-essential amino acids

NPC1 ..... Niemann Pick C1

nSREBP ..... nuclear form of SREBP

ORF ..... open reading frame

P450scc ..... P450 cholesterol side chain cleavage enzyme

PBR ..... peripheral benzodiazepine receptor

PBS ..... phosphate buffered saline

PCOS ..... polycystic ovary syndrome

PH ..... pleckstrin homology

PKA ..... protein kinase A

PKC ..... protein kinase C

PMA phorbol-12-myristate-13-acetate

RER ..... rough endoplasmic reticulum

SBP ..... sterol-binding pocket

SCAP ..... SREBP cleavage-activating protein

SDS ..... sodium dodecyl sulfate

SER..... smooth endoplasmic reticulum

SF-1 ..... steroidogenic factor-1

SR-BI..... scavenger receptor BI

SRE..... sterol regulatory element

SREBP..... sterol regulatory element binding protein

StAR ..... steroidogenic acute regulatory protein

STARD ..... START domain protein

STARD1 ..... START domain protein 1

STARD2 ..... START domain protein 2

STARD3 ..... START domain protein 3

STARD4 ..... START domain protein 4

STARD5 ..... START domain protein 5

STARD6 ..... START domain protein 6

STARD7 ..... START domain protein 7

STARD8 ..... START domain protein 8

STARD9 ..... START domain protein 9

STARD10 .....START domain protein 10

STARD11 .....START domain protein 11

STARD12 .....START domain protein 12

STARD13 .....START domain protein 13

STARD14 .....START domain protein 14

STARD15 .....START domain protein 15

START..... steroidogenic acute regulatory protein-related lipid transfer

TBS.....tris buffered saline

TGFα .....transforming growth factor alpha

TGFα .....transforming growth factor alpha

TTBS .....TBS-Tween

UPR .....unfolded protein response

VDAC.....voltage-dependent anion channel

WCE .....whole cell extract

Chapter I: Introduction

1.1 Introduction overview

Steroidogenesis, the process of making steroid hormones, occurs in many tissues. Large scale *de novo* steroidogenesis is restricted to the gonads, the adrenals, and placentas of some species. The adrenal cortex produces essential mineralocorticoid and glucocorticoid hormones necessary for life. In some species, like humans, sex steroid hormones are also made by the adrenal. The ovaries of females and testes of males are the major sites for sex steroid hormone production. All steroid hormones can be derived from the first synthesized steroid hormone product, pregnenolone, if the appropriate modifying enzymes are present. As pregnenolone is the first hormone produced by *de novo* steroidogenesis from cholesterol substrate, this section will review cholesterol regulation and cholesterol access to the enzymatic machinery within the mitochondria. The role of steroidogenic acute regulatory protein (StAR) also called STAR-related lipid transfer (START) domain protein 1 (STARD1), the major protein controlling cholesterol entry into the mitochondrion, will be reviewed. In addition, other relevant START domain proteins of the START domain family, STARD4 and STARD6, of interest to our study will be reviewed.

1.2 Cholesterol regulation

Cholesterol is not only a critical component of cell membranes, but also has functions as metabolites or precursors (Edwards and Ericsson, 1999). Humans are able to get cholesterol from the diet as well as produce cholesterol from acetate. However, too much cholesterol loading in the cell is noxious, and much research shows that atherosclerotic vascular disease is related to the levels of low density lipoprotein-borne cholesterol. Therefore, cholesterol levels need to be controlled to keep them at a certain level, not too low or too high. There are two major protein families that transcriptionally regulate cholesterol level, liver X receptors (LXRs) and sterol regulatory element binding proteins (SREBPs) (Edwards and Ericsson, 1999). When cholesterol concentration is deficient, LXR is inactive, yet under the same conditions SREBP is cleaved to an active form. Cleaved SREBP moves into nucleus and activates certain genes for the synthesis and uptake of cholesterol. On the other hand, when cholesterol level is high, SREBPs are inactive. In contrast, when LXR binds oxysterol it stimulates the transcription of the genes to reverse cholesterol transport (Edwards et al, 2000).

Acetyl-CoA can be used to synthesize cholesterol through a process that requires no less than twenty-three enzymes (Clark 2012). The expression of genes coding for many of these enzymes are under the control of the SREBP family. SREBPs are a group of transcription factors, belonging to the helix–loop–helix leucine zipper (bHLH-Zip) family (Horton et al, 2002) where the bHLH-Zip region is the DNA binding domain (Sato et al, 1994). There are three members in this protein family, SREBP-1a, SREBP-1c, and

SREBP-2 (Goldstein et al, 2002). The three proteins reside in the membrane of the endoplasmic reticulum (ER). The three proteins are separated to three parts: amino-terminal (N-terminus), carboxyl-terminal (C-terminus), and the part between the two domains. The N-terminus consists of about a 500 amino acid sequence which includes the bHLH-Zip domain. The C-terminus contains around a 590 amino acid sequence is the functional domain. The middle region has two transmembrane segments, and the two segments are linked by about 30 amino acids. The N-terminus region, which is the transactivation domain, can be cut from the membrane by proteases, and imports into nucleus to activate the transcription level of lipid related genes (Horton et al, 2003).

If SREBP resides in the ER membrane, its C-terminus region links to SREBP cleavage-activating protein (SCAP). SCAP is a sensor for lipid level. If the cholesterol level of the ER membrane decreases to a threshold, the protein complex of SREBP and SCAP moves to the golgi. In the golgi, the complex is cut twice by enzymes, and releases the nuclear form of SREBP (nSREBP) into nucleus. In the nucleus, nSREBP recognizes a 10 base pair repeat sequence in DNA within the promoters of target genes related to cholesterol synthesis or metabolism (Goldstein et al, 2002). On the other hand, if the cholesterol concentration of the ER membrane is plentiful, SCAP maintains SREBP in the ER membrane with the help of insulin-induced genes 1 (INSIG1) and insulin-induced genes 2 (INSIG2) (Yabe et al, 2002; Yang et al, 2002). Thus, the active domain is unable to be delivered to the nucleus, so the transcription level of cholesterol related genes cannot be enhanced.

The three proteins, SREBP-1a, SREBP-1c, and SREBP-2 regulate cholesterol synthesis and fatty acid synthesis in different ways. First, in liver, both SREBP-1a and SREBP-2 can promote both synthetic pathways. Nonetheless, SREBP-1a is more sensitive to the fatty acid pathways, but cholesterol level is more dramatically enhanced by SREBP-2. Moreover, SREBP-1c only increases fatty acid production (Horton et al, 2002; Horton et al, 2003).

1.3 Steroid hormone synthesis in the corpus luteum

The corpus luteum (CL) is a transient endocrine structure essential to support pregnancy. It is formed from the residual somatic cells of an ovarian follicle after it has released its ovum at ovulation. The CL produces mainly the steroid hormone progesterone but also can produce estrogen in some species. The CL exists for only a short period of time, but it has remarkable function for synthesizing more than 40 mg of progesterone daily for humans (Christenson and Devoto, 2003). As steroid hormones are released upon synthesis, continued steroid hormone production is required to maintain high plasma levels. Steroid hormone synthesis by the CL is regulated by different hormones in different animal species. For example, the progesterone level in the CL of humans and monkeys is under the control of luteinizing hormone (LH) which stimulates steroidogenesis through the cAMP or PKA pathway (Niswender et al, 2000). On the contrary, although LH is the initial agent to promote CL function, prolactin and estradiol

maintain CL steroidogenic ability in rodents and rabbits, and human chorionic gonadotropin (hCG) maintains it in humans (Christenson and Devoto, 2003).

The first step for *de novo* steroidogenesis in luteal cells is producing pregnenolone from cholesterol. This initial event occurs in the mitochondria and is highly regulated. Steroid hormone production efficiency is limited by cholesterol transport to the inner mitochondria. Cholesterol itself can be synthesized via 3-hydroxy-3-methylglutaryl-coenzyme A (HMG-CoA) reductase activity, but this is a minor source of cholesterol in the CL. The major source of cholesterol is via cellular uptake of low density lipoprotein (LDL), which is rich with cholesterol, or high density lipoprotein (HDL) which contains cholesterol esters. The preferred source of extracellular lipoprotein used for steroidogenesis is dependent on the species. Humans and pigs prefer LDL as cholesterol source which is obtained via LDL receptors at the cell membrane (Brannian and Stouffer, 1993); on the other hand, for rodents and ruminants, scavenger receptor BI (SR-BI) in the plasma membrane can obtain HDL (Christenson and Devoto, 2003).

There are two forms of cholesterol which existed in cells or in plasma lipoproteins. They are free cholesterol and cholesterol esters. The free cholesterol is a critical substrate, or precursor, which is involved in steroidogenesis. Cholesterol is esterified through its 3β-hydroxyl group to polyunsaturated fatty acids or to sulfate which is catalyzed by an enzyme called microsomal acyl coenzyme A: cholesterolacyltransferase (ACAT). The cholesterol esters are produced in the rough endoplasmic reticulum (RER), and then they

are transported to lipid droplets which localize in the cytosol to vesicles. Lipid droplet abundance is a crucial characteristic in the luteal cells. However, cholesterol esters in these droplets cannot be a direct precursor in the process of steroidogenesis, or be a structural compound serving in the cellular membrane system as free cholesterol does. On the other hand, these cholesterol esters can be hydrolyzed by neutral cholesterol ester hydrolase (NCEH), and the hydrolysis product, free cholesterol, can be used for steroid production or structural functions. Furthermore, NCEH is sensitive to many tropic hormones, such as hCG (which mimics LH), follicle-stimulating hormone (FSH), and LH, in steroidogenic ovarian cells (Christenson and Devoto, 2003).

In women, after the LH surge or injecting hCG, the progesterone concentration in serum is raised immediately (Christenson and Devoto, 2003). This observation demonstrates that the enzymes for producing progesterone have to exist or be induced quickly in the steroidogenic cells. In luteal cells, researchers have found several enzymes that are involved in steroid hormone production. However, there are only two major steps to synthesize progesterone from cholesterol. First, the P450 cholesterol side chain cleavage enzyme (P450scc) complex (which includes the P450scc enzyme, adrenodoxin and adrenodoxin reductase) converts cholesterol to pregnenolone at the inner membrane of the mitochondria. To synthesize progesterone, pregnenolone is further altered by 3β-hydroxysteroid dehydrogenase (3β-HSD) which resides in the smooth endoplasmic reticulum (SER). However, to reach the inner mitochondrial membrane, cholesterol must associate with STARD1 in luteal cells (Devoto et al, 2002). The action of STARD1 is

believed to be the true rate-limiting step in *de novo* steroidogenesis (Lavoie and King, 2009).

In *de novo* steroidogenesis, STARD1 delivers cholesterol, and several publications have focused on its regulation or function in ovarian cells or other steroidogenic tissue cells (Stocco 2000). The ovarian follicle is composed of theca cells, granulosa cells, and the oocyte. Steroids hormones are synthesized in theca cells and granulosa cells which are surround the oocyte in follicles of the ovary. In the follicle, the androgens are produced *de novo* in theca cells which locates at the outermost layer of the follicle. The androgens are then converted to estradiol in the granulosa cells for most mammals. The theca cells of some species can use the androgens for estradiol production. Both LH and FSH stimulate progesterone production in cultured cells, however, *in vivo*, within the maturing ovarian follicle before the LH surge, STARD1 cannot be detected in the granulosa cells of most species, and thus progesterone production from cholesterol is limited. On the contrary, STARD1 protein is highly expressed in the periovulatory theca cells in order to synthesize androgens which are produced from cholesterol through pregnenolone. Moreover, in the preovulatory human follicle, STARD1 can be found in granulosa from the starting point of the LH surge (Kiriakidou et al, 1996). Thus, with the LH surge and ovulation, the major developmental change occurs in the granulosa cell layer of the follicle. The residual theca and granulosa cells of the ovulated follicle become the luteal cells of the corpus luteum. STARD1 RNA and protein levels climb to a peak and are maintained in the early luteal phase and mid-luteal phase, respectively, and

their expression are decreased during the late luteal phase in human CL and the CL of numerous other species (Devoto et al, 2001; Juengel et al, 1995).

1.4 START domain protein family

The START domain proteins are very different among animals, plants and protists. In mammals including humans, all the START domains are close to the C-terminus of each protein, but this domain does not reside on the C-terminus in other species. The domain sits about 470 amino acids from the C-terminus in rice and *Arabidopsis*. In addition, some plants proteins locate the START domain in the middle of two other domains (Schrick et al, 2004).

Plants have more kinds of STARD proteins than animals. For example, *Arabidopsis* has thirty-five proteins, and twenty-nine for rice. Yet mouse and human only possess fifteen STARD proteins. On the other hand, *C. elegans* contains 7, and 4 for *D. melanogaster*, and for protists and bacteria, there are no more than two kinds (Soccio and Breslow, 2003). Moreover, some STARD proteins contain more than one domain. In human, six out of the total fifteen are multidomain proteins. *Arabidopsis* encodes twenty-six multidomain STARD proteins, and rice encodes twenty-two. Most multidomain proteins in *Arabidopsis* and rice contain a homeodomain (HD), and a small part contains pleckstrin homology (PH) domains. The homeodomain of STARD proteins only exists in plants, and some proteins with the homeodomain play roles in localization, signaling, or enzymatic activity (Iyer et al, 2001; Ponting and Aravind, 1999).

For humans, STARD family contains a preserved sequence with around 210 amino acids, and the amino acids fold into an α/β helix-grip structure , which consists of four α helices and nine anti-parallel β sheets, and these secondary structures form a hydrophobic pocket which is able to maintain one molecule of lipid, called the sterol-binding pocket (SBP) (Mathieu et al, 2002; Yaworsky et al, 2005). The C-terminus α helix forms a hydrophobic pocket which acts as a ligand binding site, and the C-terminus requires a conformational change when lipid enters into the pocket (Baker et al, 2005; Bose et al, 2008a; Bose et al, 2008b). The model of tertiary structure demonstrates the C-helix is stable since the neighboring amino acids are bound by a series of hydrogen bonds, for example, a salt bridge which is formed by Asp 106 and resides at the loop of sheets β1 and β2 (Mathieu et al, 2002; Yaworsky et al, 2005). The loop is close to the C-helix unless the structure is in acidic microenvironment (Baker et al, 2005).

This START domain protein family participates in non-vesicular transport for lipids, such as cholesterol, oxysterol, and other lipids (Clark, 2012). The human START domain protein family contains 15 members, and the 15 proteins are separated into 6 subfamilies (Soccio et al, 2002): 1) STARD1 group (STARD1 and STARD3), 2) STARD4 group (STARD4, STARD5 and STARD6), 3) the phospholipid- and sphingolipid-binding group (STARD2, STARD7, STARD10 and STARD11), 4) the group with putative Rho GTPase function (STARD8, STARD12 and STARD13), 5) the thioesterase group (STARD14 and STARD15), and 6) STARD9 (Alpy and Tomasetto, 2005).

1.5 STARD1

For several decades, data supported the idea that an unknown protein mediated cholesterol entry into the mitochondrion to initiate steroidogenesis, however, a candidate protein was not found until 1994 (Clark et al, 1994). In heterologous transient transfection experiments, a cDNA for a protein candidate led to enhanced synthesis of steroid hormones, and it was called StAR (Clark et al, 1994). Because it was the first member of STARD family, StAR is also named STARD1. STARD1 primarily expresses in adrenal and gonadal cells. Overwhelming evidence shows that STARD1 play a major role in cholesterol transport into the steroidogenic pathway (Stocco and Clark, 1996). Importantly, humans with inactivating mutations of STARD1 suffer from congenital lipoid adrenal hyperplasia (CLAH), a disease characterized by the inability to make steroid hormones.

STARD1 contains a START domain motif of about 210 amino acids which forms a hydrophobic pocket that is able to hold a cholesterol molecule. It also contains an amino-terminal α helix sequence that can target into the membrane of mitochondria. Thus, it binds to and helps cholesterol transfer from the outer membrane of mitochondria to the inner membrane so as to facilitate steroid production. This protein is a 37 kDa precursor when just translated in and present in the cytosol. Then it is cut into a 32 kDa intermediate during its transfers into the mitochondria. Finally, a mature protein with 30 kDa localizes in the matrix of mitochondria (Stocco and Clark, 1996). One report illustrates that the newly synthesized 37 kDa precursor is critical for cholesterol transport.

Other evidence supports that STARD1 increases the transfer rate of cholesterol (Arakane et al, 1998; Arakane et al, 1996; Artemenko et al, 2001; Baker et al, 2007; Bose et al, 2002). Still yet, other evidence shows that STARD1 phosphorylation happens at the mitochondria (Dyson et al, 2008). The presence of the 30 kDa form of STARD1 positively correlates with increased *de novo* steroidogenesis.

STARD1 is activated after phosphorylation by 3'-5'-cyclic adenosine monophosphate (cAMP)-dependent PKA. Serine 57 and serine 195 are two conserved sites in STARD1 for phosphorylation (Arakane et al, 1997). If the serine 195 is mutated to alanine which cannot be phosphorylated, the ability for cholesterol transport will decline more than 50%. In contrast, if the serine 195 is substituted by aspartic acid which is more positive charged and mimics phosphorylation, the steroidogenic activity STARD1 will be higher than the activity of the wild type. However, if this residue is mutated to a nonpolar amino acid, such as alanine, and it cannot be phosphorylated, the protein still maintains most activity (Fleury et al, 2004). These results show that posttranslational modification of the protein can increase the ability of cholesterol transport through the PKA pathway (Strauss, III et al, 2003).

1.6 STARD1 in steroidogenic cells

STARD1 is crucial for steroid hormone synthesis in steroidogenic cells. Steroid hormone synthesis occurs in response to the stimulation by tropic hormone. As mentioned previously, the first step for steroid hormone production is the process of

converting cholesterol to pregnenolone. This step needs the P450scc complex which resides in the inner membrane of mitochondria. The reaction occurs in the mitochondria, yet cholesterol is produced in the ER, or transferred into the cells by LDL receptors or SR-BIs. The hydrophobic cholesterol needs to move across the hydrophilic space between the two membranes of mitochondria, and therefore, the speed of cholesterol transport across mitochondrial membrane becomes the rate-limiting step for the steroid hormone production, and this limiting step is acutely under the control of a non-vesicular lipid transport protein, STARD1, and its expression also responds to the tropic hormone stimulation (King and LaVoie, 2012, Chark, 1994).

1.7 STARD1 in liver

STARD1 participates in bile acid biosynthesis in hepatocytes by transmitting cholesterol into mitochondria. STARD1 overexpression leads to increase the levels of 27-Hydroxycholesterol (27HC) and bile acid production in rodent primary liver cells and human HepG2 cell line (Hall et al, 2005; Pandak et al, 2002; Ren et al, 2004). One study demonstrated the rate limiting process, cholesterol transport from the outer membrane to the inner membrane of mitochondria, is needed for bile acid production by the Cytochrome P450, Family 27, Subfamily A, Polypeptide 1 (CYP27A1) pathway (Pandak et al,). The expression of STARD1 in liver cells does not only increase oxysterol synthesis in which liver X receptor participates, but also enhances bile acid production which helps clear cholesterol in blood vessels. As a result, its expression leads to

anti-atherogenic action. Thereby, increasing the level of STARD1 expression may theoretically be a method to adjust dyslipidemia or decrease atherosclerosis (Ning et al, 2009).

1.8 Mechanism of STARD1 transport

STARD1 is believed to deliver cholesterol after inserting into mitochondria through its N-terminus targeting sequence. Mutated STARD1 protein which is lacking of 62 amino acids in the N-terminus, called N-62 STARD1 protein, has a similarly effective transport rate for cholesterol in cytosol, compared with the wild type protein (Christenson and Strauss, III, 2000). However, the N-62 and normal STARD1 proteins do not work in exactly the same way. N-62 STARD1 protein scatters in the cytosol, but the wild type mostly localizes in the mitochondria. On the other hand, if more than 10 amino acids from the C-terminus are cut off, the ability of steroidogenesis decreases distinctly. With deletion of more than 28 amino acids in the C-terminus, the STARD1 protein is totally inactive. Importantly, patients with CLAH have C-terminus mutations. In summary, STARD1 protein can be separated into two independent parts: the N-terminus targeting motif and C-terminus functioning motif (Bose et al, 2002). The N-62 STARD1 protein can increase steroid hormone synthesis in a few minutes in mitochondria in COS-1 cells with only nanomolar concentration (Arakane et al, 1998).

STARD1 is able to deliver hundreds of cholesterol molecules, but one molecule of STARD1 protein can transport only one molecule of cholesterol at one time. Therefore,

this transporter should work in the intramembranous matrix of mitochondria so as to help cholesterol molecules pass through the space between the two membranes (Tsujishita and Hurley, 2000). In the 1990s, there were two hypotheses for how STARD1 targets into the mitochondria and transports cholesterol across the membrane of mitochondria. First, the C-terminus of STARD1 connects to the outer mitochondrial membrane where is rich with cholesterol, and STARD1 then uptakes cholesterol and delivers it to the inner membrane that is sterol poor. In order to terminate cholesterol transfer, the protein enters through the inner membrane, and this process occurs fast. When STARD1 passes across the inner membrane, it will not be able to transport cholesterol. Hence, the transporter is synthesized fast. The other assumption is shuttle model: the STARD1 goes back and forth between the two membranes. Nonetheless, this later model is not supported by abundant evidence(Strauss, III et al, 2003).

To summarize some of the key points regarding STARD1, the leading peptide locates in the N-terminus of the STARD1, and it is used to target STARD1 to mitochondria. The C-terminus is the functional group for cholesterol transfer. The transporter has to be recycled since one molecule of this protein delivers hundreds of cholesterol molecules through the intramembranous matrix, and converts into pregnenolone by the actions of P450scc enzyme complex. Maintaining the activity of STARD1 requires a proton pump, and disturbing the electrochemical gradient of mitochondrial membranes causes decreased function of STARD1 (Allen et al, 2004). This protein forms a molten globule molecule through a pH-dependent transition state in

liquid in vitro (Bose et al, 1999) or onto artificial membranes (Christensen et al, 2001; Song et al, 2001). Lastly, some papers show that STARD1 interacts with a protein localized in the outer membrane of mitochondria, called the peripheral benzodiazepine receptor (PBR), during the cholesterol import process (Hauet et al, 2005; West et al, 2001). Other studies have failed to confirm this.

After STARD1 is synthesized as a 37 kDa protein, the leader peptide at the N-terminus targets to the outer mitochondrial membrane. Then the whole protein anchors into the membrane, and participates in steroidogenesis. Localizing in the membrane, STARD1 delivers the cholesterol which has already been in the outer mitochondrial membrane. The cholesterol molecules in the outer membrane can be separated into two groups by their function. First, those stabilized in the membrane as a structural component of the membrane; second, the molecules which are unstable and can be imported to the inner membrane for steroidogenesis. Although the two kinds are the same chemical form, they are different in the physical states for how they link to the outer membrane.

PBR may participate in the process of STARD1 transport (Hauet et al, 2005). PBR is made up of five transmembrane domains and its C-terminus, a 26 amino acid sequence, is exposed to the cytosol (Joseph-Liauzun et al, 1998). The C-terminus forms a cholesterol recognition/interaction amino acid consensus (CRAC) domain, which consists of a helical structure, which comprises a hydrophobic pocket in order to hold only one cholesterol molecule (Jamin et al, 2005; Li et al, 2001).

As a consequence, a new model for the transport mechanism is suggested. Unstable cholesterol first binds to the CRAC domain of PBR, and the cholesterol molecule transmits to STARD1 which is through proton-induced molten globule transition. Then some other proteins form a hydrophobic channel, perhaps the voltage-dependent anion channel (VDAC) and the adenine nucleotide-binding protein (McEnery et al, 1992), pick up the cholesterol molecule and transfer it to P450scc enzyme to produce pregnenolone (Soccio et al, 2002).

1.9 Hormonal control of STARD1

Injecting hCG into women leads to differential effects on the mRNA and protein levels of STARD1 in theca-lutein cells and granulosa-lutein cells during the mid-luteal phase. Their expression is increased sharply in theca-lutein cells while they are increased moderately in granulosa-lutein cells (Kohen et al, 2003). Nonetheless, the protein and mRNA expression are enhanced in both theca-lutein cells and granulosa-lutein cells. Moreover, gonadotropin hormone regulates the mRNA level of STARD1, and the mRNA level of STARD1 is under the control of the cAMP pathway by LH in Leydig cells. In addition, hCG can bind to LH receptor so as to enhance the transcription of STARD1. The mRNA level of STARD1 is also controlled by the PKC pathway which is also activated by high concentrations of LH and some growth factors, such as insulin-like growth factor 1 (IGF-1), epidermal growth factor (EGF), fibroblast growth factor (FGF) and transforming growth factor alpha (TGFα) in primary Leydig and some Leydig tumor

cell lines (King and LaVoie, 2012). The transcriptional level of STARD1 is also enhanced by increased hCG which acts through PKA and PKC signaling in Leydig cells (Jo et al, 2005; Lin et al, 1998; Manna et al, 2006a; Manna et al, 2002; Manna et al, 2006b). Low dose phorbol ester (10 nM) acting through PKC increases STARD1 mRNA in Leydig cells (Manna et al, 2009). Moreover, the granulosa cell also expresses STARD1 followed the LH surge in the ovary (LaVoie and King, 2009). Interestingly, in cultured human luteinized granulosa cells; higher phorbol ester concentrations (162 nM) suppressed cAMP-stimulated STARD1 mRNA (Kiriakidou et al, 1996).

1.10 STARD1 transactivators

Early publications have shown that the protein level of STARD1 can be stimulated by cAMP by increasing transcription (Christenson and Strauss, III, 2000). However, later studies show that the promoter of this protein is lacking a canonical cAMP-responsive element (CRE) (Christenson and Devoto, 2003). Nevertheless, it is found that all STARD1 gene promoters identified thus far contain steroidogenic factor-1 (SF-1) binding sites. SF-1 belongs to the nuclear receptor superfamily, and it can promote the transcription levels of many steroidogenic genes following increased cAMP (Parker and Schimmer, 1997). Also, all the SF-1 binding sites of the human STARD1 gene are regulated by cAMP. Moreover, liver receptor homologue-1 (LRH-1) a related protein also acts on SF-1 binding sites (Galarneau et al, 1996). LRH-1 exists in granulosa cells

prior to LH surge, the protein level raises after LH surge, and maintains a high expression if progesterone production is enhanced as shown in rodent luteal tissue.

The most active promoter region of STARD1 genes resides at -119 bp to -58 bp, of the 5′-flanking region of the gene. The two transcription factors, SF-1 and LRH-1, bind at -105 to -95 bp, -42 to -35 bp and -926 to -918 bp of the human gene (Sugawara et al, 1997). Mutation of -105 to -95 bp also causes a decreased promoter activity in granulosa cells in rodent ovarian cells (Yivgi-Ohana et al, 2009). The STARD1 promoter of humans is influenced by SF-1/LRH-1 recognition sites with sites from -3400 bp to -3000 bp (Mizutani et al, 2010). Deletion of LRH-1 leads to impaired ovulation and reduced levels of STARD1 and progesterone synthesis in rodent granulosa cells (Duggavathi et al, 2008). Furthermore, the promoters of STARD1 in humans and rodents have an element that binds to CCAAT/enhancer-binding proteins (CEBPs), and CEBPβ can also enhance the STARD1 gene expression with addition of cAMP. It has shown a synergistic effect on cAMP-dependent activity of STARD1 gene promoter by overexpression both SF-1 and CEBPβ (LaVoie and King, 2009).

Two members of GATA family, GATA4 and GATA6, regulate the STARD1 level in somatic steroidogenic cells in testis and ovary (LaVoie 2003). With the treatment of cAMP analog, the binding of transcription factor GATA4 increases, and which activates STARD1 promoter in MA-10 Leydig cell line (Hiroi et al, 2004). Also, in granulosa cells, the two transcription factors bind from a proximal GATA sequence, and enhance the promoter activity (Gillio-Meina et al, 2003; LaVoie et al, 2004). GATA6 can partly

substitute for GATA4, and elevate the mRNA level of STARD1 in luteal cells (King and LaVoie, 2012).

1.11 STARD4 subfamily

The three members of the STARD4 subfamily, STARD4, STARD5 and STARD6. They contain 205 to 233 amino acids and share 26% to 32% identical residues. STARD4 and STARD5 are widely expressed in different cell types, such as in kidney cells and hepatocytes, but STARD6 is only found in testis, and nerve cells (Soccio et al, 2002). Recently, our lab also localized STARD6 to ovary (LaVoie et al., 2011).

There are three pieces of evidence show that the STARD4 subfamily proteins bind to lipids and cholesterol. First, STARD4 is involved in cholesterol homeostasis and is under the control of SREBPs. SREBPs also regulate other molecules involved in lipid metabolism (Edwards et al, 2000). Moreover, the three members of this subfamily are most similar with STARD1 which binds to cholesterol (Soccio et al, 2002). Last, the crystal structure of STARD4 has been elucidated, and revealed a hydrophobic pocket (Romanowski et al, 2002).

STARD4 and STARD5 share about 30% identical sequence, and both proteins contain a START domain. The STARD4 gene is under the control of SREBPs via a sterol regulatory element (SRE) within its promoter, but STARD5 is not regulated by sterol level. The two proteins have similar activity to STARD1 in terms of cholesterol transport.

In addition, both of them may activate the alternative bile acid production pathway (Soccio et al, 2005b).

1.12 STARD4

The mouse STARD4 contains only an α/β domain which consists of four α helixes (αA to αD) and ten β sheets (β1 to β10). Most β sheets are anti-parallel, but β8 and β9 are parallel. Two α helixes localize at the two ends, and the other two insert between β3 and β4. Moreover, the three dimensional structure contains a hydrophobic pocket which may hold a lipid molecule (Renet al, 2004).

In experiments with SREBP transgenic mice, STARD4 was more highly induced by SREBP-2 compared to SREBP-1a. The STARD4 level of wild-type mice dropped dramatically within one day of feeding with a high cholesterol diet. Moreover, STARD4 level was not influenced by activated SREBP-1c. Therefore, STARD4 was more sensitive to SREBP-2 than SREBP-1a and SREBP-1c (Soccio et al, 2005).

During the six days when monocytes differentiate to macrophages, the expression of SREBP-1 and its target genes increased. On the contrary, the SREBP-2 level declined, so that the expression of its target genes also decreased (Ecker et al, 2010). As STARD4 was preferentially regulated by SREBP-2 rather than SREBP-1 and since STARD4 increased in macrophages while SREBP-2 decreased, the enhanced STARD4 protein level may result from the increased expression of activating transcription factor 6α

(ATF6α) which occurred during the differentiation process of macrophages (Rodriguez-Agudo et al, 2011).

Peptides are synthesized by the ER in eukaryotic cells. If unfolded and misfolded proteins build up within the ER, such as when the cellular environment is perturbed, the cell induces several pathways in order to reduce such ER stress. This is referred to as the unfolded protein response (UPR). UPR simulates the transcription level of genes encoding ER-resident chaperones or folding catalysts. STARD4 level is increased during the early phase of ER stress, and this protein is one of the target genes for the UPR, Moreover, the promoter of STARD4 can be activated by ATF6, which is stimulated in the early stage of ER stress (Yamada et al, 2006).

STARD4 promotes the rate of cholesterol esterification from exogenously derived cholesterol. This protein transports cholesterol to ACAT, and the delivery efficiency of cholesterol to ACAT decides the rate of cholesteryl ester production. Also, STARD4 promotes cholesterol transport to the ER and mitochondria. Thus, this protein plays an important role in cholesterol metabolism (Rodriguez-Agudo et al, 2008).

Riegelhaupt et al. (2010) investigated of the role of STARD4 in knockout mice to clarify the function of this protein in cholesterol metabolism. Homozygous STARD4 knockout mice had reduced body weight compared to the wild type mice, and this result was not caused by altered food intake or energy metabolism (Riegelhaupt et al, 2010), but may have resulted from a defect during the development.

It has also been shown that STARD4 is able to promote steroidogenesis after P450scc complex and 3β-HSD cDNAs are transfected into nonsteroidogenicCOS-1 cells. Therefore, knocking out STARD4 might lead to impaired steroid hormone synthesis during development, but there is no data to support this concept at present. Furthermore, there was no significant difference between the knockout mice and wild type mice in body composition, including the heart, kidney, liver, lung, spleen, and the epididymal fat pads. Compared to the wild types, STARD4 null mice also showed no significant difference in plasma and liver lipid content, when fed normal chow diet. However, the levels of bile cholesterol and phospholipid were lower in gallbladders of the female knockout mice compared to the controls (Riegelhaupt et al, 2010).

STARD4 null mice were also fed a diet of 0.2% lovastatin to reduce the cholesterol concentration in blood. The result did not show any significant alteration between the STARD4 null mice and wild type controls. Nevertheless, with a 0.5% cholesterol diet, the levels of total cholesterol, LDL, and cholesterol ester have a moderate decline in female knockout mice. Based on microarray analyses, the mRNA levels of most genes did not have significant differences between the two groups with the exception of Niemann Pick C1 (NPC1). NPC1 mRNA level dropped 2.5 fold in the knockout mice. Therefore, decreasing of NPC1 expression may be a compensatory mechanism for lack of STARD4 in the intracellular cholesterol transport pathway (Riegelhaupt et al, 2010).

Taken together, these data support the role of STARD4 in cholesterol transport: knocking out this protein did not yield on apparent change in cholesterol metabolism.

Hence, several proteins may have overlapping functions and compensate for the impairment of STARD4's function in cholesterol regulation in the knockout mice (Riegelhaupt et al, 2010).

In the STARD4 knockdown cells, the ability of cholesterol to regulate SREBP-2 decreases sharply, and cholesterol builds up in the cells. After the injection of methyl-β-cyclodextrin (MCD) a simple steroid transporter, into the cytosol, the cholesterol accumulation is reversed in STARD4 silenced cells. It seems that MCD can mimic the cholesterol transport that is normally mediated by STARD4 (Mesmin et al, 2011).

A 2011 publication showed that STARD4 was controlled by sterol levels in 3T3-L1 cells and THP-1 macrophages. Moreover, this protein was associated with the ER and ER-derived vesicles rich in ACAT-1. STARD4 and ACAT-1 co-localized outside of lipid droplets. STARD4 was able to enhance the ACAT-1 activity of cholesterol esterfication, and this observation shows it was possible for STARD4 to deliver cholesterol to or into the ER. In addition, it played a crucial role to regulate cholesterol homeostasis in hepatocytes and Kupffer cells which were two major cell types in the liver (Rodriguez-Agudo et al, 2011).

Purified recombinant STARD4 protein can increase ACAT activity (cholesteryl ester formation) by 2 fold in vitro (Rodriguez-Agudo et al, 2011). This observation was consistent with the result that overexpressing the STARD4 protein promoted cholesterol esterfication in macrophages and liver cells (Rodriguez-Agudo et al, 2008). Therefore,

these results demonstrated that STARD4 is able to activate ACAT enzyme localized to the ER (Rodriguez-Agudo et al, 2011).

As an overview of STARD4 action, first, this protein is involved in cholesterol delivery to ACAT, and promotes the activity of ACAT for cholesteryl ester formation. Second, it plays a central role in cholesterol distribution from ER as a non-vesicular transport pathway, so as to regulate cholesterol homeostasis in the ER. Thus, this protein may be involved in the ER stress which is induced by the altered level of free cholesterol, and hence, it is possible for STARD4 to play a role in the atherosclerosis development (Rodriguez-Agudoetal, 2011).

Elbadawy and his coworkers (Elbadawy et al, 2011) focused on the STARD4 function in a hepatocarcinoma cell line, HepG2. The expression of this protein was increased when the HepG2 cells are grown in lipoprotein deficient serum (LPDS), where cholesterol was depleted, when compared with the cells grown in normal serum. The free cholesterol was preserved in the plasma membrane, and the ER associated cholesterol was decreased in the STARD4 knockdown cells under the cholesterol deficient environment. Moreover, in the knockdown, the cholesterol poor condition caused decreased ACAT activity of cholesteryl ester synthesis. In other words, ER associated cholesterol esterification was reduced when the expression of STARD4 was reduced in the cholesterol deficient condition. Under conditions which restore cholesterol for a short period of time, STARD4 knockdown cells showed a decreased rate of fluorescent recovery after photobleaching (FRAP) in the endocytic recycling compartment when

dehydroergosterol (DHE) was used. DHE is a nontoxic cholesterol analog with natural fluorescence, and can mimic cholesterol characteristics in different sorts of cells. In summary, STARD4 can transport cholesterol between the ER, plasma membrane and endocytic recycling compartment in order to maintain cellular cholesterol homeostasis in *in vitro* models.

1.13 STARD6

To date, there are few studies that have examined the distribution and function of STARD6. Bose and his colleagues showed recombinant mouse STARD6 can promote steroidogenesis in isolated pig mitochondria *in vitro*, similar to STARD1. STARD6 was also able to bind cholesterol better than STARD1. Furthermore, both of the two proteins show similar patterning during the process of unfolding or refolding.

The cDNA of rat STARD6 is 1146 bp long, and the longest open reading frame (ORF) can translate a 227 amino acid long peptide. In rat testis, the mRNA appeared from the third week after birth, and the mRNA kept increasing until adulthood. STARD6 protein only expresses during the maturation of germ cells and in spermatids in the testis. According to result of Western Blots, rat STARD6 is a 28 kDa protein, and immunohistochemistry data also demonstrates that it expresses in mature germ cells (Gomes et al, 2005). Therefore, it may participate in spermatogenesis during meiosis and the process of sperm cell maturation (Soccio et al, 2002). Subsequently, STARD6 was found in Leydig cells in testes of the rat under hypothyroid conditions during puberty.

Hence, perhaps it is involved in both spermatogenesis and steroidogenesis in rats (Chang et al, 2007b).

Immunoreactivity data showed that STARD6 protein was found in the nucleus rather than cytosol in neurons and the glia of the brain, spinal cord and dorsal root ganglion. Thus, STARD6 may also play roles in sensory conduction control and lipid sensing of the nervous system (Chang et al, 2007a). Chang and his coworkers (Chang et al, 2010) showed that the immunoreactivity of this protein was mostly found in nucleus and the intensity was weaker in cytosol in the cultured neuron cells, and STARD6 may play critical roles in cholesterol homeostasis (Chang et al, 2010). Just recently, their lab also inferred the possiblity that STARD6 is a neuroprotective protein, and it may be influenced by excitotoxic stimuli (Chang et al, 2013).

1.14 START proteins and diseases involving steroid production

The mutation of the STARD1 gene can lead to a disease, congenital lipoid adrenal hyperplasia, and this disease is due to the lack of the steroidogenesis in both the gonads and adrenals (Lin et al, 1995). Most of the patients are lacking of adrenocorticoids within 2 weeks after born with poor feeding, dehydration, lethargy, hyperkalemia, hyponatremia, hypoglycemia, and acidosis (Richmod et al, 2001). CLAH, in most cases, is due to failed cholesterol transport to the inner membrane of mitochondria for steroid production. With this condition, cholesterol accumulates in the cytoplasm which ultimately damages the steroidogenic cells (Bose et al, 1996). Similarly, in *stard1* knockout mice, the

accumulation of lipid and the deficiency of steroid hormones, mice live only a short period of time after birth unless given supplemental steroid hormones (Caron et al, 1997). These animals are infertile even when maintained on supplemental steroids as are humans.

Diminished ovarian reserve (DOR) is a common diagnosis in infertility patients, but it is also one of the least well-studied diseases of infertility. The cause of DOR is unclear and yet there is some association with age and is characterized by fewer follicles capable of development and ovulation. A comparison of normal ovarian reserve women's and DOR patients' luteinized granulosa cells from obtained from assisted reproduction protocols revealed DOR patients expressed a higher level of STARD1 and STARD4 mRNA (Skiadas et al, 2012); this study was also the first to identify STARD4 in ovarian cells. Another common infertility disorder in women, polycystic ovary syndrome (PCOS), is associated with high androgen production in theca cells of the ovary. *In vitro*, STARD1 level in primary theca cells was not different between PCOS and control groups, however specific enzymes involved with androgen synthesis have been shown to be elevated in PCOS (Wood et al, 2003).

1.15 Aims of this study

This study is part of a larger ongoing study to determine the roles of STARD4 and STARD6 in ovarian function. The first aim of this thesis study was: to determine the levels of STARD1, STARD4, and STARD6 mRNAs and proteins in human luteinized

granulosa cells with treatments that stimulate progesterone production, and to test the effect of cholesterol depletion, cholesterol supplementation, and inhibition of progesterone synthesis on these endpoints. As a prelude to studies with ovarian granulosa cells, a second aim was: to determine the subcellular localization of recombinant human STARD4 and STARD6 in COS-1 cells. To provide confirmation of our lab's prior results showing the steroidogenic potential of human STARD6 using the COS-F2 assay, a third aim was: to utilize the COS-F2 assay to show that STARD6 can increase pregnenolone production in COS-1 cells transfected with components of the P450scc complex.

These aims are based on the following hypotheses and rationale. Cyclic AMP acting through PKA is known to stimulate STARD1 mRNA and protein in human granulosa cells and high doses of phorbol ester inhibit it (Kiriakidou et al, 1996), but the effect of low dose phorbol-12-myristate-13-acetate (PMA) is not known. STARD1 protein is functional after phosphorylation, and this process is catalyzed through the PKA pathway. In MA-10 cells, a low dose of PMA can enhance the STARD1 protein expression but not phosphorylated STARD1 (Jo et al, 2005). Because these cells have little phosphorylated STARD1, low dose PMA had little effect on increasing progesterone synthesis. However, our lab's preliminary data (not shown) revealed that PMA can increase progesterone production. Therefore, we hypothesize that in the human luteinized granulosa cells, low dose PMA is able to increase the protein level of STARD1 and phosphorylated STARD1. This occurrence would be most likely due to the presence of the higher basal levels of PKA activity (Bogan and Niswender, 2007).

STARD4 and STARD6 have only been recently identified in the ovary, and almost nothing is known about their regulation or possible functions in the ovary. Both of these molecules have the potential to act like STARD1 in certain settings. As we found that STARD1 mRNA and protein was increased by cAMP and low dose PMA in granulosa cells, we hypothesized that STARD4 and STARD6 may be similarly regulated. Since STARD1, STARD4, and STARD6 have a START domain and the ability to bind and transport cholesterol, we also hypothesized that intracellular cholesterol availability would regulate the mRNA and protein levels. There are three steps to test these hypotheses. First, we tested if the mRNA, protein level of STARD4 and STARD6 are affected by PKA and PKC pathways by treating granulosa cells with 8-Bromoadenosine 3',5'-cyclic monophosphate (8Br-cAMP) and low dose PMA. We then altered the intracellular cholesterol levels by preventing cholesterol usage by the steroidogenic pathway and manipulating cellular cholesterol content by pretreating cells in lipoprotein deficient media or resupplying human low density lipoprotein during treatment to observe the effects on the mRNA and protein levels of STARD1, STARD4 and STARD6. As steroidogenesis requires cholesterol to be transported to the mitochondria, and STARD1 is localized to mitochondria, we hypothesized that STARD4 and STARD6 may localize to mitochondria. To test this we performed preliminary subcellular localization studies of recombinant STARD4 and STARD6 in transfected COS-1 cells using the fluorescent-antibodies. Both STARD1 and STARD4 have the ability to increase steroidogenesis in an artificial system which utilizes COS-1 cells transfected to express

steroidogenic machinery (Soccio et al, 2005). We therefore hypothesized that STARD6, when overexpressed in COS-1 with co-expression of the P450scc system, would be able to increase pregnenolone production. In total, these studies will provide novel data on the regulation and localization of STARD4 and STARD6, and the function of STARD6.

Chapter II: Materials and Methods

2.1 Human granulosa cell isolation

Human follicular fluid containing residual granulosa cells isolated from women undergoing assisted reproduction techniques were obtained from Advanced Fertility and Reproductive Endocrinology Institute, LLC in West Columbia, SC. Follicular fluid was transported on ice as soon as possible to the University of South Carolina. A protocol for the use of these cells was reviewed by the institutional IRB and found exempt from further review. The follicular fluid containing granulosa cells and blood was transferred to one or more 50 ml tubes (depending on volume) and cells were pelleted at 2000 rpm in a Beckman TJ-6 refrigerated swinging rotor centrifuge for 15 minutes. A filtered solution of hyaluronidase (4 mg/ml) and DNase (0.25 mg/ml) was prepared fresh in media containing antibiotics. The media used was Dulbecco's Modification of Eagle's Medium (DMEM)/Ham's F12 (F12) (1:1) containing antibiotics (0.1% Gentamicin, 1 % antibiotic/antimycotic solution (AMAB)). Following centrifugation, the supernatant of the follicular fluid was discarded and each cell pellet was resuspended in 2.5-3 ml of enzyme solution, mixed well, and incubated in the culture incubator (37 ^{o}C 5% CO2) for 10 minutes. Percoll gradients were used to remove contaminating blood cells. During this time Percoll gradients were prepared consisting of 4 ml of 70% Percoll in saline overlaid

with 4 ml of 35% Percoll in DMEM/F12 in a 15 ml tube. After enzyme incubation, DMEM/F12 + antibiotics (ab) was added to each pellet up to 4 ml. The cell mixture was gently overlaid onto the Percoll gradient. The gradients were spun at 2000 rpm for 30 minutes. The white band(s) was collected from each gradient and placed in a clean tube then poured through a 70 μm cell strainer into a clean 50 ml tube to remove any clumps. Sample volume was adjusted to 22-25 mls with DMEM/F12 + ab medium and the sample was spun at 2000 rpm for 20 minutes. The supernatant was poured off, and the cell pellet was retained and resuspended in 300 to 600 μl DMEM/F12 + ab medium and the total volume was measured. For counting, 10 μl of cell suspension was taken, and 1 ml DMEM/F12 + ab medium were added to the suspension with 100 μl trypan blue dye. Cells were plated at approximately 0.5 to 2 x 10^6 live cells per well in 1 ml DMEM/F12 complete medium (same as above except containing 10% fetal bovine serum (FBS)) in 12 well Falcon plates. In some experiments the FCS was replaced with lipoprotein deficient serum (LPDS) to deplete cells of intracellular cholesterol stores. Cells were cultured at 37^{o}Cwith 5% CO_2 in humidified cell culture incubator. The medium was changed daily at approximately 24 h intervals for 3 days after plating. Cells were treated on day 4 in serum-free DMEM/F12 + ab medium.

2.2 Human granulosa cell treatment

Cells were treated in 1 ml serum-free DMEM/F12 + ab supplemented with vehicle(s) or treatments. Treatments included cell-permeable cyclic AMP analog 8Br-cAMP, (0.25

or 1 mM) to activate the PKA pathway, and phorbol ester, PMA (1 or 20 nM, low dose), to activate the PKC pathway. For time course studies, cells were initially cultured in complete medium for 4 days prior to treatment in serum-free medium with the above compounds for 6 or 24 h.

Aminoglutethimide (AG) is an inhibitor of 450scc enzyme and blocks cholesterol utilization for de novo steroidogenesis and its use reduces progesterone production. In order to determine the effect of reducing the use of cholesterol (and therefore its intracellular depletion) for steroidogenesis, AG (100 μM in dimethyl sulfoxide (DMSO)) was co-added to cultures with vehicle, 8Br-cAMP (1 mM), or PMA (20 nM). DMSO solvent was used as a vehicle in place of AG. Treatments were for 24 h.

To evaluate the effects of cholesterol depletion on human granulosa cell endpoints of interest, some cells were precultured for the initial 4 days with complete media containing 10% LPDS. Cells from the same patient were also precultured under normal conditions (complete media with 10% FCS) for the same period. On day 4, cells were treated with vehicle, 8Br-cAMP (1 mM), or PMA (20 nM) alone or in the presence of human low density lipoprotein (hLDL, 50 μg/ml) or its saline/EDTA vehicle. hLDL served as an exogenous source of cholesterol. Treatments were for 24 h.

2.3 Whole cell extracts

Whole cell extract (WCE) buffer was used to lyse cells for protein isolation and was composed of 50 mM Tris (pH 7.5), 1% NP-40, 0.5% sodium deoxycholate, 0.1% sodium

dodecyl sulfate (SDS), 150 mM NaCl, 1 mM EDTA, 0.3% ALLN, 1% Pierce protease inhibitor cocktail, 1% Pierce phosphatase inhibitor, and sterile distilled water. Prior to removing medium from wells, 600-800 µl of conditioned medium was collected from each well and frozen at -80^{o}C for later progesterone quantification. The residual media was aspirated from cells and cells were rinsed with 1-2 ml of room temperature Dulbecco's phosphate buffered saline (PBS). Following aspiration of PBS, ice cold WCE buffer (human granulosa cell: 100 µl, COS-1 cell: 150 µl) was added to each well. Cells were scraped into the buffer by using a rubber scraper. The cell lysate in each well was transferred into a 1.5-ml microfuge tube and incubated on ice for 30 minutes. The lysate was spun at 13,000 rpm in an Eppendorf model 5417R refrigerated microcentrifuge for 15 minutes at 4^{o}C. The supernatant was collected and transferred to a new labeled tube on ice. The volume of these supernatant was measured for the purposes of calculating total protein. Samples were stored at -80^{o}C until use.

2.4 Protein quantification

Protein was quantified by method of Bradford using Bio-Rad dye reagent and a spectrophotometer set to 595 nm. A standard curve with known amounts of protein (bovine serum albumin, BSA, 0-8 µg/ml) was generated in each assay and sample quantities were extrapolated from the linear standard curve. Protein (20-30 µg) was aliquoted for SDS-PAGE and Western blotting.

2.5 SDS-polyacrylamide gel electrophoresis

Separating acrylamide gels of 10% and 12% were prepared in 20 ml volumes constituted of 6.6 ml and 8 ml, respectively of 30% acrylamide stock, 7.7 ml 1 M Tris, pH 8.8, 0.2 ml 10% SDS, 150 µl 10% APS, 15 µl TEMED and 5.3 ml or 3.94 ml sterile water. The 5% stacking gel was constituted of 0.8 ml 30% acrylamide stock, 0.625 ml 1M Tris, pH 6.8, 50 µl 10% SDS, 50 µl 10% APS, 5 µl TEMED, and 3.481 ml sterile water. In some cases, 4-20% precast gradient gels (Pierce, ThermoScientific) were utilized.

After assembling the gel apparatus, 800 ml of 1X running buffer was made of 80 ml of 10X running buffer, and 720 ml nanopure water. The 10X running buffer was made of 57.3 g glycine, 12.1 g Trizma Base, and 4 g SDS, and filled up to 500 ml with nanopure water. Wells were flushed prior to loading. On ice protein samples were combined with a 5X bromophenol blue loading dye containing 5% 2-mercaptoethanol. The protein samples were boiled for 8 minutes prior to loading. The samples were loaded into wells, and the gel was run at 200 V for 45 min to 1 h.

2.6 Immunoblotting

Protein in gels was transferred to Hybond-P PVDF membrane after wetting the membrane briefly in methanol. Transfer buffer was constituted of 2.93 g glycine, 5.82 g Trizma Base, and 200 ml methanol, and nanopure water up to 1 liter with nanopure water. Semi-dry electroblotting (Owl Panther semi-dry electroblotter) was used for protein

transfer. The transfer stack consisted of three sheets of the pre-cut, pre-wet Whatman paper, the gel, the PDVF membrane, and three additional sheets of Whatman paper. The transfer occurred under conditions of constant current, starting at a voltage of 9-10 and for 90 minutes.

2.7 Western blot

The membrane was blocked in 5% nonfat dry milk (Carnation)/1X tris buffered saline (TBS) -Tween TTBS. TTBS (1X) contained 100 ml 10X TBS, 900 ml nanopure water and 0.5 ml Tween-20 per liter. 10X TBS was constituted of 24.2 g Trizma Base, 292 g NaCl, and filled up to 1 liter with nanopure water. After 1 hour blocking, the membrane was washed with 1X TTBS for 3 times, 10 minutes for each time. The membrane was placed in a small container. STARD1 (concentration unknown, 1:1500) and phosphorylated-STARD1 (p-STARD1, concentration unknown, 1:500) antibodies were gifts from Dr. Douglas Stocco and Dr. Steven King, respectively (Texas Tech University, Lubbock, TX). STARD4 (0.5 µg/ml, Cat. # AP12801a, Lot # SA110414AR,), STARD6 (2.5 µg/ml, Cat. # AP11832b, Lot # SA 110210AB,) and CYP11A1 (0.5 µg/ml, Cat. # AP7899a, Lot # SH081229L) antibodies were from Abgent (Atlanta, GA). The actin antibody (concentration unknown, 1:500) was obtained from Cell Signaling (Cat. # 4967, Lot # 6, Danvers, MA), SREBP2 (0.5 to 1 µg/ml, Cat. # sc-5603, Lot #D1712) from Santa Cruz Biotechnology (Santa Cruz, CA) antibodies from was obtained from InVitrogen/Life Technologies (Carlsbad, CA). With a couple of exceptions, primary

antibodies was diluted in 1% nonfat dry milk/1X TTBS, and applied to the membrane. The exceptions were STARD1 antibody, where the primary antibody was diluted in 5% milk, and p-STARD1 antibody which was diluted in 4% milk, 1XTBS containing 0.01% Tween (as recommend by the source). At least 3 ml of antibody solution was used. The container was placed at 4 ^{o}C overnight (cold room) on a shaker. Goat anti-rabbit secondary antibody (Zymed, Cat. # 65-6120) which was obtained from InVitrogen/Life Technologies 3 µl, 3 µl BSA, and 94 µl PBS was mixed together in a 50 ml tube in order to pre-absorb the secondary antibody overnight at 4 ^{o}C.

The following day the membrane was transferred to a plastic box for washing. The membrane was washed with 1X TTBS for 3 times, 10 minutes for each time. The pre-absorbed secondary antibody was diluted with 5% nonfat dry milk/1X TTBS (or 4% milk/1XTTBS 0.01% Tween) with a final concentration of 1:4000 for the goat anti-rabbit secondary antibody. The membrane was placed in a container for antibody application and incubated on the shaker for 1 hour at room temperature. Afterwards, the membrane was washed with 1X TTBS for 5 times, 10 minutes for each time. ECL solution was prepared by adding 1:1 Reagent 1 and Reagent 2 of the ECL kit. The ECL solution was mixed well, and added onto well-drained membrane for 1 minute. The membrane was drained extremely well without touching protein lanes, and then the membrane was placed inside two pieces of transparency plastic inside a film cassette. A spectrum of timed film exposures was performed and developed. After exposure, the membrane was washed with 1X TTBS 3 times, 5 minutes each time. Then the membrane was ready for

reblocking or was stripped. If two proteins of interest were of sufficiently different size, then another primary antibody was applied without stripping off the first antibody.

2.8 Stripping immunoblots

The membrane was washed with 1X TTBS 3 times, 5 minutes each time. The 1X TTBS was poured off and approximately 50 ml of erasing buffer was added for each membrane in a small box. The erasing buffer for 50 ml was made up of 3.125 ml 1 M Tris-Cl, pH 6.8, 10 ml 10% SDS, 0.35 ml 2-mercaptoethanol, and 36.5 ml nanopure water. The membrane was placed in a hybridization oven at 60 ^{o}C, with agitation for 45 minutes. The easing buffer was poured off, and the membrane was washed 4-5 times in 1X TTBS for 10-15 minutes each over the course of an hour. A 2 hour blocking period was used before applying another primary antibody.

2.9 RNA isolation

Prior to removing medium from wells, 600-800 µl of conditioned medium was collected from each well and frozen at -80^{o}C for later progesterone quantification. Residual medium was aspirated from each well of cells. Trizol (800 µl) was added to each well and incubated 10 minutes at room temperature to lyse cells, and lysates were transferred to microfuge tubes and stored at -80^{o}C until use. All the following spins were at 15,000 g in an Eppendorf refrigerated microfuge. Directzol spin columns, RNA wash buffer and RNA prewash buffer were used from the Zymo Research Directzol kit. After

thawing and equilibrating to room temperature, an equal volume of 95-100% ETOH was added to tubes containing the Trizol lysates and vortexed. Samples were loaded into a spin column and centrifuged for 1 minute. The flow-through was discarded. Each column was placed to a new tube and 400 µl of RNA wash buffer was added into each column and centrifuged for 1 minute. The flow-through was discarded. DNase cocktail (80 µl) was added into each column and incubated 15-20 min at room temperature. The DNase cocktail contained 6.25% DNase (from Zymo Research Directzol kit), 1X DNase reaction buffer (from Zymo Research Directzol kit), 3.75% kit water, and 80% RNA wash buffer. All columns were centrifuged for 30 seconds followed by addition of 400 µl RNA prewash buffer and centrifugation for 1 minute. The flow-through was discarded. The RNA prewash buffer was added and then centrifuged again, and the flow-through was discarded. RNA wash buffer (700 µl) was added to each column, centrifuged for 1 minute, and the flow-through was discarded. Columns were centrifuged for another 2 minutes in order to dry the columns. Each column was transferred to a new tube. RNase/DNase-free kit water (30 µl) was added to columns, and incubated at room temperature for 5 minutes. Columns with tubes were centrifuged for 2 minutes to elute RNA, and then kept on ice for use or stored at -80 ^{o}C. RNA was transferred into new tubes. Quantification of RNA was performed at 260 nm using a Biophotometer (Eppendorf). The dilutions were made for cDNA synthesis, and then stored at -80^{o}C.

2.10 cDNA synthesis

The cDNA synthesis reaction consisted of 15 µl of RNA, 4 µl of 5X iScript reaction mix, and 1 µl of iScript Reverse Transcriptase enzyme (Bio-Rad iScript cDNA synthesis kit). After assembly, reactions were placed in the room temperature for 2 minutes. cDNA synthesis was carried out in a thermal cycler (Effendorf, Hauppauge, NY). The cycle consisted of 25 ^{o}C for 5 minutes, 42 ^{o}C for 30 minutes, 85 ^{o}C for 5 minutes, and a 4 ^{o}C hold. After cDNA synthesis, each sample of the cDNA was diluted with DNase/RNase-free water to 10 ng/µl when possible. In some cases cDNA was diluted to 3-5 ng/µl. The cDNA was stored at -20^{o}C and later used for real time PCR.

2.11 Real time PCR

Quantification of hTBP (human TATA-box binding protein, an internal control), hSTARD1, hSTARD4, and hSTARD6 was performed by real-time PCR using the method of Pfaffl(Pfaffl 2001). The PCR primers for hTBP yielded an 87-bp amplicon and were derived from GenBank accession no. NM_003194.3. The upstream primer was 5'-CACGGCACTGATTTTCAGTTC-3' and the downstream primer was 5'-TCTTGCTGCCAGTCTGGACT-3'. The PCR primers for hSTARD1 (157-bp amplicon) were upstream 5'-TACGTGGCTACTCAGCATCG-3' and downstream 5'-ACAGCAGGCTGGTCTTCAAC-3'. The PCR primers for hSTARD4 (135-bp amplicon) were upstream 5'-CAAAGCCCAAGGTGTTATAGATGAC-3' and downstream 5'-ACAGCAATTCTCTTCAAAGTTCTCC-3'. The hSTARD6 primers

(203-bp amplicon) were upstream 5'-TTCATATGTCATACCATTACACAAAG-3' and downstream 5'-CTCATTTCTGTCTGGACAAACATCAC-3'. All primers were obtained from InVitrogen/Life Technologies.

cDNA samples were amplified in 2-3 well replicates (or more as needed) and a water negative control was included in each PCR run. Each PCR 20 µl reaction was composed of 0.2-1.0 ng/µl (according to different patients) cDNA, 1X SSoAdvanced SYBR Green Supermix, 312.5 nM (for hTBP, hSTARD1 and hSTARD6) or 600 nM (for hSTARD4) of upstream primer, and the same amount of downstream primer. The real-time PCR was performed in iCycler (Bio-Rad, Hercules, CA) with the initial denaturation, 1X, 95^{o}C for 1.5 min, followed by 40 cycles (for hTBP, hSTARD1 and hSTARD4) or 45 cycles (for hSTARD6) of denaturation for 15 seconds, 95^{o}C, annealing for 30 seconds, 60^{o}C (for hSTARD1 and hSTARD6), or 62^{o}C (for hTBP and hSTARD4), elongation for 30 seconds, 72^{o}C, followed by 10 min final extension at 72^{o}C, and a melt curve using 80 cycles of 0.5^{o}C increments starting at 60^{o}C. A single product was confirmed by a single melt curve peak. The amplicons of non-SYBR green PCR reactions were previously sequenced by the lab to confirm their identities.

2.12 COS-1 cell culture

COS-1 cells were maintained in complete COS-1 medium in 10-cm dishes, and the cells were cultured at 37 ^{o}C with 5% CO_2 in the incubator. Complete medium (100 ml) for COS-1 cells contained 88 ml of DMEM, 1X AMAB, 1X non-essential amino acids

(NEAA), and 10 ml of new born calf serum (NBCS). When the cells were confluent they were passaged by standard technique using Trypsin-EDTA solution followed by addition of complete medium and pelleted. For experiments, cells were resuspended in complete medium and seeded into 6-well plates containing a sterile coverslip and 2 ml of complete medium. One 10-cm plate of cells was used to seed one 6-well plate and resulted in cells being approximately 50-80% confluent on the next day. The cells were cultured in the incubator.

2.13 Plasmid transfection into COS-1 cells for confocal staining and imaging

The pSTARD4 and pSTARD6 plasmids which were from Origene (Rockville, MD) contained a human full-length cDNA sequence and an additional Myc-DDK (Flag) tag sequence which is added at the C-terminus of the protein. Plasmids were purified from bacteria using appropriate antibiotic selection and a QiagenMaxiprep kit.

When the COS-1 cells were more than 50% confluent, they were transfected. Individual plates of cells were transfected with pcDNA3.1 (empty expression vector), which was from InVitrogen/Life Technologies, pSTARD6, or pSTARD4. In some experiments, a plate of cells that received no transfection was included. The cells were rinsed by replacing media with 2 ml of serum-free antibiotic-free DMEM media per well. The transfection mix for each well was DMEM/NEAA media containing 1 or 2 µg of pSTARD1 or D6 plasmid or pcDNA3.1 plasmid, and 8 µl of Lipofectamine per ml of media. The plates were incubated at 37 ^{o}C with 5% CO_2 for 5-6 hours. The transfection

mix was removed and complete medium (2 ml) was added to each well. The plates were incubated for 18 hours for recovery and plasmid expression, and then the cells were ready fixed. The pSTARD1 and the F2 plasmids were gifts from Dr. Himangshu Bose (Mercer University, Savannah, GA).

Cells were fixed as follows. Media were aspirated off, and 2 ml of Phosphate Buffered Saline (PBS) was added to each well of the plates. PBS was removed, and 1.5 ml 2% paraformaldehyde was added in each well. The cells were incubated in room temperature for 15 minutes. The paraformaldehyde was removed, and 2 ml of PBS was added. After 5 minutes the PBS was removed and another 2 ml of PBS was added. The edges of the plates were sealed with parafilm, and the plates were store at 4 ^{o}C in the fridge.

2.14 COS-1 F2 steroid assay to evaluate the steroidogenic potential of hSTARD6

To determine if human STARD6 had the potential to facilitate de novo steroidogenesis, the COS-1 F2 assay was used. The F2 and human STARD1 plasmids were a generous gift of Himangshu Bose (Mercer University). Several 6-well plates (Plates I to V) of COS-1 cells were set up for this assay using the same plating procedure as above except without coverslips (Table 2.1). Plate V was not transfected and received media changes only. Plates I-IV received the F2 plasmid (1 ug/well) which codes for the 3 components of the P450scc complex needed for de novo steroid synthesis. Plates I-IV also received a renilla luciferase (ptk-RL-luc) plasmid (10 ng/well) which was used for

assessing transfection efficiency. The plates received 1 µg of the following plasmids: Plate I, pSTARD1 (positive control), II, pSTARD6 (experimental), Plates III and IV, pcDNA3.1 (empty expression vector). The transfection mix was made with the indicated amount of plasmids and 8 µl Lipofectamine in DMEM/NEAA media. Cells were incubated with the transfection mix for 5.5-6 h and then the medium was replaced with 2 ml complete COS-1 medium and cells were allowed an 18 h recovery/expression period. At the end of the recovery period, medium was changed to 1 ml complete medium. Plates I-IV were treated with vehicle or 0.25 mM 8Br-cAMP (half the wells for each plate received one treatment). Plate IV also received 5 µM 22(*R*)-hydroxy-cholesterol (22R-OH-Chol) as a positive control. 22R-OH-Chol is able to directly permeate the mitochondrion can be converted to pregnenolone by P450scc complex without the need for a STARD molecule. Cell treatments were for 24 h.

At the end of the treatment time, 0.6 ml of medium was collected from each well and media from like wells pooled. Residual medium was removed and cells were rinsed with PBS. One of the three wells of cells was lysed for renilla luciferase assay by using Passive Lysis Buffer (Dual Luciferase Assay System, Promega), and the other two wells were lysed with WCE buffer to measure total protein and for later used in western blot. Renilla luciferase activity in cleared lysates was measured using a Turner luminometer and renilla luciferin substrate (Promega). Pregnenolone in the undiluted culture media was measured by ELISA (Alpco, Salem NH). Pregnenolone concentrations were normalized to protein content of wells or luciferase activity.

2.15 Staining cells for confocal imaging

The coverslips were moved into a new 6-well plate for staining. Cells were washed with 1.5 ml PBS per well for 5 to 10 minutes, three times. An aspirator was used to remove the liquid in the wells. Cells were incubated in 1 ml PBS/0.01 M glycine/0.1% Trition-X per well for 15 minutes, three times. Cells were incubated in 1 ml 5% BSA/PBS per well for 10 minutes. Cells were incubated in 1 ml 5% normal donkey serum (dissolved in 1% BSA/PBS) per well for 10 minutes. One ml primary antibody (dissolved in 1% BSA/PBS) was added in each well, and the plate was incubated at 37 ^{o}C for 1 h. The primary antibodies included STARD4 (2.5 μg/ml), STARD6 C-term (2.5 μg/ml), and DDK (Flag) tag (5 μg/ml) for incubation. Cells were washed with 1.5 ml 1% BSA/PBS per well for 15 minutes, twice. Cells were incubated in 1 ml 5% donkey normal serum (which was dissolved in 1% BSA/PBS) per well for 10 minutes. The plate was covered with foil for all subsequent steps. One ml secondary antibody (dissolved in 1% BSA/PBS) was added in each well, and the plate was incubated at 37^{o}C for 1 h, and the secondary antibody included donkey anti-rabbit Cyanine 3 (DAR-Cy3, Cat. # 711-165-152, Lot # 108392) (15 μg/ml) and donkey anti-mouse Cyanine 3 (DAM-Cy3, Cat.# 715-165-112, Lot # 107821) (15 μg/ml) in the experiments. Both of them were obtained from Jackson ImmunoResearch (West Grove, PA). Wells were washed with 1.5 ml 1%BSA/PBS for 15 minutes, three times. PBS (1.5 ml) was added to wash each well for 15 minutes. Nuclei were stained with 1 ml of 5 μg/ml

4',6-diamidino-2-phenylindole (DAPI) per well for 15 minutes. Cells were washed in 1.5 ml PBS per well for 15 minutes, twice. One drop of 1,4-diazabicyclo [2.2.2] octane (DABCO) solution was dropped on the middle of the slide, and slowly pulling the coverslip down to the slide to avoid bubbles. DABCO solution (100 ml) was made of 1 g of DABCO powder, 25 ml PBS, and 75 ml glycerol.

2.16 Confocal imaging

A LSM 510 META ZEISS confocal microscope (Carl Zeiss Micro Imaging Inc.) was used to image. The excitation/emission spectrum for DAPI complexes was 358 nm /461 nm. The excitation/emission spectrum for Cy3 complexes was 550 nm/570 nm.

2.17 Statistical analyses

GraphPad Prism version 3.02 for Windows (GraphPad Software, San Diego, CA) was used for statistical analysis for at least three independent sets of samples of human granulosa cells for all real-time PCR data. The mean and standard error of the mean were calculated for all groups. Data was analyzed by ANOVA followed by Tukey's post-hoc test to determine if there were differences in mRNA expression between control conditions of with the appropriate vehicle treatment. For studies with LPDS pretreatment, the values were compared with those of FCS pretreated vehicle controls. Paired T-tests were used to determine if there were significant changes when only two groups were analyzed. Differences were determined to be significant if the P-value was ≤ 0.05.

Table 2.1 information for plasmid transfections and treatments of COS-1 F2 steroid assay

plate number	I	II	III	IV	V
number of wells with cells	6	6	6	6	3
F2 plasmid	Y	Y	Y	Y	N
renilla luciferase plasmid	Y	Y	Y	Y	N
hSTARD1 plasmid	Y	N	N	N	N
hSTARD6 plasmid	N	Y	N	N	N
pcDNA3.1 plasmid	N	N	Y	Y	N
treated with 5 μM 22R-OH-Chol	N	N	N	Y	N
water control	Y	Y	Y	Y	Y
treated with 0.25mM 8Br-cAMP	Y	Y	Y	Y	N

Chapter III: Result

3.1 Comparison of 8Br-cAMP and phorbol ester effects on STARD1, STARD4, and STARD6 mRNA levels in human luteinized granulosa cells

In order to compare the effects of cAMP analog and phorbol ester on STARD1, STARD4, and STARD6 mRNA levels, cultured human luteinized granulosa cells were treated with 8Br-cAMP (0.25 mM and 1 mM) or low dose PMA (1 nM and 20 nM) for 6 or 24 h. STARD1 mRNA was significantly increased by 0.25 mM 8Br-cAMP at 24 h and increased by 1 mM 8Br-cAMP at both 6 and 24 h treatment (Figure 3.1). STARD1 mRNA was significantly increased by 20 nM PMA at both 6 and 24 h treatment. PMA increases in STARD1 mRNA levels were lower than those observed with cAMP. STARD4 mRNA was significantly increased by 0.25 mM 8Br-cAMP at 24 h and increased by 1 mM 8Br-cAMP at both 6 and 24 h treatment (Figure 3.2). STARD4 mRNA was significantly increased by 20 nM PMA at both 6 and 24 h treatment. PMA increases in STAR mRNA levels were similar to those observed with cAMP. STARD6 mRNA levels were not significantly altered by treatment with cAMP analog or PMA (Figure 3.3)

3.2 Effects of blocking cholesterol utilization with the P450scc inhibitor Aminoglutethimide on STARD1, STARD4, and STARD6 mRNA levels

In human luteinized granulosa cells, under serum-free conditions, intracellular cholesterol is depleted by agonists that stimulate progesterone production which utilizes P450scc. We tested the effect of blocking P450scc enzyme activity with Aminoglutethimide, to block the utilization of cholesterol for de novo steroidogenesis. In other experiments in our laboratory we verified that that progesterone levels were decreased by ~50% with 100 μM AG (data not shown). The increase of STARD1 mRNA level by either 8Br-cAMP (1 mM) or PMA (20 nM) with the 24 hour treatment was not altered Aminoglutethimide treatment (Figure 3.4). STARD4 showed a different response to Aminoglutethimide. The increase in STARD4 mRNA level by 8Br-cAMP with 24 h treatment was significantly reduced by Aminoglutethimide (Figure 3.5). There was no effect of Aminoglutethimide on PMA-stimulated STARD4 mRNA. STARD6 mRNA levels were not affected by Aminoglutethimide at 24 h treatment (Figure 3.6). However, the fold-change in STARD6 mRNA was significantly reduced by Aminoglutethimide in cells treated with PMA (Table 3.1).

3.3 Effects of cholesterol depletion and supplementation on STARD1, STARD4, and STARD6 mRNA levels

In order to test the effect of cellular cholesterol depletion on STARD1, STARD4, STARD6 mRNA cells were precultured under wither normal conditions (10% FCS) or

lipoprotein deficient conditions (10% LPDS) for the initial 4 days of culture. To further test the effects of sterol on the responses of these mRNAs, some samples were supplemented with exogenous hLDL during the 24-h treatment period with 8Br-cAMP (1 mM) and PMA (20 nM). The STARD1 mRNA level was significantly enhanced by 8Br-cAMP and PMA with 24 h treatment under either preculture condition (Figure 3.7). The addition of 50 μg/ml hLDL did not affect the cAMP-stimulated response of STARD1 mRNA in either preculture condition. PMA stimulated STARD1 mRNA to a similar extent with both preculture conditions. With LPDS pretreatment conditions, the addition of hLDL with PMA reduced STARD1 mRNA levels. In addition, the fold-change in STARD1 mRNA was significantly reduced by hLDL in cells with normal preculture conditions that were treated with PMA (Table 3.2). In other words, the STARD1 mRNA response to PMA was altered by the addition of exogenous hLDL under either preculture condition.

The STARD4 mRNA level was significantly enhanced by 8Br-cAMP and PMA with 24 h treatment under either preculture condition (Figure 3.8). The addition of 50 μg/ml hLDL reduced the cAMP-stimulated response of STARD4 mRNA in either preculture condition. PMA stimulated STARD1 mRNA to a similar extent with both preculture conditions. Regardless of preculture conditions, the addition of hLDL impaired the ability of PMA to stimulate STARD4 mRNA levels, as the PMA responses were not significant with hLDL. In addition, the fold-change in STARD4 mRNA in response to 8Br-cAMP

was significantly reduced by co-addition of hLDL under either pretreatment condition, whereas it was not affected with PMA treatments (Table 3.3).

There was no significant effect of cholesterol depletion (LPDS pretreatment) or cholesterol supplementation during treatment on STARD6 mRNA levels at 24 h (Figure 3.9).

3.4 The effects of 8Br-cAMP and PMA on STARD1, STARD4, STARD6, and CYP11A1 protein levels in human luteinized granulosa cells

Although we attempted to quantify the western blots densitometrically, the quality of some blots did not allow this and thus individual western blots are presented below to allow one to evaluate the range of responses between patients. Actin was used as a control to evaluate protein loading or transfer.

The western blots in Figure 3.10 with patient #1376 were performed by others and included to show the effects of the two different concentrations of 8Br-cAMP (0.25, 1 mM) and PMA (1, 20 nM) at 24 h treatment. 8Br-cAMP at either concentration increased the levels of both STARD1 protein and phosphorylated STARD1. PMA also increased STARD1 protein and phosphorylated STARD1, however in patient #1376 at 24 h treatment 20 nM PMA did not show increased STARD1 protein, yet a small amount of phosphorylated STARD1 was present (Figure 3.10C). Other patients have shown increased STARD1 and phosphorylated STARD1 with 20 nM treatment (data not shown).

When accounting for actin levels, in patient #1376 STARD4 and STARD6 protein levels showed no obvious regulation by treatments at 24 h. In this patient both 8Br-cAMP and PMA treatments led to a decrease in CYP11A1 level.

3.5 Effects of blocking cholesterol utilization with the P450scc inhibitor Aminoglutethimide on target protein levels

Figures 3.11 to 3.15 cells represent cells treated with 8Br-cAMP (1 mM) or PMA (20 nM) with either vehicle (DMSO) or Aminoglutethimide (100 μM). Both 8Br-cAMP and PMA increased the protein levels of STARD1 for the Patient #1578, #1581, and #1619, with PMA giving a lower response that than that of 8Br-cAMP. In patient #1624 blots, 8Br-cAMP increased STARD1 protein and in #1559 the data is unclear due to blot quality. In patients #1581 and 1619 Aminoglutethimide treatment appeared to modestly decrease the STARD1 protein levels, whereas for patients # 1578 and 1624 this did not occur.

In the absence of Aminoglutethimide, 8Br-cAMP increased the levels of phosphorylated STARD1 for the patients # 1578, 1581 and 1619, and PMA increased it in patient #1578. In the presence of Aminoglutethimide phosphorylated STARD1 was lower with 8Br-cAMP in patient #1581, and not # 1578 nor 1619.

STARD4 protein levels for patients # 1578, 1581, 1619, 1624, and 1559 did not show any obvious changes with 8Br-cAMP or PMA (20 nM) alone nor with Aminoglutethimide treatment.

STARD6 protein levels for patients # 1578, 1581, 1619, 1624, and 1559 did not show any obvious changes with 8Br-cAMP or PMA (20 nM) alone nor with Aminoglutethimide treatment.

Data for SREBP-2 protein was collected for patients # 1578, 1581, and 1644 and did not reveal any consistent trends with treatments.

CYP11A1 protein showed a variety of responses to treatment depending on the patient. In patient # 1578, 1619, 1559 CYP11A1 protein was unchanged by 8Br-cAMP, in # 1581 and 1624 it was decreased with cAMP analog, in # 1578 and 1644 it was decreased with PMA, and it was unchanged in # 1581, 1619 and 1559.

3.6 Effects of cholesterol depletion and supplementation on target protein levels

Figures 3.15 to 3.17 represent human granulosa cells that were either precultured under normal conditions (FCS) or lipoprotein deficient (LPDS) conditions for the initial 4 days of culture prior to treatment in serum-free medium with 8Br-cAMP (1 mM) or PMA (20 nM) with the addition of vehicle or hLDL (50 μg/ml). Under normal preculture conditions, subsequent 24 h treatment with 8Br-cAMP or PMA increased the protein levels of STARD1 for the patients # 1641 and 1644, but as mentioned above #1559 blot quality in this region was too poor to evaluate. With the LPDS preculture conditions, patient # 1559 had lower overall STARD1 protein with an increase evident with 8Br-cAMP compared to vehicle under the same conditions. Blot quality for patient # 1641 with LPDS preculture was poor, however an increase in STARD1 protein was still

evident with the cAMP treatment (no hLDL). In patient # 1644 with LPDS precultureSTARD1 protein was lower overall when considering the actin yet there was an increase still evident with 8Br-cAMP and PMA. Taken together there was a trend to have reduced level of STARD1 protein in cells with 24 h treatment in those precultured in LPDS. Phosphorylated STARD1 proteins followed the same general trends as above with consistent increases with 8Br-cAMP treatment and in some cases with PMA under normal preculture conditions.

The addition of hLDL to cells with normal pretreatment conditions showed no difference in STARD1 protein compared to non-LDL treatment in patient # 1644 but reduced the PMA-induction of STARD1 in patient # 1641. The blot quality for the LPDS preculture for patient 1641 was poor in this region and not suitable to draw conclusions from pertaining to hLDL treatment. In patient #1644, hLDL had no effect on STARD1 expression under LPDS precultured conditions.

For patients # 1559, 1641, and 1644 no discernible differences in the levels of STARD4 or STARD6 were observed (in good quality blot regions) between the normal and lipoprotein preculture conditions or with different treatments.

For patients # 1559, 1641, and 1644 lipoprotein deficient preculture conditions reduced the overall levels of CYP11A1 protein for all treatment conditions. No differences between 8Br-cAMP or PMA with or without hLDL were noted.

Due to the variable quality of these western blots comparing the normal and lipoprotein deficient preculture conditions +/- hLDL further experiments will be performed by others in the lab to provide more quantifiable blots.

3.7 The effects of 8Br-cAMP and PMA on STARD1 and phosphorylated STARD1 protein levels in human luteinized granulosa cells with 6 h treatment

In initial studies of STARD1 in human luteinized granulosa, our lab evaluated concentration and treatment time for 8Br-cAMP and PMA and the most consistent stimulation of STARD1 occurred at 24 h and thus most studies were performed with this treatment time. Figure 3.18 shows levels of STARD1 and phosphorylated STARD1 at 6 h treatment in human luteinized granulosa cells precultured under normal conditions or lipoprotein deficient conditions. STARD1 protein was stimulated to a similar extent with either preculture conditions and phosphorylated STARD1 tended to be increased to a greater extent with 8Br-cAMP or PMA treatments in lipoprotein deficient preculture conditions. The 6 h treatment with LPDS preculture conditions is representative of only 1 patient so far. Blots of STARD1 and phosphorylated STARD1 with normal preculture conditions has been repeated multiple times with several patients by others in the lab and showed fairly consistent stimulation by cAMP and PMA (data not shown).

3.8 Immunofluorescence microscopy of recombinant human STARD4 and STARD6 expressed in COS-1 cells

As a basis for future studies with human granulosa cells, COS-1 cells were utilized to for antibody testing and preliminary localization studies. COS-1 cells were transfected with expression plasmids containing the cDNAs for human STARD4 or STARD6 that would yield Flag-tagged proteins. The immunoreactivity for recombinant STARD4 protein in COS-1 cells was localized throughout the cytoplasm and nucleus with both the primary antibodies for STARD4 and the Flag-tag. In some cell nuclear staining was more predominant (Figure 3.19 and Figure 3.20). Most immunoreactivity for recombinant STARD6 proteins in COS-1 cells was localized in the cytoplasm with little evident signal in the nucleus with both the primary antibodies for STARD6 and the Flag-tag (Figure 3.21 and Figure 3.22).

3.9 STARD6 can facilitate *de novo* steroidogenesis in the COS-1 F2 assay

Using the COS-1 F2 assay, which involves transfecting the machinery for *de novo* steroidogenesis into non-steroidogenic COS-1 cell, both recombinant STARD1 and STARD6 have both shown to increase pregnenolone production to differing extents. To determine if STARD6 has the potential to increase *de novo* steroidogenesis, STARD6 was expressed along with the F2 plasmid and pregnenolone levels measured in the media. The data presented here is one experiment which was performed to replicate previous data in the lab.

Whole cell extracts were isolated from cells to verify protein expression.STARD1, STARD6 and CYP11A1 proteins were detected in the appropriate cells which meant all the plasmids were successfully transfected and expressed (Figure 3.25A). The vector only transfection (pcDNA3.1) showed a low concentration of pregnenolone in cells with or without 8Br-cAMP treatment (Figure 3.25B). The pregnenolone level increased 2.80 fold with vehicle and 4.37 fold with 8Br-cAMP treatment in the STARD6 transfected cells compared to the vector only control group. With STARD1 transfection (a positive control), the level increased 10.7 fold with vehicle and 12.0 fold with 8Br-cAMP. As a positive control for the P450scc complex activity, a group of the cells transfected with vector only was treated with 5 μM 22R-OH-cholesterol, a mitochondrial permeable form of cholesterol, and in these cells the pregnenolone concentration increased to 14.1 and 15.4 fold with or without 8Br-cAMP, respectively.

Table 3.1. The fold-change in STARD6 mRNA in response to cAMP or phorbol ester treatment in the presence of vehicle (-AG) or Aminoglutethimide (AG) at 24 h.

Treatment	Fold-response with cAMP or PMA		AG effect Significance
Br-cAMP	-AG 0.89 ± 0.14	+AG 1.12 ± 0.34	ns P= 0.41
PMA	0.85 ± 0.10	0.37 ± 0.10	P = 0.03

ns = not significant

Table 3.2. The fold-change in STARD1 mRNA in response to cAMP or phorbol ester treatment in the presence of vehicle (-LDL) or low density lipoprotein at 24 h, following normal or lipoprotein deficient preculture (Pretrt) conditions.

Treatment	FCS Pretrt		P	LPDS Pretrt		P
8Br-cAMP	-LDL 10.44±2.52	+LDL 10.09±3.48	ns	-LDL 11.43±2.64	+LDL 9.48±1.46	ns
PMA	5.29±1.27	2.67±0.52	0.003	7.89±1.85	2.96±1.15	ns 0.07

ns = not significant

Table 3.3. The fold-change in STARD4 mRNA in response to cAMP or phorbol ester treatment in the presence of vehicle (-LDL) or low density lipoprotein at 24 h, following normal or lipoprotein deficient preculture (Pretrt) conditions.

Treatment	FCS Pretrt		P	LPDS Pretrt		P
8Br-cAMP	-LDL 4.98±0.09	+LDL 2.92±0.60	0.04	-LDL 3.12±0.53	+LDL 1.65±0.54	0.05
PMA	5.10±0.87	5.85±1.00	ns 0.35	2.67±0.64	4.16±0.88	ns 0.12

ns = not significant

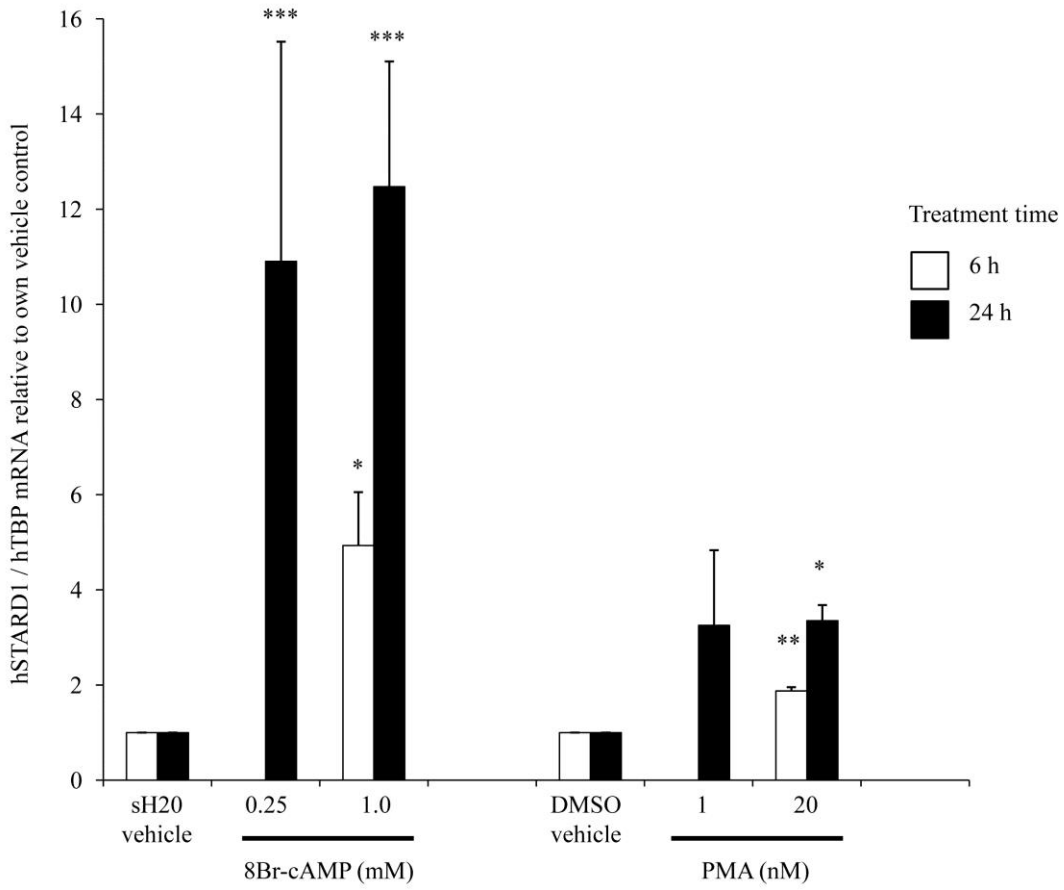

Figure 3.1. The effect of cyclic AMP analog (0.25 or 1 mM) or low dose phorbol ester (1 or 20 nM) treatment on STARD1 mRNA levels in human luteinized granulosa cells. Human luteinized granulosa cells were cultured for 4 days with 10% FCS prior to treatment in serum-free media for 6 or 24 h. Data are mean + SEM from n = 3-4 experiments per time point, each with a different patient. Data for sH20/8Br-cAMP treatments and DMSO/PMA treatments were analyzed separately. Six-hour data were analyzed by T-test, and 24-h hour data were analyzed by ANOVA and Tukey's post hoc test. *, **, and *** indicate there is a significant difference between the treatment and its vehicle control at the same time point at $P<0.05$, 0.01, and 0.001, respectively.

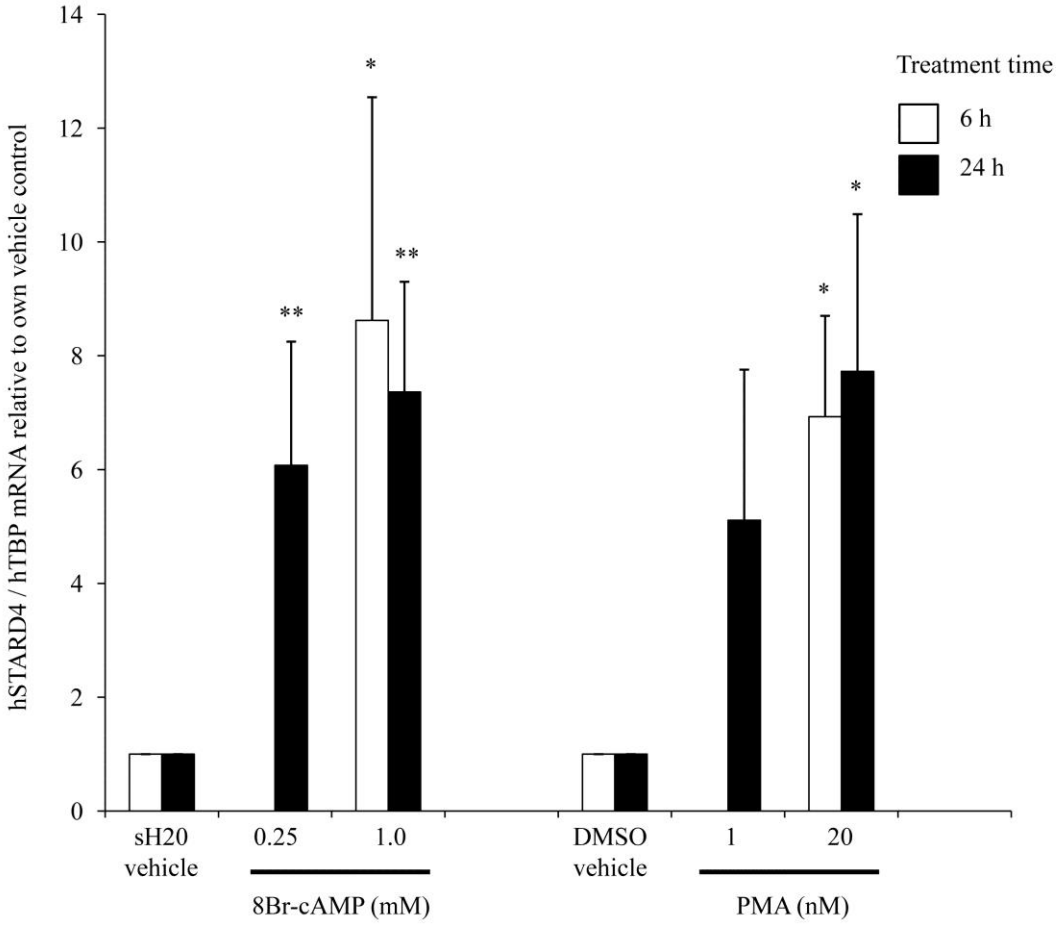

Figure 3.2. The effect of cyclic AMP analog (0.25 or 1 mM) or low dose phorbol ester (1 or 20 nM) treatment on STARD4 mRNA levels in human luteinized granulosa cells. Human luteinized granulosa cells were cultured for 4 days with 10% FCS prior to treatment in serum-free media for 6 or 24 h. Data are mean + SEM from n = 3-4 experiments per time point, each with a different patient. Data for sH20/8Br-cAMP treatments and DMSO/PMA treatments were analyzed separately. Six-hour data were analyzed by T-test, and 24-h hour data were analyzed by ANOVA and Tukey's post hoc test. * or ** indicate there is a significant difference between the treatment and its vehicle control at the same time point at $P<0.05$ and $P<0.01$, respectively.

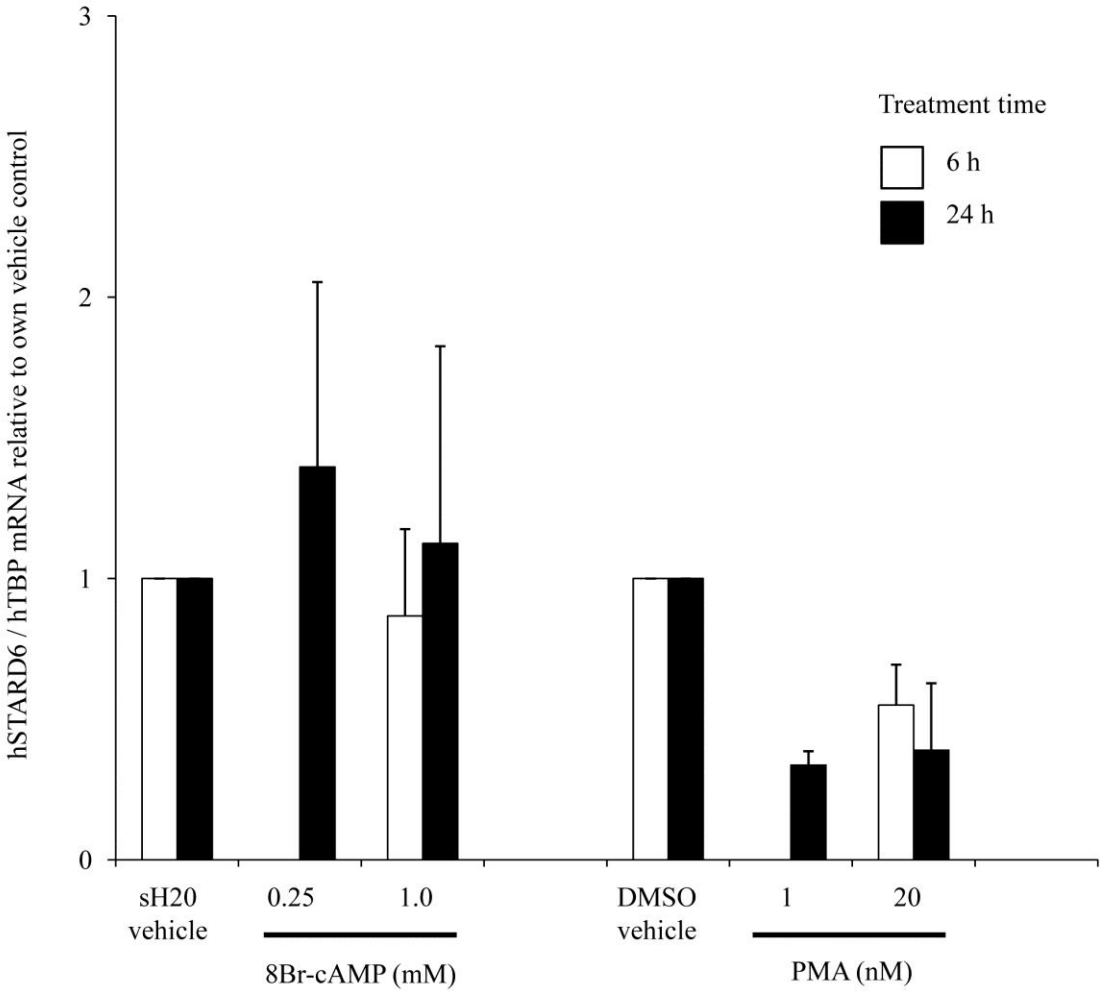

Figure 3.3. The effect of cyclic AMP analog (0.25 or 1 mM) or low dose phorbol ester (1 or 20 nM) treatment on STARD6 mRNA levels in human luteinized granulosa cells. Human luteinized granulosa cells were cultured for 4 days with 10% FCS prior to treatment in serum-free media for 6 or 24 h. Data are mean + SEM from n = 3-4 experiments per time point, each with a different patient. Data for sH20/8Br-cAMP treatments and DMSO/PMA treatments were analyzed separately. Six-hour data were analyzed by T-test, and 24-h hour data were analyzed by ANOVA and Tukey's post hoc test. There were no significant differences.

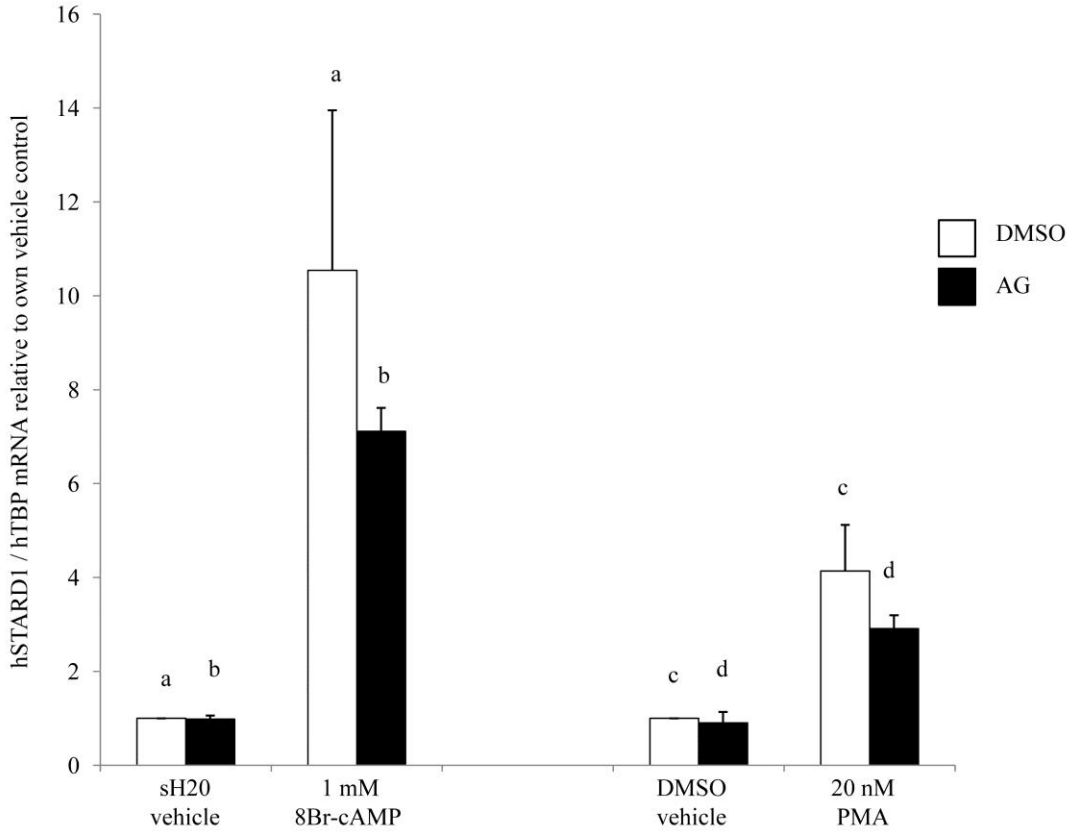

Figure 3.4.The effect of blocking cholesterol utilization with the P450scc inhibitor Aminoglutethimide (AG) on STARD1 mRNA levels. Human luteinized granulosa cells were cultured for 4 days with 10% FCS prior to treatment in serum-free media for 24 h with 8Br-cAMP or PMA in the presence of vehicle (DMSO) or P450scc inhibitor Aminoglutethimide (100 μM) to block cholesterol conversion to pregnenolone and thus prevent cellular depletion of cholesterol. Data represent mean + SEM of 3-4 experiments, each with 1 patient. Bars with the same letters are significantly different from each other by ANOVA and Tukey's post-hoc test, $P<0.05$. Only relevant are comparisons shown.

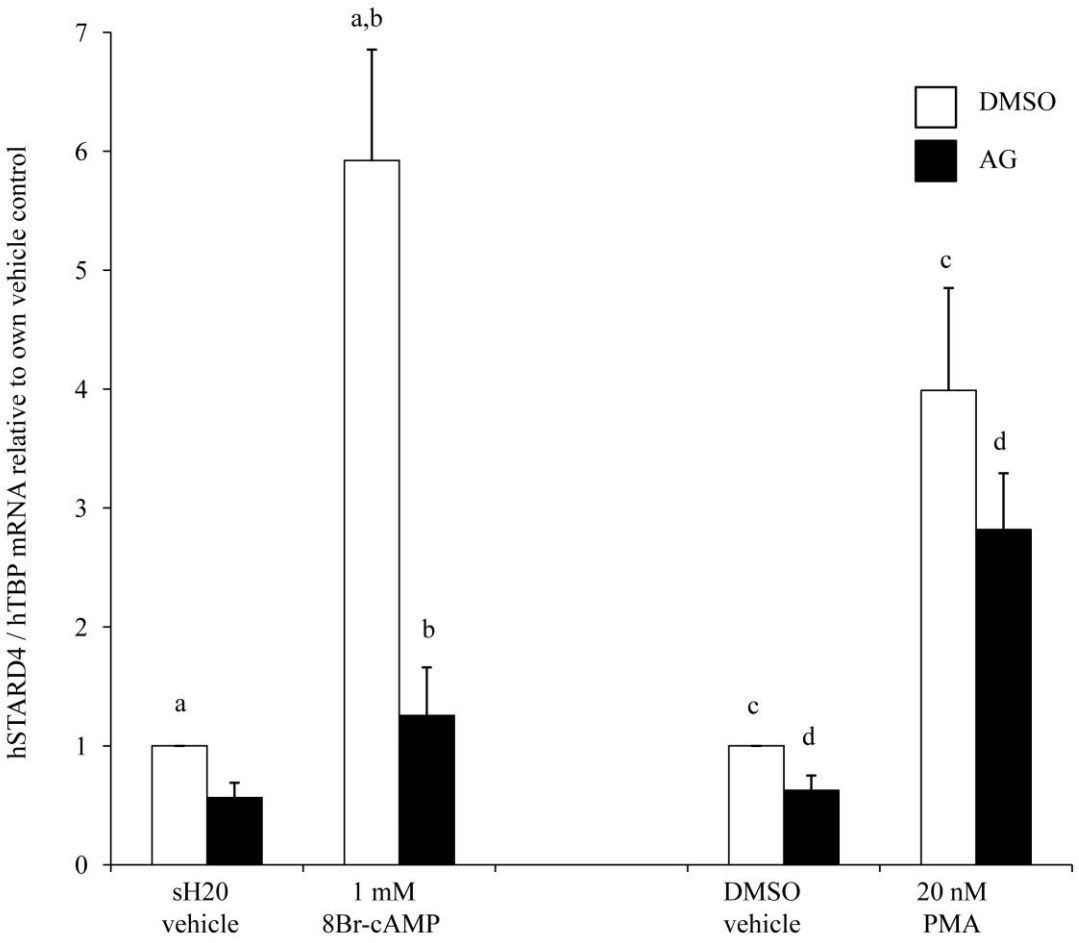

Figure 3.5.The effect of blocking cholesterol utilization with the P450scc inhibitor Aminoglutethimide (AG) on STARD4 mRNA levels. Human luteinized granulosa cells were cultured for 4 days with 10% FCS prior to treatment in serum-free media for 24 h with 8Br-cAMP or PMA in the presence of vehicle (DMSO) or P450scc inhibitor Aminoglutethimide (100 μM) to block cholesterol conversion to pregnenolone and thus prevent cellular depletion of cholesterol. Data represent mean + SEM of 3-4 experiments, each with 1 patient. Bars with the same letters are significantly different from each other by ANOVA and Tukey's post-hoc test, $P<0.05$. Only relevant are comparisons shown.

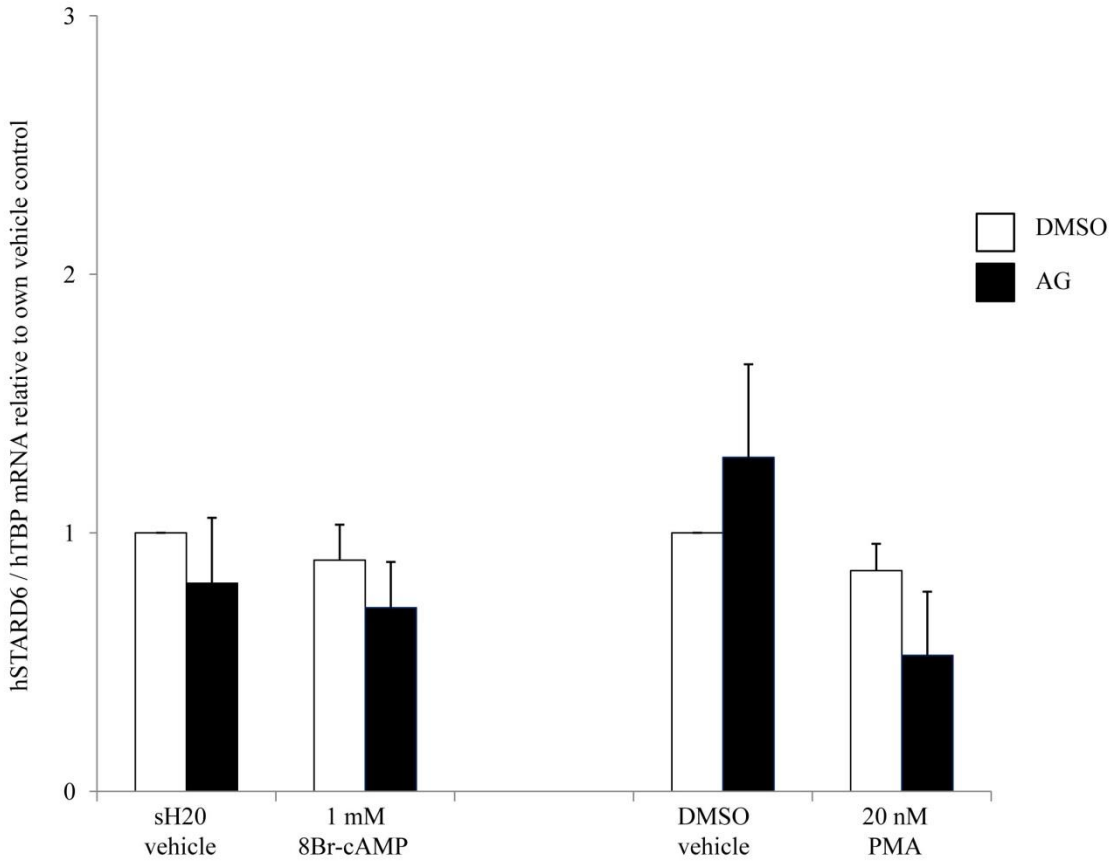

Figure 3.6.The effect of blocking cholesterol utilization with the P450scc inhibitor Aminoglutethimide (AG) on STARD6 mRNA levels. Human luteinized granulosa cells were cultured for 4 days with 10% FCS prior to treatment in serum-free media for 24 h with 8Br-cAMP or PMA in the presence of vehicle (DMSO) or P450scc inhibitor Aminoglutethimide (100 μM) to block cholesterol conversion to pregnenolone and thus prevent cellular depletion of cholesterol. Data represent mean + SEM of 3-4 experiments, each with 1 patient. There were no significant differences.

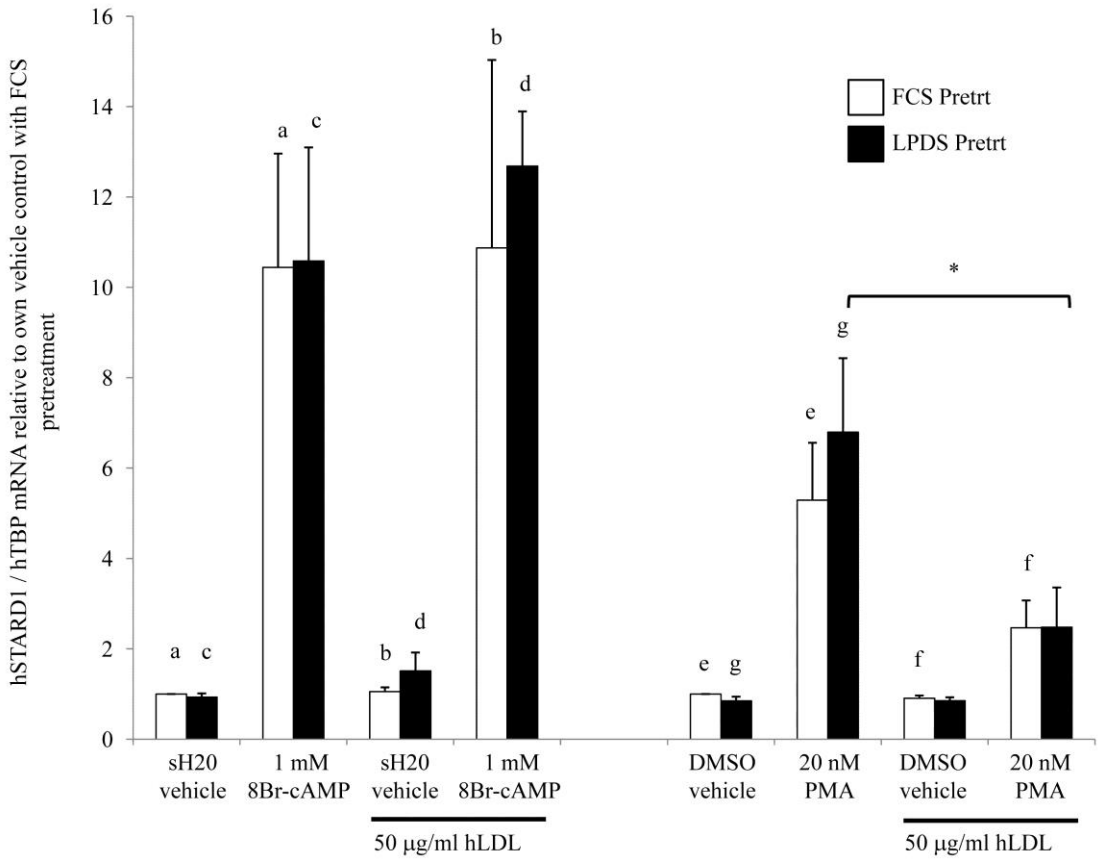

Figure 3.7. Comparison of pre-culturing human luteinized granulosa cells in fetal calf serum (FCS) or lipoprotein deficient serum (LPDS), followed by treatment in serum-free medium with cAMP analog or phorbol ester in the presence or absence of exogenous human low density lipoprotein (hLDL) on STARD1 mRNA. Cells were initially cultured for 4 days under normal conditions (10% FCS) or lipoprotein deficient serum (10% LPDS) and then treated in serum-free medium for 24 h with the indicated agents. Data are mean + SEM from n = 4 experiments, each with a different patient. Data for sH20/8Br-cAMP treatments and DMSO/PMA treatments were analyzed separately. Data were analyzed by ANOVA followed by Tukey's post hoc test. Bars with common letters are significantly different with $P < 0.05$. * indicates a significant difference between the two treatments, $P < 0.05$. Only relevant comparisons are shown.

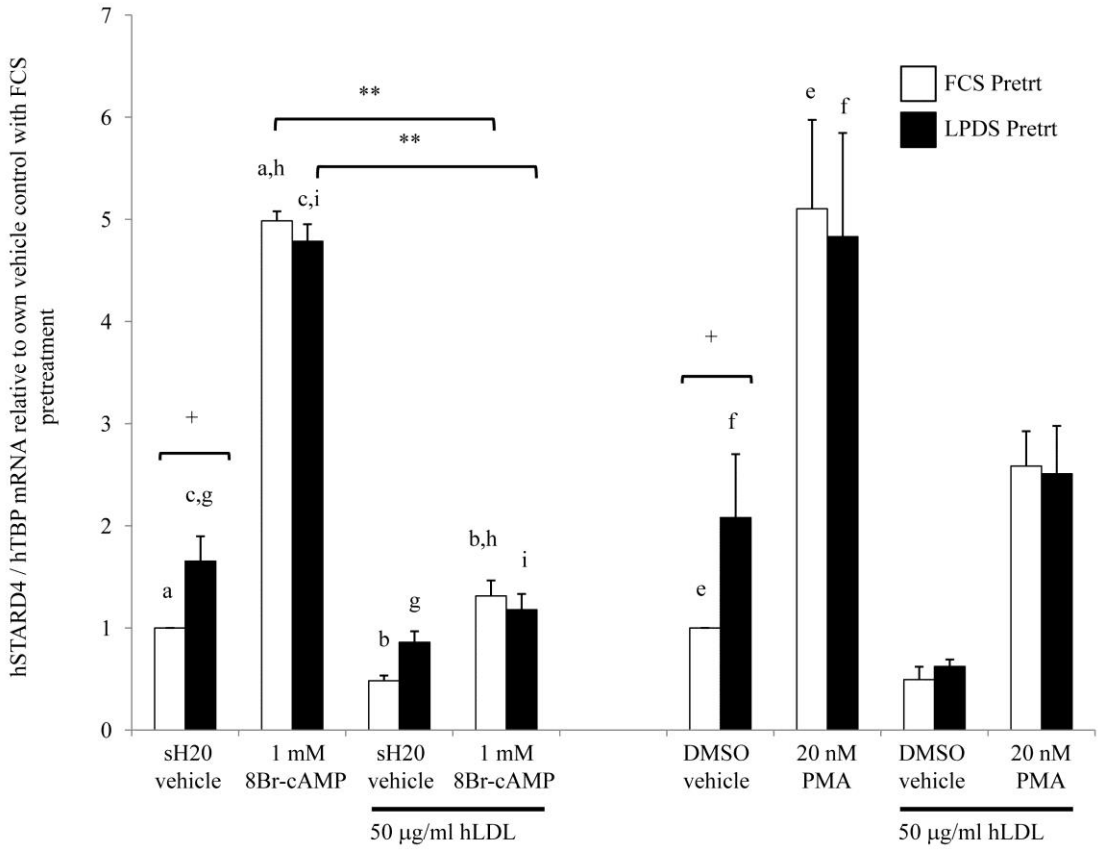

Figure 3.8. Comparison of pre-culturing human luteinized granulosa cells in fetal calf serum (FCS) or lipoprotein deficient serum (LPDS), followed by treatment in serum-free medium with cAMP analog or phorbol ester in the presence or absence of exogenous human low density lipoprotein on STARD4 mRNA. Cells were initially cultured for 4 days under normal conditions (10% FCS) or lipoprotein deficient serum (10% LPDS) and then treated in serum-free medium for 24 h with the indicated agents. Data are mean + SEM from n = 4 experiments, each with a different patient. Data for sH20/8Br-cAMP treatments and DMSO/PMA treatments were analyzed separately. Data were analyzed by ANOVA followed by Tukey's post hoc test. Bars with common letters are significantly different with $P < 0.05$. ** indicates that the two treatments were different, $P<0.001$. + indicates that the two treatments were different by T-test ($P<0.05$) and shows basal STARD4 mRNA levels increased with LPDS pretreatment (which reduces intracellular cholesterol stores). Only relevant comparisons are shown.

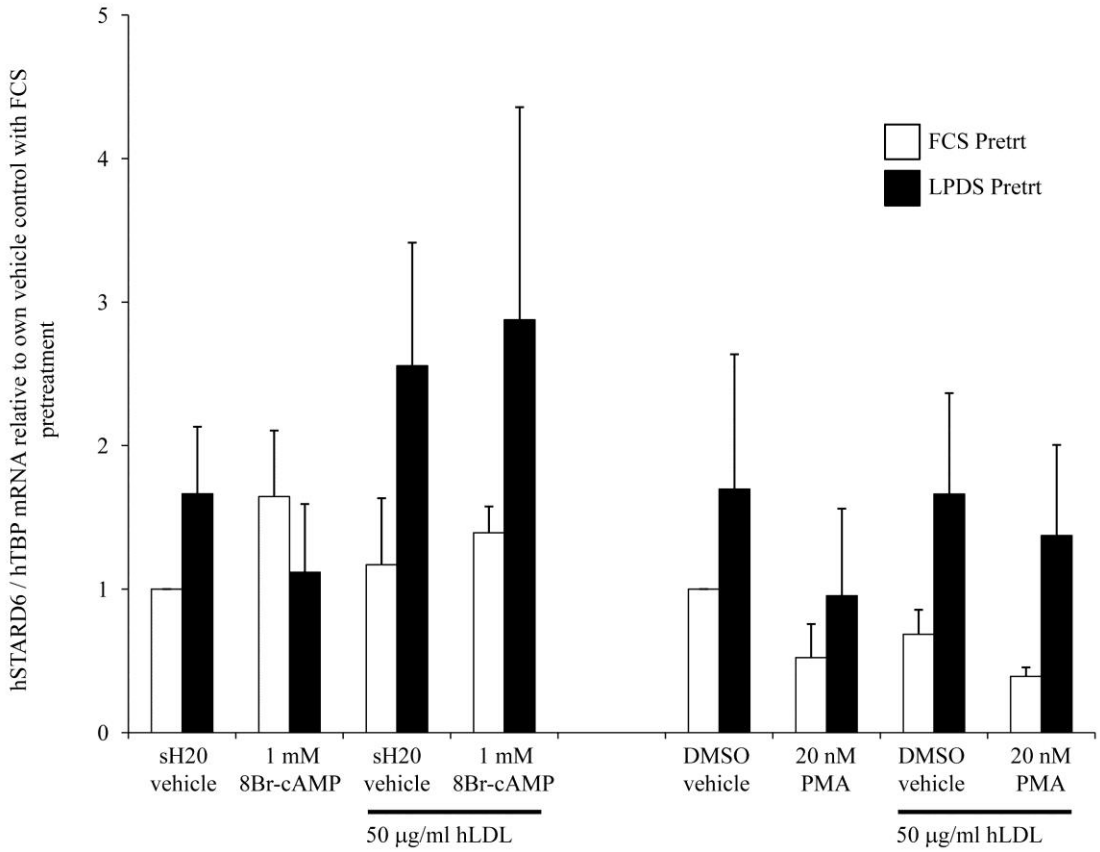

Figure 3.9. Comparison of pre-culturing human luteinized granulosa cells in fetal calf serum (FCS) or lipoprotein deficient serum (LPDS), followed by treatment in serum-free medium with cAMP analog or phorbol ester in the presence or absence of exogenous human low density lipoprotein on STARD6 mRNA. Cells were initially cultured for 4 days under normal conditions (10% FCS) or lipoprotein deficient serum (10% LPDS) and then treated in serum-free medium for 24 h with the indicated agents. Data are mean + SEM from n = 4 experiments, each with a different patient. Data for sH20/8Br-cAMP treatments and DMSO/PMA treatments were analyzed separately. Data were analyzed by ANOVA followed by Tukey's post hoc test. There were no significant differences.

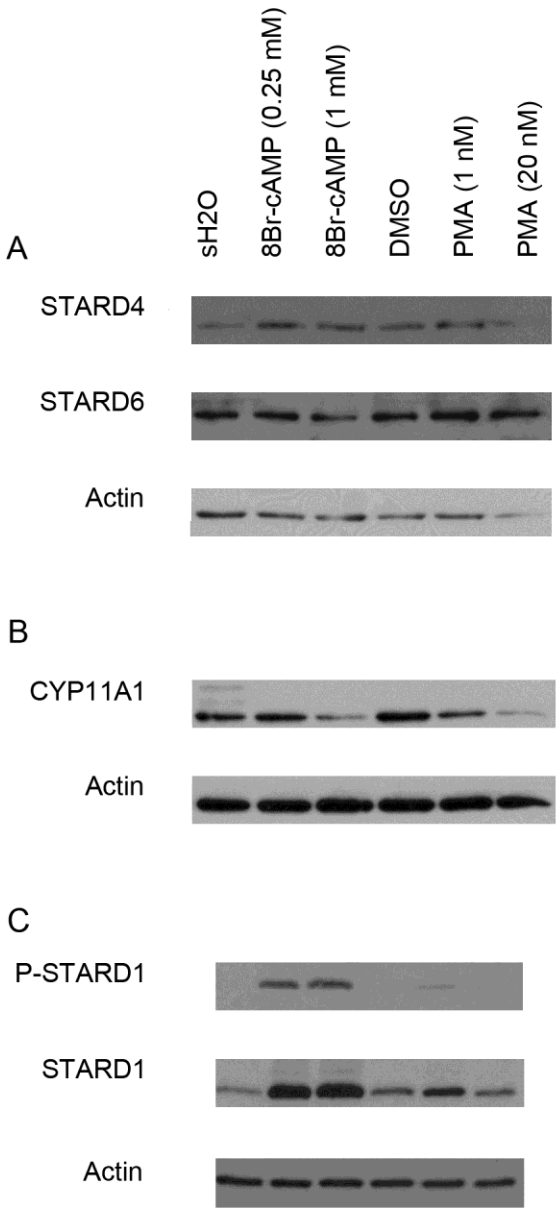

Figure 3.10. Western blot analyses of STARD1, phosphorylated STARD1, STARD4, STARD6, CYP11A1, and actin proteins. The effects of cAMP and PMA on protein levels at 24-h treatment. Human luteinized granulosa cells from Patient #1376 were cultured for 4 days with 10% FCS prior to treatment with 8Br-cAMP (0.25 mM and 1 mM) and PMA (1 nM and 20 nM) in serum-free media for 24 h. Whole cellular protein extracts were separated by SDS-polyacrylamide gel electrophoresis using 12% gels and transferred to PVDF membranes and probed with antibodies for the indicated proteins.(A) Membrane 1 (B) Membrane 2 (C) Membrane 3. Membrane 3 data was provided by Dr. Steven King of Doug Stocco's laboratory (Texas Tech University, Lubbock, TX). This

experiment has been performed with at least three different patients and although there is patient to patient variation, it is consistent with the overall trends with the exception that 20 nM PMA was usually stimulatory to STARD1 in most patients.

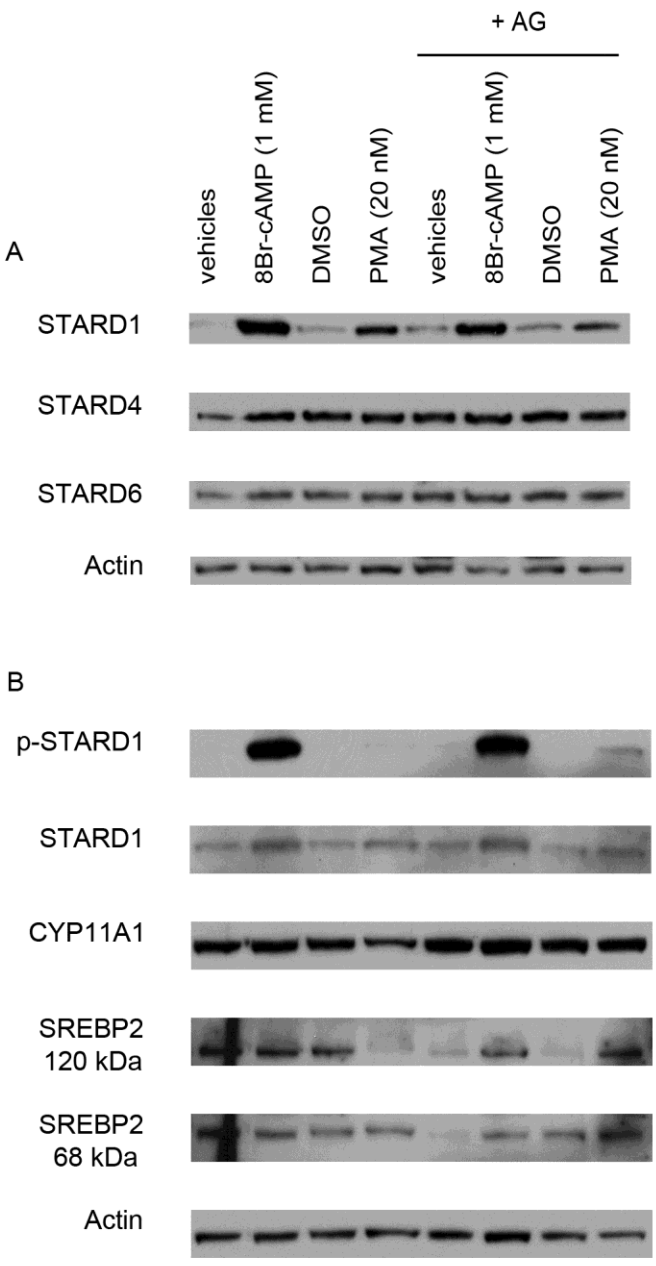

Figure 3.11. Western blot analyses of STARD1, phosphorylated STARD1, STARD4, STARD6, CYP11A1, SREBP2 (68 kDa and 120 kDa), and actin proteins. The effects of Aminoglutethimide on protein levels. Human luteinized granulosa cells from Patient #1578 were cultured for 4 days with 10% FCS prior to treatment with 8Br-cAMP (1 mM), PMA (20 nM), and vehicle (DMSO) or AG (100 μM) in serum-free media for 24 h. Whole cellular protein extracts were separated by SDS-polyacrylamide gel electrophoresis using 4-20% gradient gels and transferred to PVDF membranes and probed with antibodies for the indicated proteins. (A) Membrane 1. (B) Membrane 2.

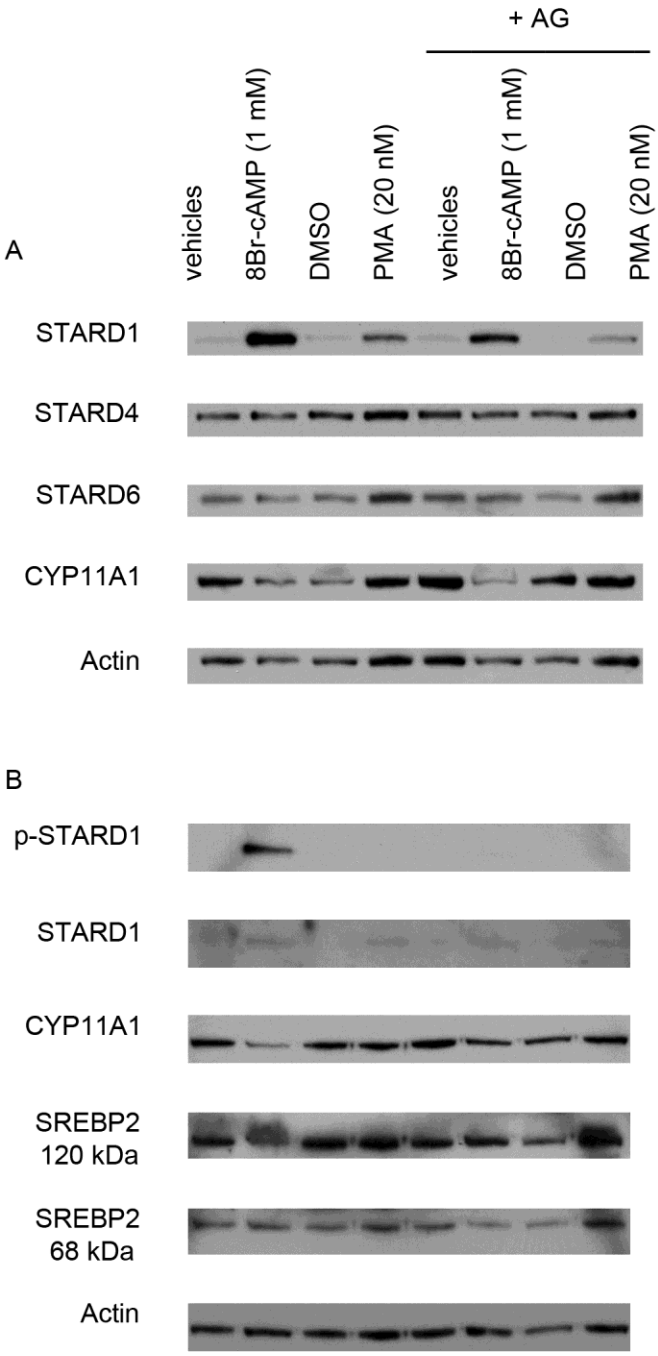

Figure 3.12. Western blot analyses of STARD1, phosphorylated STARD1, STARD4, STARD6, CYP11A1, SREBP2 (68 kDa and 120 kDa), and actin proteins. The effects of Aminoglutethimide (AG) on protein levels. Human luteinized granulosa cells from Patient #1581 were cultured for 4 days with 10% FCS prior to treatment with 8Br-cAMP (1 mM), PMA (20 nM), and vehicle (DMSO) or AG (100 μM) in serum-free media for 24 h. Whole cellular protein extracts were separated by SDS-polyacrylamide gel

electrophoresis using 4-20% gradient gels and transferred to PVDF membranes and probed with antibodies for the indicated proteins. (A) Membrane 1. (B) Membrane 2.

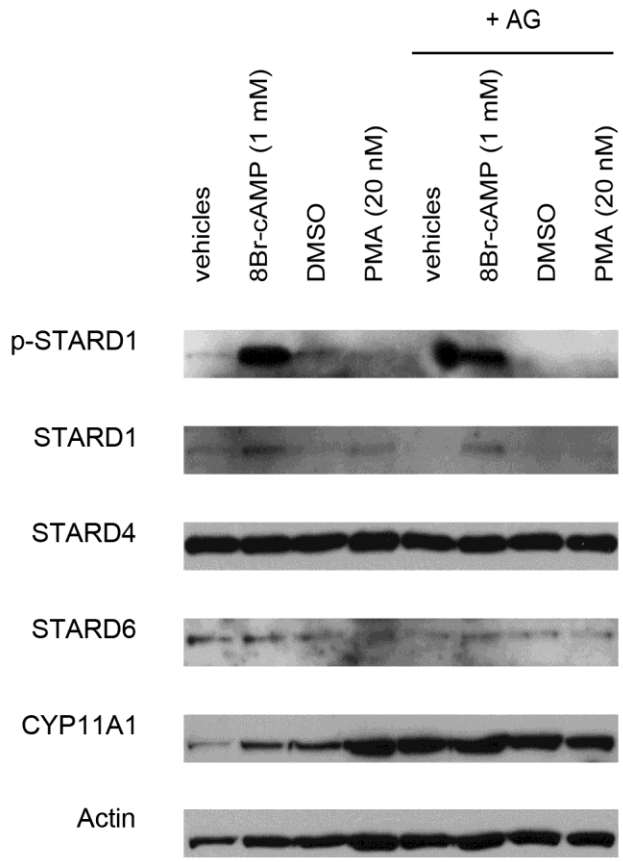

Figure 3.13. Western blot analyses of STARD1, phosphorylated STARD1, STARD4, STARD6, CYP11A1, and actin proteins. The effects of Aminoglutethimide (AG) on protein levels. Human luteinized granulosa cells from Patient #1619 were cultured for 4 days with 10% FCS prior to treatment with 8Br-cAMP (1 mM), PMA (20 nM), and vehicle (DMSO) or AG (100 μM) in serum-free media for 24 h. Whole cellular protein extracts were separated by SDS-polyacrylamide gel electrophoresis using 4-20% gradient gels and transferred to PVDF membranes and probed with antibodies for the indicated proteins.

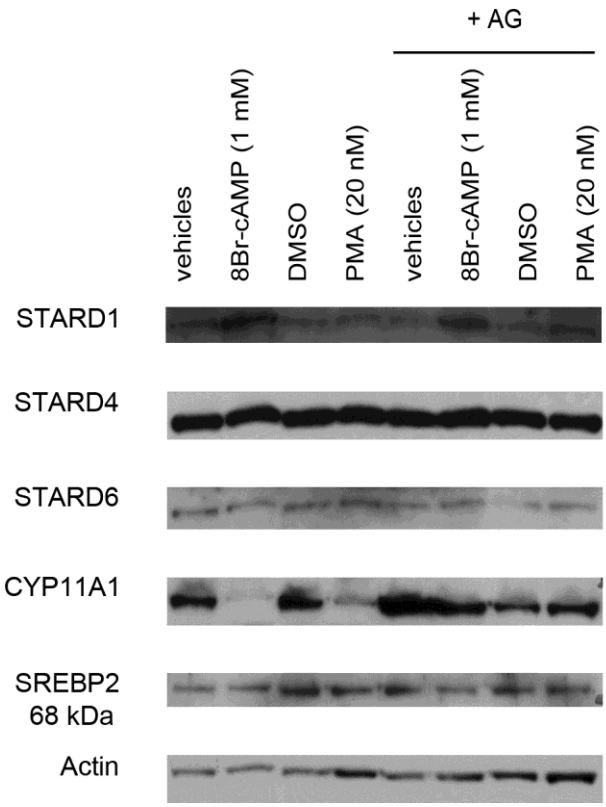

Figure 3.14.Western blot analyses of STARD1, STARD4, STARD6, CYP11A1, SREBP2 (68 kDa), and actin proteins. The effects of Aminoglutethimide (AG) on protein levels. Human luteinized granulosa cells from Patient #1624 were cultured for 4 days with 10% FCS prior to treatment with 8Br-cAMP (1 mM), PMA (20 nM), and vehicle (DMSO) or AG (100 μM) in serum-free media for 24 h. Whole cellular protein extracts were separated by SDS-polyacrylamide gel electrophoresis using 4-20% gradient gels and transferred to PVDF membrane and probed with antibodies for the indicated proteins.

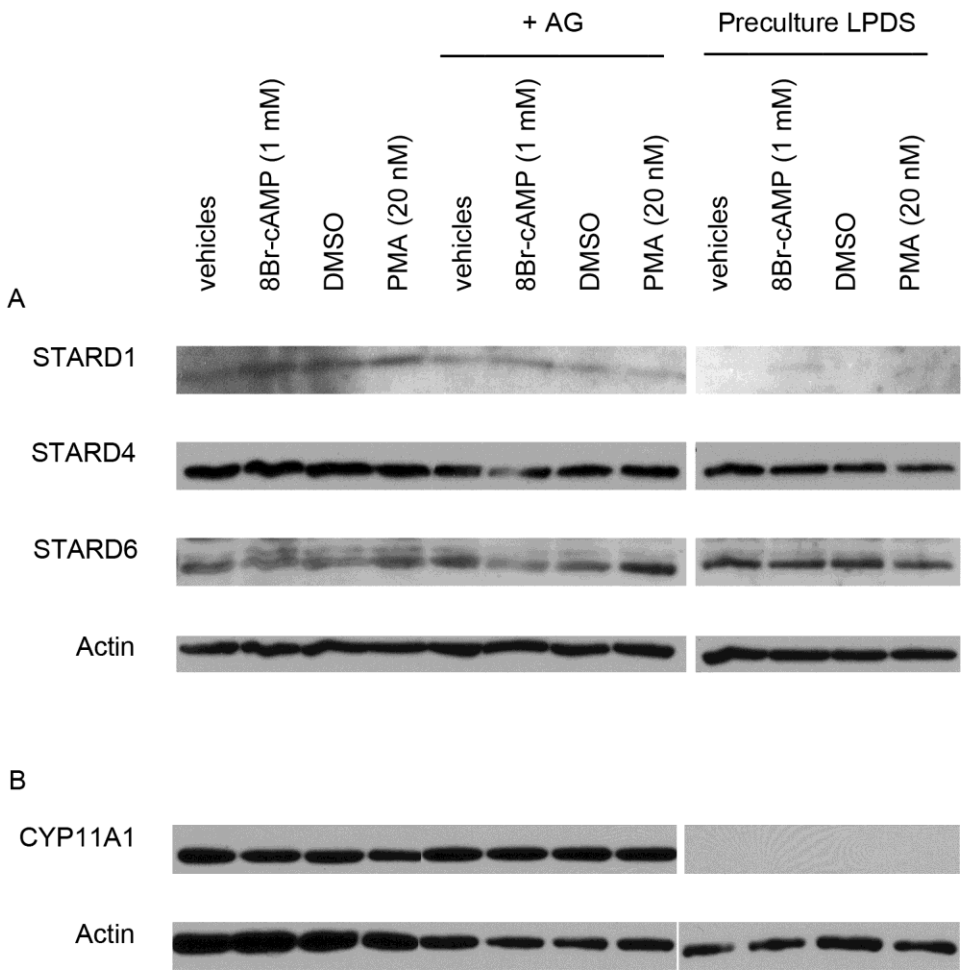

Figure 3.15. Western blot analyses of STARD1, STARD4, STARD6, CYP11A1, and actin proteins. The effects of lipoprotein deficient serum (LPDS) pre-culture or Aminoglutethimide (AG) on protein levels. Human luteinized granulosa cells from Patient #1559 were cultured for 4 days with 10% FCS or 10% LPDS prior to treatment with 8Br-cAMP (1 mM), PMA (20 nM), and vehicle (DMSO) or AG (100 μM) in serum-free media for 24 h. Whole cellular protein extracts were separated by SDS-polyacrylamide gel electrophoresis using 10% or 12% gels and transferred to PVDF membranes and probed with antibodies for the indicated proteins. (A) Membrane 1 from a 12% gel. (B) Membrane 2 from a 10% gel.

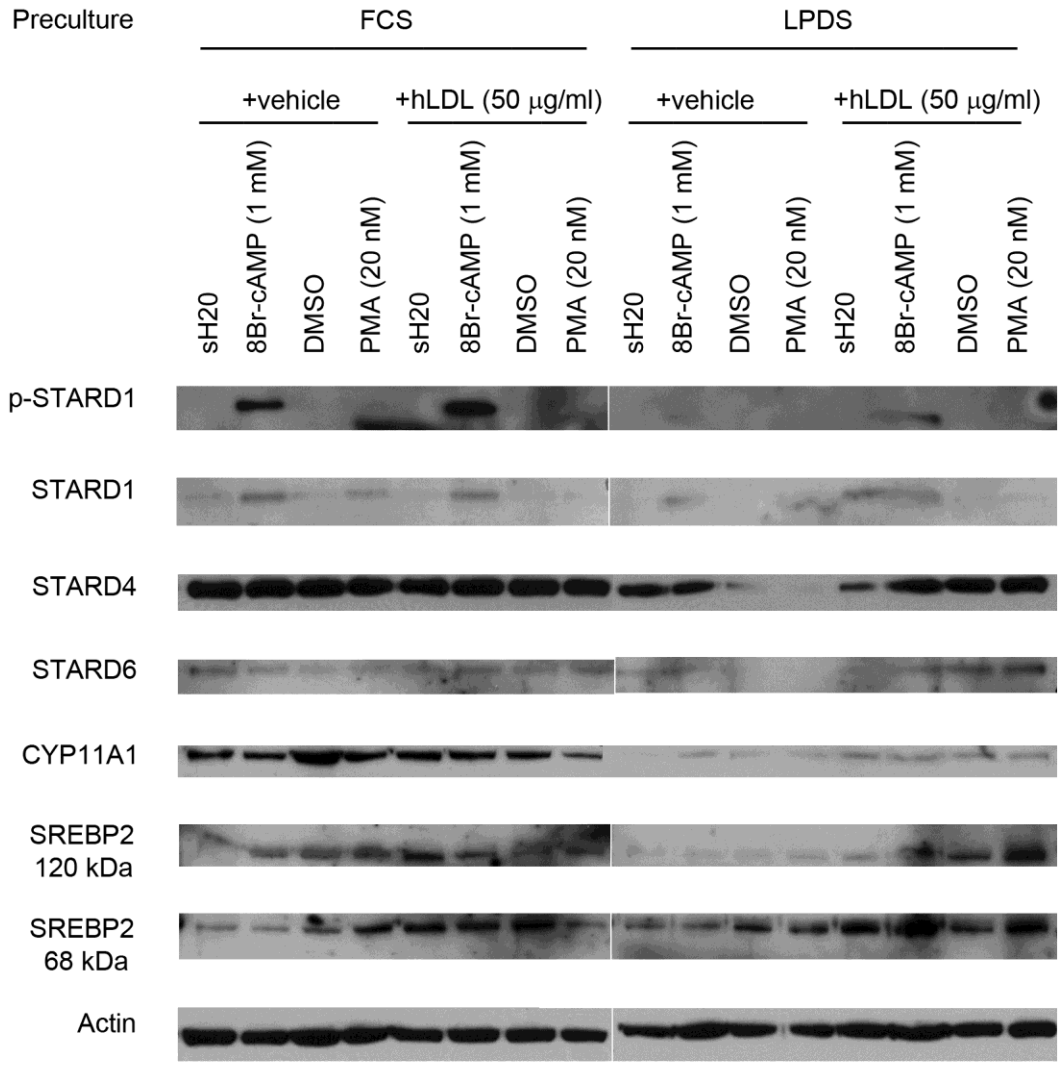

Figure 3.16. Western blot analyses of STARD1, phosphorylated STARD1, STARD4, STARD6, CYP11A1, SREBP2 (68 kDa and 120 kDa), and actin proteins. The effects of lipoprotein deficient serum (LPDS) pre-culture on protein levels. Human luteinized granulosa cells from Patient #1641 were cultured for 4 days with 10% FCS or 10% LPDS prior to treatment with 8Br-cAMP (1 mM), PMA (20 nM), and vehicle (saline/EDTA) or human LDL (hLDL, 50 μg/ml) in serum-free media for 24 h. Whole cellular protein extracts were separated by SDS-polyacrylamide gel electrophoresis using 4-20% gradient gels and transferred to PVDF membranes and probed with antibodies for the indicated proteins. There was a big bubble at the site from row 10-13 of the membrane and thus protein levels in this region are underrepresented.

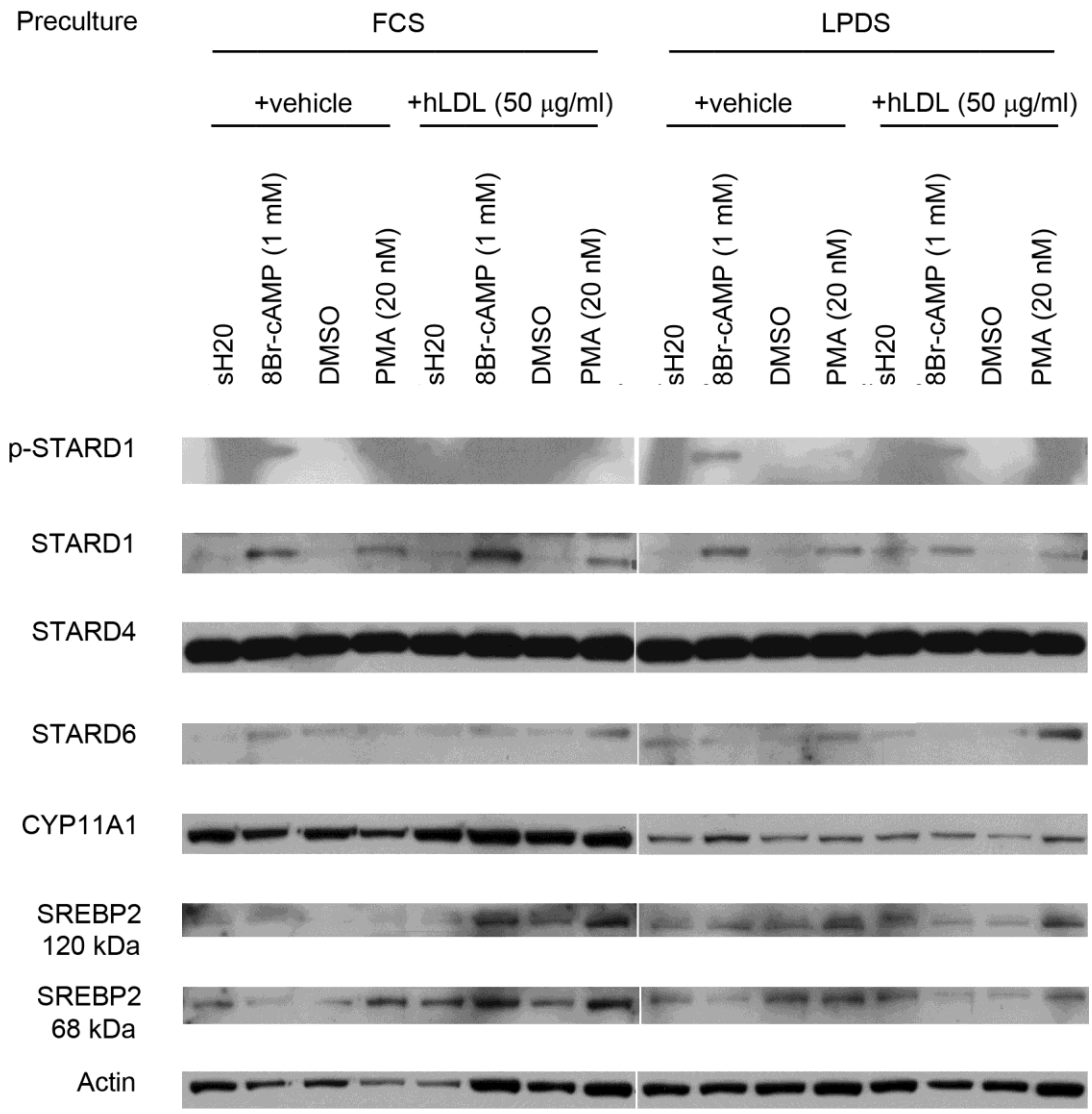

Figure 3.17. Western blot analyses of STARD1, phosphorylated STARD1, STARD4, STARD6, CYP11A1, SREBP2 (68 kDa and 120 kDa), and actin proteins. The effects of lipoprotein deficient serum (LPDS) pre-culture on protein levels. Human luteinized granulosa cells from Patient #1644 were cultured for 4 days with 10% FCS or 10% LPDS prior to treatment with 8Br-cAMP (1 mM), PMA (20 nM) and vehicle (saline/EDTA) or human LDL (hLDL, 50 μg/ml) in serum-free media for 24 h. Whole cellular protein extracts were separated by SDS-polyacrylamide gel electrophoresis using 4-20% gradient gels and transferred to PVDF membranes and probed with antibodies for the indicated proteins.

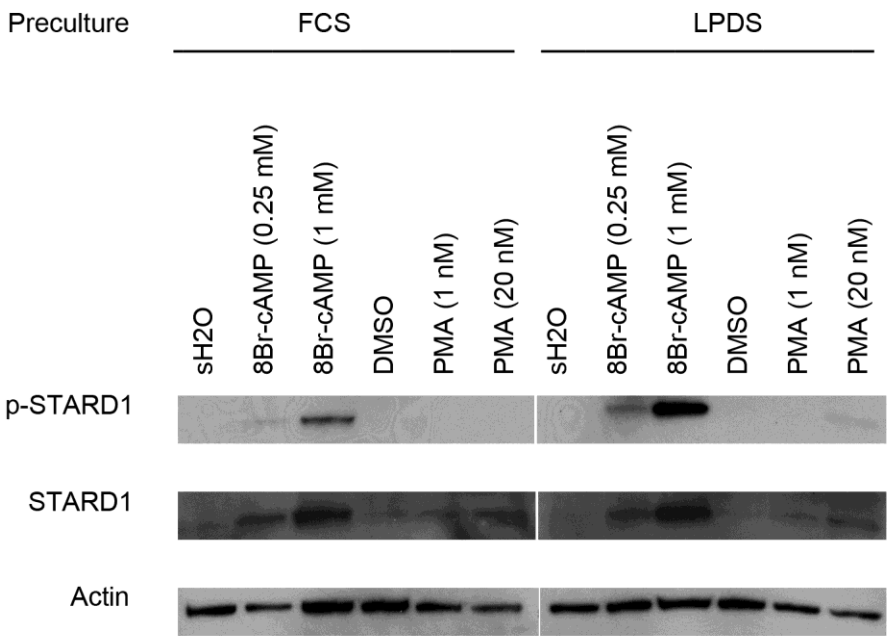

Figure 3.18. Western blot analyses of STARD1, phosphorylated STARD1, and actin proteins. The effects of lipoprotein deficient serum (LPDS) pre-culture on protein levels with 6 h treatments. Human luteinized granulosa cells from Patient #1688 were cultured for 4 days with 10% FCS or 10% LPDS prior to treatment with 8Br-cAMP (0.25 mM and 1 mM) and PMA (1 nM and 20 nM), in serum-free media for 6 h. Whole cellular protein extracts were separated by SDS-polyacrylamide gel electrophoresis using 4-20% gradient gels and transferred to PVDF membranes and probed with antibodies for the indicated proteins. Data with FCS pretreatment are representative of at least three different patients.

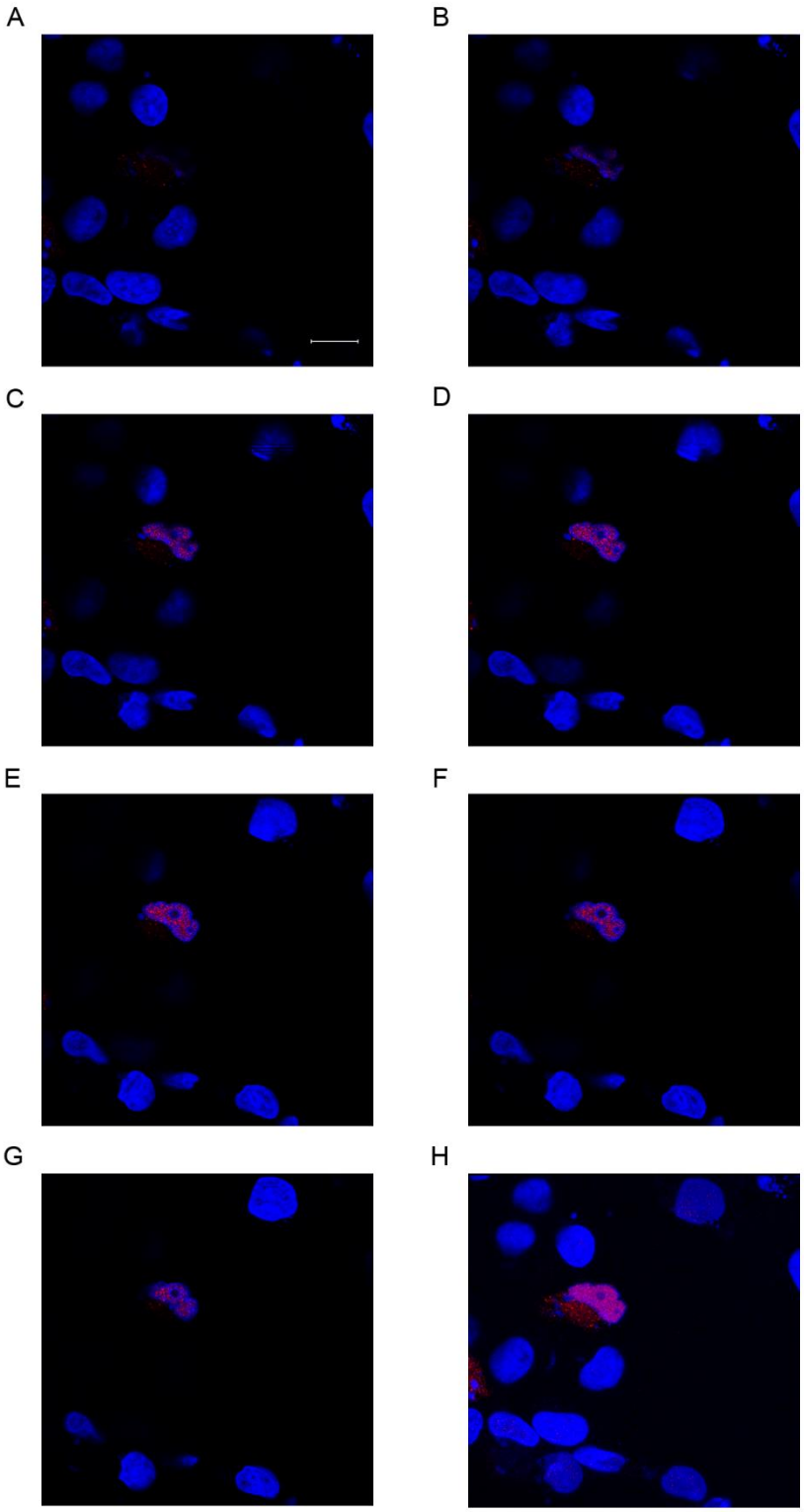

Figure 3.19.The distribution of recombinant human STARD4 in transfected COS-1 cell as assessed by immunofluorescence confocal microscopy using the STARD4

primary antibody. COS-1 cells were cultured and transfected on coverslips and processed for immunofluorescence confocal microscopy. A-G represent serial images from a Z-stack (63X), and H represents a 3D image for the same visual field under the microscope. DAPI is shown in blue and STARD4 primary antibody detected by Cy3-labeled donkey anti-rabbit secondary antibody is shown in red. The majority of positive immunoreactivity was present in the nucleus. Scale bar represents 20 μm.

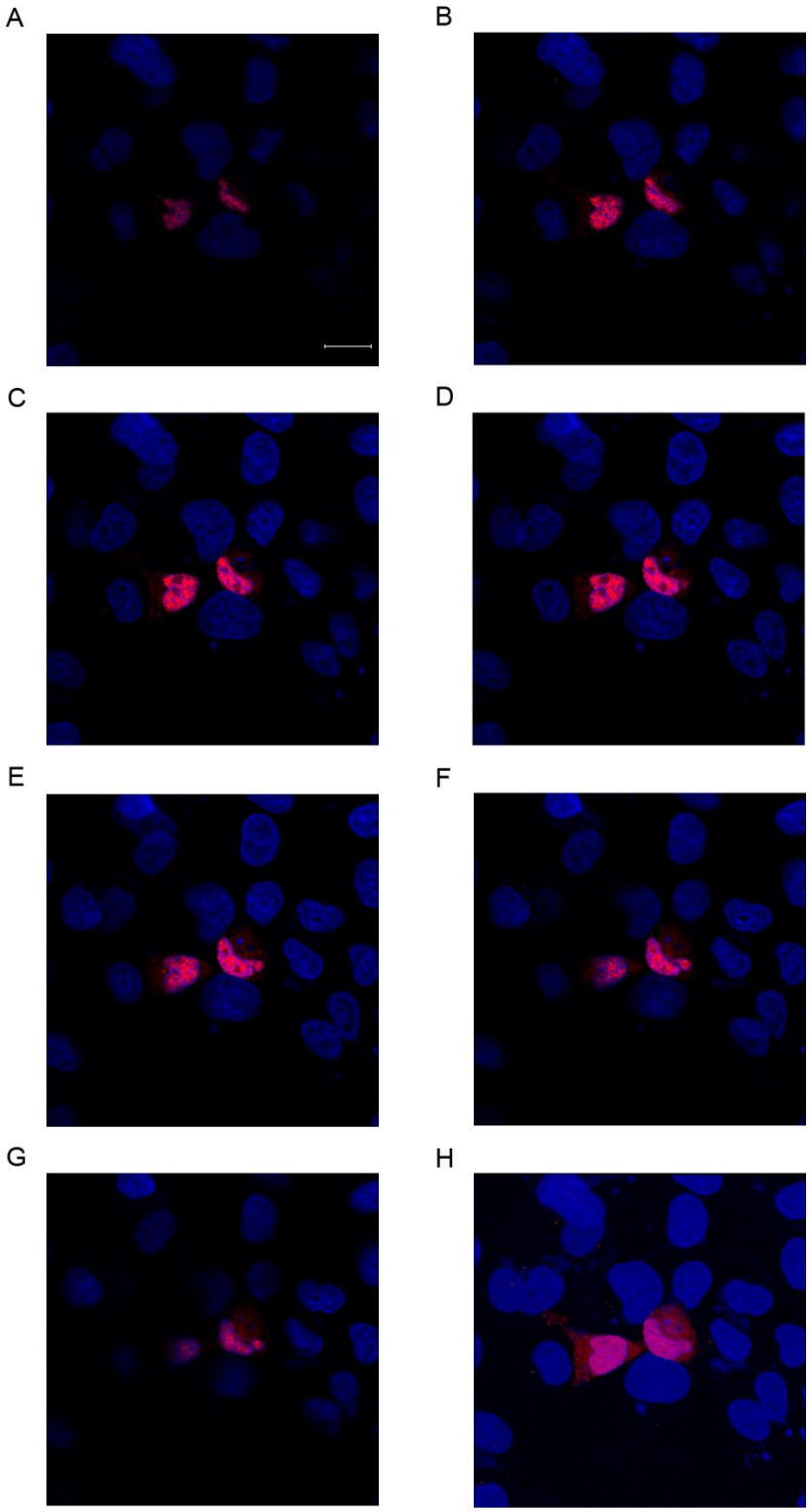

Figure 3.20.The distribution of recombinant human STARD4 in transfected COS-1 cell as assessed by immunofluorescence confocal microscopy using the DDK-tag

primary antibody to detect human STARD4. COS-1 cells were cultured and transfected on coverslips and processed for immunofluorescence confocal microscopy. A-G represent serial images from a Z-stack (63X), and H represents a 3D image for the same visual field under the microscope. DAPI is shown in blue and DDK (Flag)-tag primary antibody which should recognize Flag-tagged STARD4 was detected by Cy3-labeled donkey anti-mouse secondary antibody is shown in red. The majority of positive immunoreactivity was present in the nucleus. Scale bar represents 20 μm.

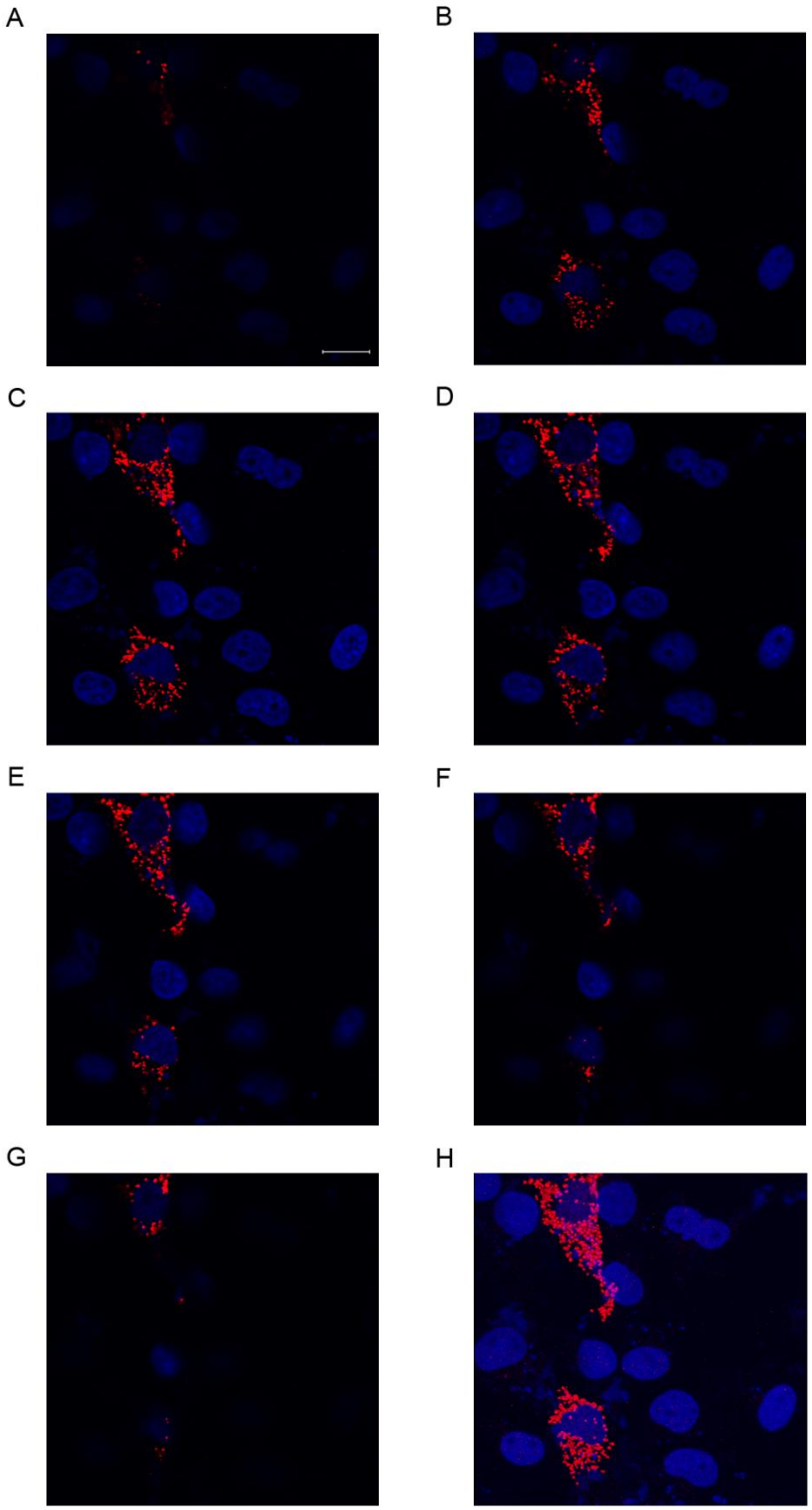

Figure 3.21.The distribution of recombinant human STARD6 in transfected COS-1 cell as assessed by immunofluorescence confocal microscopy using the STARD6

primary antibody. COS-1 cells were cultured and transfected on coverslips and processed for immunofluorescence confocal microscopy. A-G represent serial images from a Z-stack (63X), and H represents a 3D image for the same visual field under the microscope. DAPI is shown in blue and STARD6 primary antibody detected by Cy3-labeled donkey anti-rabbit secondary antibody is shown in red. The majority of positive immunoreactivity was present in the cytoplasm. Scale bar represents 20 μm.

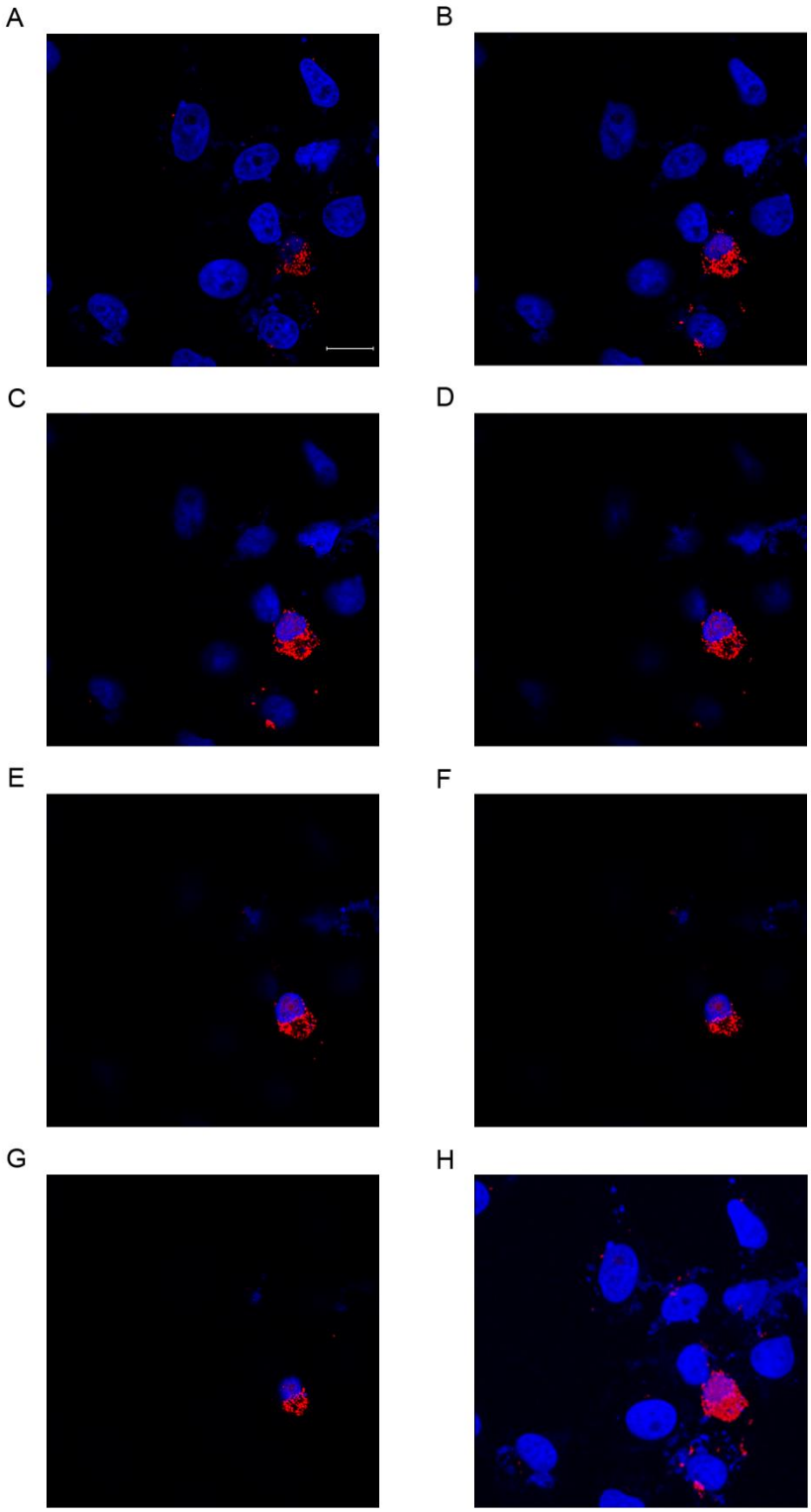

Figure 3.22.The distribution of recombinant human STARD6 in transfected COS-1 cell as assessed by immunofluorescence confocal microscopy using the DDK-tag

primary antibody to detect human STARD6. COS-1 cells were cultured and transfected on coverslips and processed for immunofluorescence confocal microscopy. A-G represent serial images from a Z-stack (63X), and H represents a 3D image for the same visual field under the microscope. DAPI is shown in blue and DDK (Flag)-tag primary antibody which should recognize Flag-tagged STARD6 was detected by Cy3-labeled donkey anti-mouse secondary antibody is shown in red. The majority of positive immunoreactivity was present in the cytoplasm with some evident in the nucleus. Scale bar represents 20 μm.

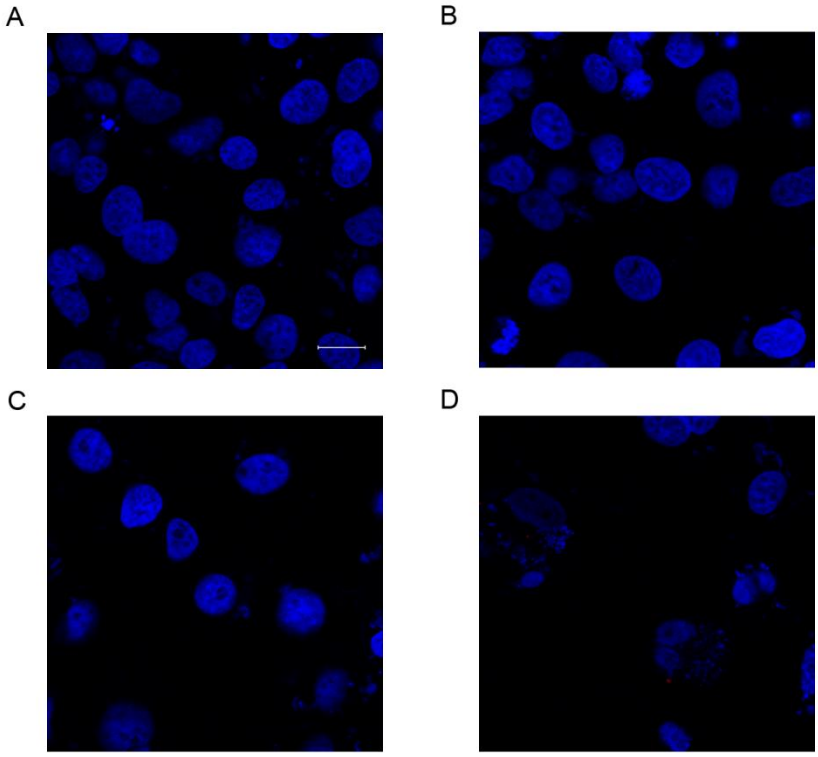

Figure 3.23. Negative control images for COS-1 cells transfected with either STARD4 or STARD6. Cells were cultured and transfected on coverslips and processed for immunofluorescence confocal microscopy. Images were taken at 63X. (A) a negative control image for STARD4 antibody staining (shown in Figure 3.19) using the Cy3-labeled donkey anti-rabbit secondary antibody only (B) a negative control image for the DDK (Flag) tag antibody used for STARD4 staining (shown in Figure 3.20) using the Cy3-labeled donkey anti-mouse secondary antibody only, (C) a negative control for STARD6 antibody staining (shown in Figure 3.21) using the Cy3-labeled donkey anti-rabbit secondary antibody only, (D) a negative control for DDK (Flag) tag antibody used for STARD6 staining (shown in Figure 3.22) showing images with Cy3-labeled donkey anti-mouse secondary antibody only. DAPI is shown in blue and Cy3 signal would be red if present. Scale bar indicates 20 μm.

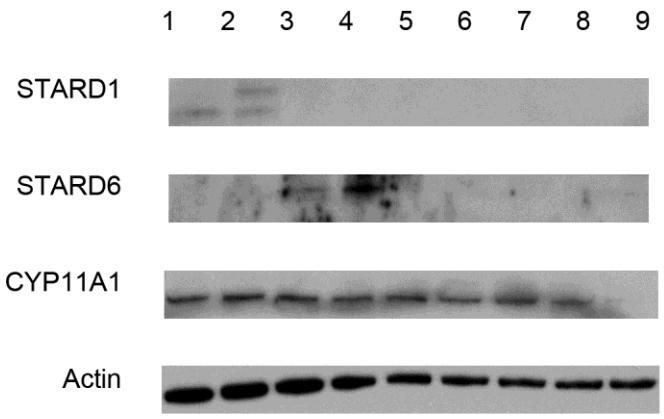

Figure 3.24.Western blot analysis of transfected COS-1 cells used for the F2 steroid assay showing STARD1, STARD6, CYP11A1 and actin proteins. COS-1 cells were transfected with expression plasmids for human STARD1, human STARD6, or pcDNA3.1 (empty vector), and F2 (P450scc complex). After a pre-expression period cells were treated with vehicle, 0.25 mM 8Br-cAMP and/or 5μM 22R-OH-Chol for 24 hours. Whole cellular protein extracts were separated by SDS-polyacrylamide gel electrophoresis using 4-20% gradient gels and transferred to PVDF membranes and probed with antibodies for the indicated proteins. Lane # 1: STARD1 and F2 plasmids; # 2: STARD1 and F2 plasmids, 8Br-cAMP treatment; # 3: STARD6 and F2 plasmids; # 4: STARD6 and F2 plasmids, 8Br-cAMP treatment; # 5: pcDNA3.1 and F2 plasmids; # 6: pcDNA3.1 and F2 plasmids, 8Br-cAMP treatment; # 7: pcDNA3.1 and F2 plasmids, and 22R-OH-Chol treatment; # 8: pcDNA3.1 and F2 plasmids, 8Br-Camp and 22R-OH-Choltreatment; # 9: without transfection or treatment.

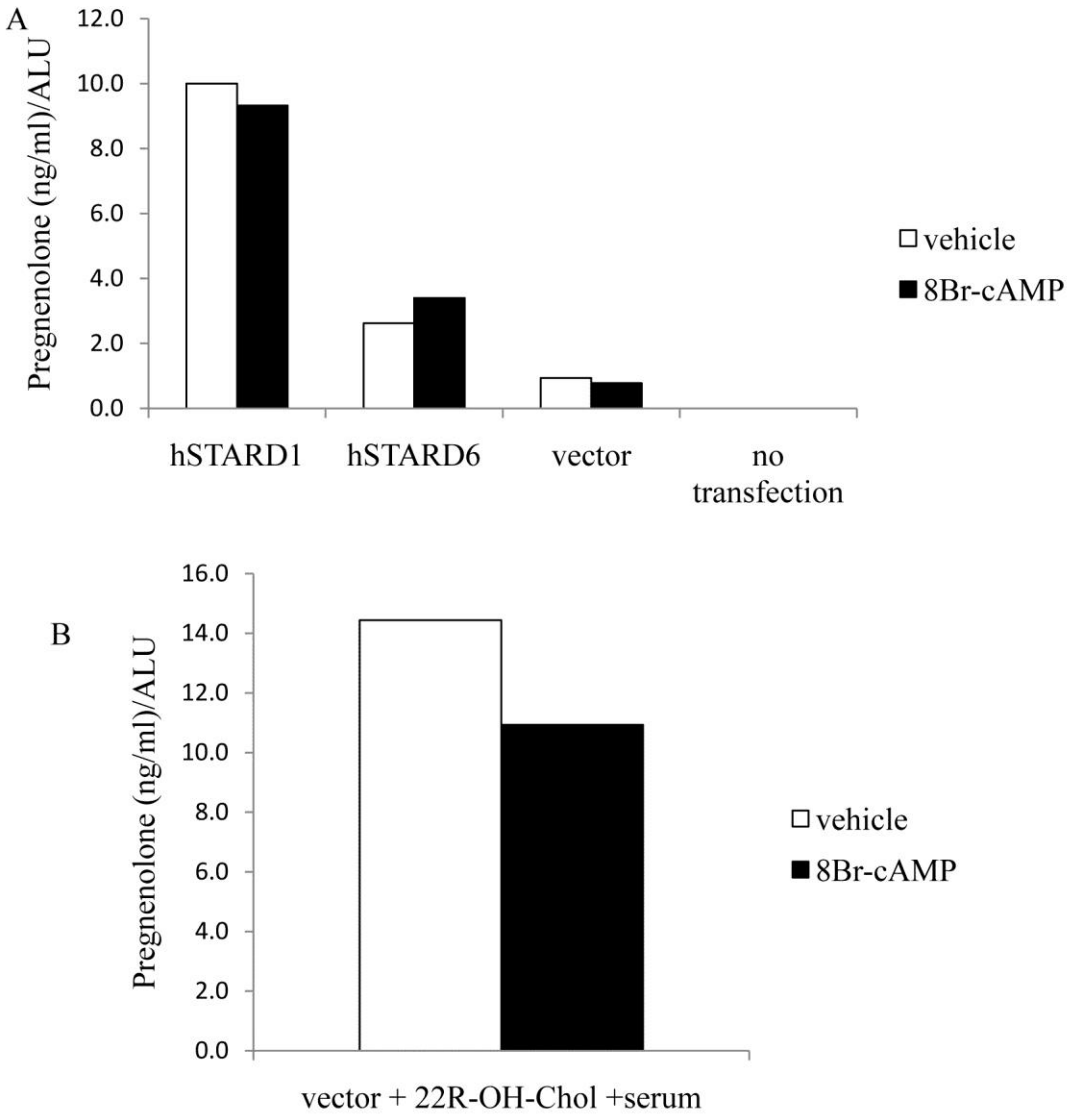

Figure 3.25.Pregnenolone production by transfected COS-1 cells using the F2 steroid assay. COS-1 cells were transfected with the F2 plasmid and the indicated expression plasmid, and following a recovery period, cells were treated with vehicle or 0.25 mM 8Br-cAMP for 24 hours. Pregnenolone concentrations in the media were measured by ELISA and normalized for renilla luciferase values (arbitrary light units, ALU) to control for transfection efficiency.(A) pregnenolone production in the presence of STARD1, STARD6, or pcDNA3.1 and the F2 plasmid or in the non-transfected control, (B) pregnenolone production in the pcDNA3.1/F2 transfection treated with 5 μM 22R-OH-cholesterol (22R-OH-Chol) which freely permeates the mitochondria and served as a positive control.

Chapter IV: Discussion

Our data showed that with 6 hour treatment or 24 hour treatment, cAMP analog increased the mRNA and protein level of STARD1 which occurred most likely through the PKA pathway in human granulosa cells. Several publications have showed similar results in MA-10 Leydig cell lines (Clark et al, 1994) and proliferating human granulosa cells (Devoto et al, 1999) on the protein level. For the mRNA level, another *in vitro* study showed that there was a 5-fold increase for STARD1 mRNA level with 24 hour treatment with 8Br-cAMP in the proliferating granulosa lutein cells (Kiriakidou et al, 1996), and it was similar with our result. However, in the same study fresh luteinized granulosa cells showed a significant increase in STARD1 mRNA with 6 hour treatment and not later, which differs from our observations where STARD1 was still up at 24 hours. Although 1 mM 8Br-cAMP was used in both our and their experiments, the culture conditions were different such that we used DMEM/F12 and they used DMEM, which may explain the difference in part. Also the hormone regimen used to stimulate follicle growth in patients might have been quite different.

We found that 20 nM PMA increased mRNA level of STARD1 significantly, and there was numerically nonsignificant stimulation by 1 nM PMA due to a larger variation among different patients. Moreover, the protein levels in most patients except patients

#1581, #1624 and #1641, were also shown to increase under the stimulation of 20 nM PMA, and this result is consistent with Manna et al (2009) which showed 10 nM PMA increased STARD1 protein level in MA-10 cells. Nonetheless, Kiriakidou et al. (1996) showed that PMA decreased its expression in granulosa lutein cells. This result may because of the higher concentration of PMA (162 nM) used in their experiment, as higher concentrations of phorbol ester can lead to a decrease in PKC activity.

We found that in several patients that low dose PMA increased not only STARD1 protein but that the protein was phosphorylated supporting our hypothesis. The study of Jo et al. (2005) gave a different result in the MA-10 Leydig cell line, but similar result in R2C Leydig cells. MA-10 cells only express STARD1 and synthesize steroid hormones when the cells were stimulated by trophic hormones or cAMP analog. On the other hand, R2C cells had a basal level of STARD1 protein and steroid production without any exogenous hormone stimulation. The result of MA-10 cells showed that PKC activation (with low dose PMA) increased the protein level of STARD1, but without the phosphorylation lacked its function and thus unable to produce steroid hormone. Moreover, when R2C cells were treated with PKA inhibitor, the cells expressed lower levels of STARD1 proteins and steroid hormones (Rao et al, 2003). This result showed that R2C cells have their own PKA signaling activity. Our data are also consistent with work in ovine luteal cells were STARD1 is present as a phosphorylated protein in the presence of PMA due to high endogenous PKA activity characteristic of these fully luteinized cells (Bogan and Niswender, 2007). In our experiment, human luteinized

granulosa cells are collected after the simulated LH surge (hGC injection), and thus their phenotype is more like the mature ovine luteal cells. As a consequence, the higher level of phosphorylated STARD1 with the low dose PMA treatment is likely due to the presence of the basal level of PKA activity induced by luteinization.

As PKA and PKC pathways regulate STARD1 and progesterone production in human ovarian cells, patients that lack STARD1, such as in CLAH, would not make significant levels of sex steroid hormones in response to activation of these pathways, which is supported by the fact they are infertile. Furthermore, without STARD1, accumulated cholesterol in the cytoplasm is harmful and finally kills the steroidogenic cells. On the other hand, excess STARD1 during ovarian follicle maturation, such as in the case of diminished ovarian reserve patients (Skiadas et al, 2012) may result in too much steroid synthesis causing a premature increase in pregnenolone or progesterone which may interfere with ovulation, oocyte quality, or implantation. STARD4 has also been shown to be elevated in diminished ovarian reserve patients and could potentially facilitate cholesterol transport to the mitochondrion resulting in abnormally high steroid production as well. There are no studies yet to indicate STARD6 is abnormal in any disease. Taken together, abnormalities on both STARD1 and STARD4 levels may affect steroidogenesis by reduced or excessive cholesterol transport leading to ovarian dysfunction.

STARD4 has previously been shown to be regulated by sterol content (Clark, 2012). LPDS pretreatment, which results in cells with lower cholesterol stores, led to an

increased basal level of the expression of STARD4 mRNA level, but not protein level. A new study also showed a similar result in HepG2 for the mRNA level, and also showed an increase in protein level (Garbarino et al, 2012) --This reference is incorrect-please insert correct one. One possibility for STARD4 mRNA and proteins being not coupled in our cells may be due to the stability of STARD4 proteins. The difference also may be the results of the different cell types. It may also be a temporal difference between the mRNA and protein regulation such that we need to evaluate longer treatment times. It is interesting that cholesterol depletion can cause increased basal level of STARD4 mRNA, because the transcription level of the STARD4 gene is regulated by SREBP2 (Soccio et al, 2005). When the cholesterol concentration of the ER declines, SREBP2 will be activated to increase cholesterol related gene transcription (including STARD4 gene) in the nucleus. This is most likely why the basal level of STARD4 mRNA increased. However, STARD4 mRNA was not shown to further increase under stimulatory treatments beyond that of FCS pretreated cells receiving cAMP or PMA, which infers that there is maximum response of the STARD4 gene that can be achieved by these cells when challenged with such agonists.

STARD4 mRNA was lower in the presence of hLDL. hLDL is an exogenous cholesterol source that upon uptake contributes to the intracellular cholesterol pool. In FCS pretreated cells it slows the depletion of cholesterol by stimulated steroidogenesis. It can partly restore the loss of cholesterol resulting from the LPDS pretreatment. Also hLDL blunted the increase of STARD4 mRNA level. Although in the presence of hLDL

the PMA affect was not significantly lower than the same treatments without hLDL, PMA in the presence of hLDL failed to significantly increase STARD4 above vehicle levels showing that cholesterol content did affect the STARD4 mRNA response also although not to the same extent as with the cAMP-treated samples. Thus, exogenous cholesterol most likely blunted the activation of SREBP2, reducing the induction of STARD4. Unfortunately, no consistent differences in the protein level of SREBP2 (68 kDa or 120 kDa) could be determined by our western blots as there was a lot of inconsistency in the blot quality and patient responses.

Our result for STARD4 localization (Figure 3.19 and Figure 3.20) found it to be nuclear and cytoplasmic in the transfected COS-1 cells. This finding was partly different than a previous study that showed STARD4 resided in the cytosol and membrane fractions in 3T3-L1 cells (Rodriguez-Agudo et al, 2011). The different findings could be the result of different cell types as 3T3-L1 cells have endogenous STARD4 protein with a role in metabolism. On the other hand, COS-1 cells do not express STARD4 protein without transfection. Furthermore, without a normal endogenous function in the COS-1 cells, STARD4 proteins does not necessarily localize to the same sites as it would in a cell where it has a metabolic role. In addition, STARD6 images showed that the most of the immunoreactivity resided outside the nucleus in the cytoplasm (Figure 3.21 and Figure 3.22.).

There is no prior evidence showing STARD4 protein nuclear localization, but studies showed the STARD6 proteins were mostly found in nucleus with less in the cytosol in

the cultured neuronal cells (Chang et al, 2010). It has been postulated that STARD6 may be involved in the transcriptional regulation of cholesterol homeostasis (Chang et al, 2013), but there is no data to support this idea. However, the STARD6 immunoreactivity in our experiment localized mostly outside the nucleus and appeared to be associated with some type of vesicle, which might be expected if it participates in sterol transport. Further studies need to be performed to answer the question of specific subcellular location are needed and should be performed with antibodies that identify organelles or other organelle markers. The future goal will be to perform these studies in the human granulosa cells.

STARD6 protein increased the pregnenolone production transfected COS-1 cells. This result showed the STARD6 protein was capable of facilitating *de novo* steroidogenesis. Similar to our studies, Soccio et al (2005) transfected STARD4 and the genes for converting cholesterol to progesterone in COS cells and found that STARD4 was able to increase progesterone production. STARD4 protein also had a similar but lower ability for cholesterol transport than STARD1.

The COS-1 cell line contains both STARD1 dependent and independent activities (Huang and Miller, 2001). Thereby, in the negative vector only control a low level of pregnenolone was observed with the F2 plasmid, and no pregnenolone was synthesized in non-transfected COS-1 in the same experiment. The same kind of studies for STARD4 and STARD5 have been done, and both of the proteins can also increase steroidogenesis, like our findings for STARD6 (Soccio et al, 2005a). Moreover, in the STARD1

transfected cells, pregnenolone levels were much higher than the levels in the STARD6 transfected cells regardless of 8Br-cAMP treatment. This result is probably because STARD1 protein has an N-terminal sequence that can target to the mitochondrial membrane. As a consequence, cholesterol delivery across the mitochondrial membrane is more efficiently transported by STARD1 protein than by STARD6 protein. Nevertheless, N-62 STARD1, which lacks targeting sequence, and wild type STARD1 had similar enhancement of steroidogenesis (Huang and Miller, 2001). N-62 STARD1 and STARD6 cannot anchor to the mitochondrial membrane, so the mechanism of the cholesterol transport abilities of N-62 STARD1 and STARD6 remains a question.

In the future research, it will be useful to localize STARD4 and STARD6 in human luteinized granulosa cells to determine the different subcellular localization of the two proteins in primary cells. This information will be critical to understanding how these proteins function in normal steroidogenic cells. These studies should be performed both under vehicle and agonist treated conditions to see if the proteins are mobilized between cellular compartments. In addition, these studies can be performed with normal conditions and other conditions that alter intracellular cholesterol content. Another avenue of study is to more thoroughly investigate STARD4 and STARD6 function in human granulosa cells by reducing each protein through the use of RNA interference technique.

In summary, we have found that STARD1 and STARD4 show somewhat similar regulation by PKA and PKC agonists, 8Br-cAMP and low dose PMA, whereas STARD6

was not regulated. STARD4 showed most regulation by manipulation of intracellular cholesterol regulation. STARD1 protein and its phosphorylation were also enhanced by agonist treatment, whereas STARD4 and STARD6 protein were not at the time points examined. Recombinant STARD4 and STARD6 expressed in COS cells showed different distributions with STARD4 being nuclear and cytoplasmic and STARD6 being mostly cytoplasmic with a punctuate appearance reminiscent of vesicular association. Finally, STARD6 when expressed in COS cells with the genes encoding the P450scc system was able to modestly enhance *de novo* steroidogenesis. These data provide new insight into the regulation of START domain proteins in a relevant primary ovarian cell.

REFERENCES

Allen J.A., Diemer T., Janus P., Hales K.H., Hales D.B. (2004). Bacterial endotoxin lipopolysaccharide and reactive oxygen species inhibit Leydig cell steroidogenesis via perturbation of mitochondria. Endocrine. 25, 265-275.

Alpy F., Tomasetto C. (2005). Give lipids a START: the StAR-related lipid transfer (START) domain in mammals. J. Cell Sci. 118, 2791-2801.

Arakane F., Kallen C.B., Watari H., Foster J.A., Sepuri N.B., Pain D., Stayrook S.E., Lewis M., Gerton G.L., Strauss J.F., III. (1998). The mechanism of action of steroidogenic acute regulatory protein (StAR). StAR acts on the outside of mitochondria to stimulate steroidogenesis. J. Biol. Chem. 273, 16339-16345.

Arakane F., King S.R., Du Y., Kallen C.B., Walsh L.P., Watari H., Stocco D.M., Strauss J.F., III. (1997). Phosphorylation of steroidogenic acute regulatory protein (StAR) modulates its steroidogenic activity. J. Biol. Chem. 272, 32656-32662.

Arakane F., Sugawara T., Nishino H., Liu Z., Holt J.A., Pain D., Stocco D.M., Miller W.L., Strauss J.F., III. (1996). Steroidogenic acute regulatory protein (StAR) retains activity in the absence of its mitochondrial import sequence: implications for the mechanism of StAR action. Proc. Natl. Acad. Sci. U. S. A. 93, 13731-13736.

Artemenko I.P., Zhao D., Hales D.B., Hales K.H., Jefcoate C.R. (2001). Mitochondrial processing of newly synthesized steroidogenic acute regulatory protein (StAR), but not total StAR, mediates cholesterol transfer to cytochrome P450 side chain cleavage enzyme in adrenal cells. J. Biol. Chem. 276, 46583-46596.

Baker B.Y., Epand R.F., Epand R.M., Miller W.L. (2007). Cholesterol binding does not predict activity of the steroidogenic acute regulatory protein, StAR. J. Biol. Chem. 282, 10223-10232.

Baker B.Y., Yaworsky D.C., Miller W.L. (2005). A pH-dependent molten globule transition is required for activity of the steroidogenic acute regulatory protein, StAR. J. Biol. Chem. 280, 41753-41760.

Bogan R.L., Niswender G.D. (2007). Constitutive steroidogenesis in ovine large luteal cells may be mediated by tonically active protein kinase A. Biol. Reprod. 77, 209-216.

Bose H.S., Lingappa V.R., Miller W.L. (2002). Rapid regulation of steroidogenesis by

mitochondrial protein import. Nature. 417, 87-91.

Bose H.S., Whittal R.M., Baldwin M.A., Miller W.L. (1999). The active form of the steroidogenic acute regulatory protein, StAR, appears to be a molten globule. Proc. Natl. Acad. Sci. U. S. A. 96, 7250-7255.

Bose H.S., Whittal R.M., Ran Y., Bose M., Baker B.Y., Miller W.L. (2008a). StAR-like activity and molten globule behavior of StARD6, a male germ-line protein. Biochemistry. 47, 2277-2288.

Bose M., Whittal R.M., Miller W.L., Bose H.S. (2008b). Steroidogenic activity of StAR requires contact with mitochondrial VDAC1 and phosphate carrier protein. J. Biol. Chem. 283, 8837-8845.

Brannian J.D., Stouffer R.L. (1993). Native and modified (acetylated) low density lipoprotein-supported steroidogenesis by macaque granulosa cells collected before and after the ovulatory stimulus: correlation with fluorescent lipoprotein uptake. Endocrinology. 132, 591-597.

Chang I.Y., Jeon Y.J., Jung S.M., Jang Y.H., Ahn J.B., Park K.S., Yoon S.P. (2010). Does the StarD6 mark the same as the StAR in the nervous system? J. Chem. Neuroanat. 40, 239-242.

Chang I.Y., Kim J.H., Cho K.W., Yoon S.P. (2013). Acute responses of DNA repair proteins and StarD6 in rat hippocampus after domoic acid-induced excitotoxicity. Acta Histochem. 115, 234-239.

Chang I.Y., Kim J.H., Hwang G., Song P.I., Song R.J., Kim J.W., Yoon S.P. (2007a). Immunohistochemical detection of StarD6 in the rat nervous system. Neuroreport. 18, 1615-1619.

Chang I.Y., Shin S.Y., Kim J.W., Yu J.M., Kim J.S., Song P.I., Yoon S.P. (2007b). The changed immunolocalization of START-domain-containing 6 (StarD6) during the development of testes in rat perinatal hypothyroidism. Acta Histochem. 109, 315-321.

Christensen K., Bose H.S., Harris F.M., Miller W.L., Bell J.D. (2001). Binding of steroidogenic acute regulatory protein to synthetic membranes suggests an active molten globule. J. Biol. Chem. 276, 17044-17051.

Christenson L.K., Devoto L. (2003). Cholesterol transport and steroidogenesis by the corpus luteum. Reprod. Biol. Endocrinol. 1, 90.

Christenson L.K., Strauss J.F., III. (2000). Steroidogenic acute regulatory protein (StAR)

and the intramitochondrial translocation of cholesterol. Biochim. Biophys. Acta. 1529, 175-187.

Clark B.J. (2012). The mammalian START domain protein family in lipid transport in health and disease. J. Endocrinol. 212, 257-275.

Clark B.J., Wells J., King S.R., Stocco D.M. (1994). The purification, cloning, and expression of a novel luteinizing hormone-induced mitochondrial protein in MA-10 mouse Leydig tumor cells. Characterization of the steroidogenic acute regulatory protein (StAR). J. Biol. Chem. 269, 28314-28322.

Devoto L., Christenson L.K., McAllister J.M., Makrigiannakis A., Strauss J.F., III. (1999). Insulin and insulin-like growth factor-I and -II modulate human granulosa-lutein cell steroidogenesis: enhancement of steroidogenic acute regulatory protein (StAR) expression. Mol. Hum. Reprod. 5, 1003-1010.

Devoto L., Kohen P., Gonzalez R.R., Castro O., Retamales I., Vega M., Carvallo P., Christenson L.K., Strauss J.F., III. (2001). Expression of steroidogenic acute regulatory protein in the human corpus luteum throughout the luteal phase. J. Clin. Endocrinol. Metab. 86, 5633-5639.

Devoto L., Vega M., Kohen P., Castro O., Carvallo P., Palomino A. (2002). Molecular regulation of progesterone secretion by the human corpus luteum throughout the menstrual cycle. J. Reprod. Immunol. 55, 11-20.

Duggavathi R., Volle D.H., Mataki C., Antal M.C., Messaddeq N., Auwerx J., Murphy B.D., Schoonjans K. (2008). Liver receptor homolog 1 is essential for ovulation. Genes Dev. 22, 1871-1876.

Dyson M.T., Jones J.K., Kowalewski M.P., Manna P.R., Alonso M., Gottesman M.E., Stocco D.M. (2008). Mitochondrial A-kinase anchoring protein 121 binds type II protein kinase A and enhances steroidogenic acute regulatory protein-mediated steroidogenesis in MA-10 mouse leydig tumor cells. Biol. Reprod. 78, 267-277.

Ecker J., Liebisch G., Englmaier M., Grandl M., Robenek H., Schmitz G. (2010). Induction of fatty acid synthesis is a key requirement for phagocytic differentiation of human monocytes. Proc. Natl. Acad. Sci. U. S. A. 107, 7817-7822.

Edwards P.A., Ericsson J. (1999). Sterols and isoprenoids: signaling molecules derived from the cholesterol biosynthetic pathway. Annu. Rev. Biochem. 68, 157-185.

Edwards P.A., Tabor D., Kast H.R., Venkateswaran A. (2000). Regulation of gene

expression by SREBP and SCAP. Biochim. Biophys. Acta. 1529, 103-113.

Elbadawy H.M., Borthwick F., Wright C., Martin P.E., Graham A. (2011). Cytosolic StAR-related lipid transfer domain 4 (STARD4) protein influences keratinocyte lipid phenotype and differentiation status. Br. J. Dermatol. 164, 628-632.

Fleury A., Mathieu A.P., Ducharme L., Hales D.B., LeHoux J.G. (2004). Phosphorylation and function of the hamster adrenal steroidogenic acute regulatory protein (StAR). J. Steroid Biochem. Mol. Biol. 91, 259-271.

Galarneau L., Pare J.F., Allard D., Hamel D., Levesque L., Tugwood J.D., Green S., Belanger L. (1996). The alpha1-fetoprotein locus is activated by a nuclear receptor of the Drosophila FTZ-F1 family. Mol. Cell Biol. 16, 3853-3865.

Gillio-Meina C., Hui Y.Y., LaVoie H.A. (2003). GATA-4 and GATA-6 transcription factors: expression, immunohistochemical localization, and possible function in the porcine ovary. Biol. Reprod. 68, 412-422.

Goldstein J.L., Rawson R.B., Brown M.S. (2002). Mutant mammalian cells as tools to delineate the sterol regulatory element-binding protein pathway for feedback regulation of lipid synthesis. Arch. Biochem. Biophys. 397, 139-148.

Gomes C., Oh S.D., Kim J.W., Chun S.Y., Lee K., Kwon H.B., Soh J. (2005). Expression of the putative sterol binding protein Stard6 gene is male germ cell specific. Biol. Reprod. 72, 651-658.

Hall E.A., Ren S., Hylemon P.B., Rodriguez-Agudo D., Redford K., Marques D., Kang D., Gil G., Pandak W.M. (2005). Detection of the steroidogenic acute regulatory protein, StAR, in human liver cells. Biochim. Biophys. Acta. 1733, 111-119.

Hauet T., Yao Z.X., Bose H.S., Wall C.T., Han Z., Li W., Hales D.B., Miller W.L., Culty M., Papadopoulos V. (2005). Peripheral-type benzodiazepine receptor-mediated action of steroidogenic acute regulatory protein on cholesterol entry into leydig cell mitochondria. Mol. Endocrinol. 19, 540-554.

Hiroi H., Christenson L.K., Chang L., Sammel M.D., Berger S.L., Strauss J.F., III. (2004). Temporal and spatial changes in transcription factor binding and histone modifications at the steroidogenic acute regulatory protein (StAR) locus associated with stAR transcription. Mol. Endocrinol. 18, 791-806.

Horton J.D., Goldstein J.L., Brown M.S. (2002). SREBPs: activators of the complete program of cholesterol and fatty acid synthesis in the liver. J. Clin. Invest. 109, 1125-1131.

Horton J.D., Shah N.A., Warrington J.A., Anderson N.N., Park S.W., Brown M.S., Goldstein J.L. (2003). Combined analysis of oligonucleotide microarray data from transgenic and knockout mice identifies direct SREBP target genes. Proc. Natl. Acad. Sci. U. S. A. 100, 12027-12032.

Huang M.C., Miller W.L. (2001). Creation and activity of COS-1 cells stably expressing the F2 fusion of the human cholesterol side-chain cleavage enzyme system. Endocrinology. 142, 2569-2576.

Iyer L.M., Koonin E.V., Aravind L. (2001). Adaptations of the helix-grip fold for ligand binding and catalysis in the START domain superfamily. Proteins. 43, 134-144.

Jamin N., Neumann J.M., Ostuni M.A., Vu T.K., Yao Z.X., Murail S., Robert J.C., Giatzakis C., Papadopoulos V., Lacapere J.J. (2005). Characterization of the cholesterol recognition amino acid consensus sequence of the peripheral-type benzodiazepine receptor. Mol. Endocrinol. 19, 588-594.

Jo Y., King S.R., Khan S.A., Stocco D.M. (2005). Involvement of protein kinase C and cyclic adenosine 3',5'-monophosphate-dependent kinase in steroidogenic acute regulatory protein expression and steroid biosynthesis in Leydig cells. Biol. Reprod. 73, 244-255.

Joseph-Liauzun E., Delmas P., Shire D., Ferrara P. (1998). Topological analysis of the peripheral benzodiazepine receptor in yeast mitochondrial membranes supports a five-transmembrane structure. J. Biol. Chem. 273, 2146-2152.

Juengel J.L., Meberg B.M., Turzillo A.M., Nett T.M., Niswender G.D. (1995). Hormonal regulation of messenger ribonucleic acid encoding steroidogenic acute regulatory protein in ovine corpora lutea. Endocrinology. 136, 5423-5429.

King S.R., LaVoie H.A. (2012). Gonadal transactivation of STARD1, CYP11A1 and HSD3B. Front Biosci. 17, 824-846.

Kiriakidou M., McAllister J.M., Sugawara T., Strauss J.F., III. (1996). Expression of steroidogenic acute regulatory protein (StAR) in the human ovary. J. Clin. Endocrinol. Metab. 81, 4122-4128.

Kohen P., Castro O., Palomino A., Munoz A., Christenson L.K., Sierralta W., Carvallo P., Strauss J.F., III, Devoto L. (2003). The steroidogenic response and corpus luteum expression of the steroidogenic acute regulatory protein after human chorionic gonadotropin administration at different times in the human luteal phase. J. Clin. Endocrinol. Metab. 88, 3421-3430.

LaVoie H.A. (2003). The role of GATA in mammalian reproduction. Exp. Biol. Med. (Maywood.). 228, 1282-1290.

Lavoie H.A., King S.R. (2009). Transcriptional regulation of steroidogenic genes: STARD1, CYP11A1 and HSD3B. Exp. Biol. Med. (Maywood.). 234, 880-907.

LaVoie H.A., Singh D., Hui Y.Y. (2004). Concerted regulation of the porcine steroidogenic acute regulatory protein gene promoter activity by follicle-stimulating hormone and insulin-like growth factor I in granulosa cells involves GATA-4 and CCAAT/enhancer binding protein beta. Endocrinology. 145, 3122-3134.

Li H., Yao Z., Degenhardt B., Teper G., Papadopoulos V. (2001). Cholesterol binding at the cholesterol recognition/ interaction amino acid consensus (CRAC) of the peripheral-type benzodiazepine receptor and inhibition of steroidogenesis by an HIV TAT-CRAC peptide. Proc. Natl. Acad. Sci. U. S. A. 98, 1267-1272.

Lin T., Wang D., Hu J., Stocco D.M. (1998). Upregulation of human chorionic gonadotrophin-induced steroidogenic acute regulatory protein by insulin-like growth factor-I in rat Leydig cells. Endocrine. 8, 73-78.

Manna P.R., Chandrala S.P., Jo Y., Stocco D.M. (2006a). cAMP-independent signaling regulates steroidogenesis in mouse Leydig cells in the absence of StAR phosphorylation. J. Mol. Endocrinol. 37, 81-95.

Manna P.R., Chandrala S.P., King S.R., Jo Y., Counis R., Huhtaniemi I.T., Stocco D.M. (2006b). Molecular mechanisms of insulin-like growth factor-I mediated regulation of the steroidogenic acute regulatory protein in mouse leydig cells. Mol. Endocrinol. 20, 362-378.

Manna P.R., Huhtaniemi I.T., Stocco D.M. (2009). Mechanisms of protein kinase C signaling in the modulation of 3',5'-cyclic adenosine monophosphate-mediated steroidogenesis in mouse gonadal cells. Endocrinology. 150, 3308-3317.

Manna P.R., Huhtaniemi I.T., Wang X.J., Eubank D.W., Stocco D.M. (2002). Mechanisms of epidermal growth factor signaling: regulation of steroid biosynthesis and the steroidogenic acute regulatory protein in mouse Leydig tumor cells. Biol. Reprod. 67, 1393-1404.

Mathieu A.P., Fleury A., Ducharme L., Lavigne P., LeHoux J.G. (2002). Insights into steroidogenic acute regulatory protein (StAR)-dependent cholesterol transfer in mitochondria: evidence from molecular modeling and structure-based thermodynamics supporting the existence of partially unfolded states of StAR. J.

Mol. Endocrinol. 29, 327-345.

McEnery M.W., Snowman A.M., Trifiletti R.R., Snyder S.H. (1992). Isolation of the mitochondrial benzodiazepine receptor: association with the voltage-dependent anion channel and the adenine nucleotide carrier. Proc. Natl. Acad. Sci. U. S. A. 89, 3170-3174.

Mesmin B., Pipalia N.H., Lund F.W., Ramlall T.F., Sokolov A., Eliezer D., Maxfield F.R. (2011). STARD4 abundance regulates sterol transport and sensing. Mol. Biol. Cell. 22, 4004-4015.

Mizutani T., Yazawa T., Ju Y., Imamichi Y., Uesaka M., Inaoka Y., Matsuura K., Kamiki Y., Oki M., Umezawa A., Miyamoto K. (2010). Identification of a novel distal control region upstream of the human steroidogenic acute regulatory protein (StAR) gene that participates in SF-1-dependent chromatin architecture. J. Biol. Chem. 285, 28240-28251.

Ning Y., Bai Q., Lu H., Li X., Pandak W.M., Zhao F., Chen S., Ren S., Yin L. (2009). Overexpression of mitochondrial cholesterol delivery protein, StAR, decreases intracellular lipids and inflammatory factors secretion in macrophages. Atherosclerosis. 204, 114-120.

Niswender G.D., Juengel J.L., Silva P.J., Rollyson M.K., McIntush E.W. (2000). Mechanisms controlling the function and life span of the corpus luteum. Physiol Rev. 80, 1-29.

Pandak W.M., Ren S., Marques D., Hall E., Redford K., Mallonee D., Bohdan P., Heuman D., Gil G., Hylemon P. (2002). Transport of cholesterol into mitochondria is rate-limiting for bile acid synthesis via the alternative pathway in primary rat hepatocytes. J. Biol. Chem. 277, 48158-48164.

Parker K.L., Schimmer B.P. (1997). Steroidogenic factor 1: a key determinant of endocrine development and function. Endocr. Rev. 18, 361-377.

Pfaffl M.W. (2001). A new mathematical model for relative quantification in real-time RT-PCR. Nucleic Acids Res. 29, e45.

Ponting C.P., Aravind L. (1999). START: a lipid-binding domain in StAR, HD-ZIP and signalling proteins. Trends Biochem. Sci. 24, 130-132.

Rao R.M., Jo Y., Leers-Sucheta S., Bose H.S., Miller W.L., Azhar S., Stocco D.M. (2003). Differential regulation of steroid hormone biosynthesis in R2C and MA-10 Leydig tumor cells: role of SR-B1-mediated selective cholesteryl ester transport.

Biol. Reprod. 68, 114-121.

Ren S., Hylemon P., Marques D., Hall E., Redford K., Gil G., Pandak W.M. (2004). Effect of increasing the expression of cholesterol transporters (StAR, MLN64, and SCP-2) on bile acid synthesis. J. Lipid Res. 45, 2123-2131.

Richmond E.J., Flickinger C.J., McDonald J.A., Lovell M.A., Rogol A.D. (2001). Lipoid congenital adrenal hyperplasia (CAH): patient report and a mini-review. Clin. Pediatr. (Phila). 40, 403-407.

Riegelhaupt J.J., Waase M.P., Garbarino J., Cruz D.E., Breslow J.L. (2010). Targeted disruption of steroidogenic acute regulatory protein D4 leads to modest weight reduction and minor alterations in lipid metabolism. J. Lipid Res. 51, 1134-1143.

Rodriguez-Agudo D., Calderon-Dominguez M., Ren S., Marques D., Redford K., Medina-Torres M.A., Hylemon P., Gil G., Pandak W.M. (2011). Subcellular localization and regulation of StarD4 protein in macrophages and fibroblasts. Biochim. Biophys. Acta. 1811, 597-606.

Rodriguez-Agudo D., Ren S., Wong E., Marques D., Redford K., Gil G., Hylemon P., Pandak W.M. (2008). Intracellular cholesterol transporter StarD4 binds free cholesterol and increases cholesteryl ester formation. J. Lipid Res. 49, 1409-1419.

Romanowski M.J., Soccio R.E., Breslow J.L., Burley S.K. (2002). Crystal structure of the Mus musculus cholesterol-regulated START protein 4 (StarD4) containing a StAR-related lipid transfer domain. Proc. Natl. Acad. Sci. U. S. A. 99, 6949-6954.

Sato R., Yang J., Wang X., Evans M.J., Ho Y.K., Goldstein J.L., Brown M.S. (1994). Assignment of the membrane attachment, DNA binding, and transcriptional activation domains of sterol regulatory element-binding protein-1 (SREBP-1). J. Biol. Chem. 269, 17267-17273.

Schrick K., Nguyen D., Karlowski W.M., Mayer K.F. (2004). START lipid/sterol-binding domains are amplified in plants and are predominantly associated with homeodomain transcription factors. Genome Biol. 5, R41.

Soccio R.E., Adams R.M., Maxwell K.N., Breslow J.L. (2005b). Differential gene regulation of StarD4 and StarD5 cholesterol transfer proteins. Activation of StarD4 by sterol regulatory element-binding protein-2 and StarD5 by endoplasmic reticulum stress. J. Biol. Chem. 280, 19410-19418.

Soccio R.E., Adams R.M., Maxwell K.N., Breslow J.L. (2005a). Differential gene regulation of StarD4 and StarD5 cholesterol transfer proteins. Activation of

StarD4 by sterol regulatory element-binding protein-2 and StarD5 by endoplasmic reticulum stress. J. Biol. Chem. 280, 19410-19418.

Soccio R.E., Adams R.M., Romanowski M.J., Sehayek E., Burley S.K., Breslow J.L. (2002). The cholesterol-regulated StarD4 gene encodes a StAR-related lipid transfer protein with two closely related homologues, StarD5 and StarD6. Proc. Natl. Acad. Sci. U. S. A. 99, 6943-6948.

Soccio R.E., Breslow J.L. (2003). StAR-related lipid transfer (START) proteins: mediators of intracellular lipid metabolism. J. Biol. Chem. 278, 22183-22186.

Song M., Shao H., Mujeeb A., James T.L., Miller W.L. (2001). Molten-globule structure and membrane binding of the N-terminal protease-resistant domain (63-193) of the steroidogenic acute regulatory protein (StAR). Biochem. J. 356, 151-158.

Stocco D.M. (2000). The role of the StAR protein in steroidogenesis: challenges for the future. J. Endocrinol. 164, 247-253.

Stocco D.M., Clark B.J. (1996). Regulation of the acute production of steroids in steroidogenic cells. Endocr. Rev. 17, 221-244.

Strauss J.F., III, Kishida T., Christenson L.K., Fujimoto T., Hiroi H. (2003). START domain proteins and the intracellular trafficking of cholesterol in steroidogenic cells. Mol. Cell Endocrinol. 202, 59-65.

Sugawara T., Kiriakidou M., McAllister J.M., Kallen C.B., Strauss J.F., III. (1997). Multiple steroidogenic factor 1 binding elements in the human steroidogenic acute regulatory protein gene 5'-flanking region are required for maximal promoter activity and cyclic AMP responsiveness. Biochemistry. 36, 7249-7255.

Tsujishita Y., Hurley J.H. (2000). Structure and lipid transport mechanism of a StAR-related domain. Nat. Struct. Biol. 7, 408-414.

West L.A., Horvat R.D., Roess D.A., Barisas B.G., Juengel J.L., Niswender G.D. (2001). Steroidogenic acute regulatory protein and peripheral-type benzodiazepine receptor associate at the mitochondrial membrane. Endocrinology. 142, 502-505.

Yabe D., Brown M.S., Goldstein J.L. (2002). Insig-2, a second endoplasmic reticulum protein that binds SCAP and blocks export of sterol regulatory element-binding proteins. Proc. Natl. Acad. Sci. U. S. A. 99, 12753-12758.

Yamada S., Yamaguchi T., Hosoda A., Iwawaki T., Kohno K. (2006). Regulation of human STARD4 gene expression under endoplasmic reticulum stress. Biochem. Biophys. Res. Commun. 343, 1079-1085.

Yang T., Espenshade P.J., Wright M.E., Yabe D., Gong Y., Aebersold R., Goldstein J.L., Brown M.S. (2002). Crucial step in cholesterol homeostasis: sterols promote binding of SCAP to INSIG-1, a membrane protein that facilitates retention of SREBPs in ER. Cell. 110, 489-500.

Yaworsky D.C., Baker B.Y., Bose H.S., Best K.B., Jensen L.B., Bell J.D., Baldwin M.A., Miller W.L. (2005). pH-dependent Interactions of the carboxyl-terminal helix of steroidogenic acute regulatory protein with synthetic membranes. J. Biol. Chem. 280, 2045-2054.

Yivgi-Ohana N., Sher N., Melamed-Book N., Eimerl S., Koler M., Manna P.R., Stocco D.M., Orly J. (2009). Transcription of steroidogenic acute regulatory protein in the rodent ovary and placenta: alternative modes of cyclic adenosine 3', 5'-monophosphate dependent and independent regulation. Endocrinology. 150, 977-989.